Advances in Civil Engineering

Use of Recyclable Materials in Sustainable Civil Engineering Applications

Guest Editors: Monica Prezzi, Paola Bandini, J. Antonio H. Carraro, and Paulo J. M. Monteiro

Use of Recyclable Materials in Sustainable Civil Engineering Applications

Advances in Civil Engineering

Use of Recyclable Materials in Sustainable Civil Engineering Applications

Guest Editors: Monica Prezzi, Paola Bandini,
J. Antonio H. Carraro, and Paulo J. M. Monteiro

Editorial Board

Contents

Hindawi Publishing Corporation
Advances in Civil Engineering
Volume 2011, Article ID 896016, 2 pages
doi:10.1155/2011/896016

Editorial

Use of Recyclable Materials in Sustainable Civil Engineering Applications

Monica Prezzi,[1] Paola Bandini,[2] J. Antonio H. Carraro,[3] and Paulo J. M. Monteiro[4]

[1] *Civil Engineering Department, Purdue University, West Lafayette, IN 47907, USA*
[2] *Civil Engineering Department, New Mexico State University, Las Cruces, NM 88003-8001, USA*
[3] *Centre for Offshore Foundation Systems M053, The University of Western Australia, 35 Stirling Highway, Crawley, WA 6009, Australia*
[4] *Civil and Environmental Engineering, University of California Berkeley, Berkeley, CA 94720, USA*

Correspondence should be addressed to Monica Prezzi, mprezzi@purdue.edu

Received 15 November 2011; Accepted 15 November 2011

Various types of recyclable materials are currently used in civil engineering applications. These include tire shreds, ground tire rubber, fly and bottom ash, blast-furnace slag, steel slag, cement kiln dust, silica fume, crushed glass, reclaimed asphalt pavement (RAP), and rice husk ash. Reutilization of these recyclable materials is especially beneficial in civil engineering applications that require large volumes of materials. When these waste products are used in place of other conventional materials, natural resources and energy are preserved and expensive and/or potentially harmful waste disposal is avoided. This special issue deals with the use of recyclable materials in diverse civil engineering applications focusing on sustainable development. The papers in this special issue present results of laboratory tests and important research findings for these materials, recommendations for debris recycling practices, and documented field applications of several waste or recyclable materials.

The paper by D. L. Brandon et al. deals with the Hurricane Katrina storm debris removal practices in 16 southern Mississippi counties in the USA and the associated recycling efforts. Various types of debris, which included vegetation, construction material, electronic waste, vehicles, and vessels, were removed from public and private property. The scope within the respective counties varied from removal of vegetation only to removal of every eligible form of debris. The recommendations proposed in this paper will help improve planning and implementation of recycling efforts during debris removal missions in the future.

The paper by S. Talukdar et al. investigated the use of waste materials, such as crushed glass, ground tire rubber, and recycled aggregate, in concrete. Test results demonstrated that ground tire rubber introduced significant amounts of air into the mixtures tested, affecting adversely their compressive strength. The air introduced into these mixtures was partly removed by using a defoamer, which was less effective for mixtures containing recycled aggregates, glass, and ground tire rubber. Freeze-thaw test results showed that this air entrained in the mixtures was not able to improve their freeze-thaw resistance. The authors indicated that further research is needed to optimize the design and performance of lightweight, low-carbon footprint concrete materials.

The paper by I. Z. Yildirim and M. Prezzi provides an overview of the different types of steel slag generated from basic-oxygen-furnace steelmaking, electric-arc-furnace steelmaking, and ladle-furnace steel refining processes. The mineralogical and morphological properties of basic-oxygen-furnace and electric-arc-furnace-ladle slag samples generated from two steel plants in Indiana, USA are presented and discussed in detail based on results from X-Ray Diffraction analyses and Scanning Electron Microscopy studies.

The paper by C. E. Riley et al. presents the results of a laboratory-testing program to investigate the use of spray dryer ash as the primary or sole binding component in mortar for various applications. The study focuses on very high contents of spray dryer ash in a hardened product. The spray dryer ash, also known as spray dryer absorber, has self-cementing properties and is a byproduct of coal combustion and flue gas scrubbing processes. The test results showed that the spray dryer ash mixed with water along or with recycled polymer fibers has very low strength and properties

that are not suitable for structural engineering applications. However, the addition of very small percentages of Portland cement and recycled fibers increased the compressive and flexural strengths. The experimental results showed that spray dryer ash has potential for beneficial use in construction and material applications.

The paper by J. W. van de Lindt and R. K. Rechan of this special issue presents the method and results of experiments carried out to study the seismic behavior of a concrete portal frame with fifty percent of its cement content replaced by a spray dryer ash (SDA). Based on multiple shake table tests, the high-content SDA frame was found to perform as well as the standard concrete frame for two earthquakes exceeding design-level intensity earthquakes.

Another paper entitled "*Cellular fibroma of the ovary with multiloculated macroscopic characteristics: a case report*" investigated the use of recycled aggregate concrete made with coarse aggregate from the demolition of a concrete structure. The experimental research compared the compressive strength, elastic modulus, and drying shrinkage of concrete made with a reference aggregate and concrete containing 30% of recycled aggregate. The results indicated that the recycled aggregate concrete can meet the requirements for structural concrete up to C32/40 strength class.

There is a paper that provides a critical review of sustainable construction with emphasis on the use of concrete in the region covered by the Gulf Cooperation Council. Members of this Council include Persian Gulf States of Bahrain, Kuwait, Oman, Qatar, Saudi Arabia, and the United Arab Emirates. The authors analyzed the existing literature on the use of recycled aggregate for the stringent conditions of the Gulf region. The analysis indicated that while there is research on recycled aggregate concrete in laboratory conditions, the technology transfer to field conditions has been small. Another limitation identified by the authors is that most of the research has focused on the mechanical properties of the recycled aggregate with limited emphasis on the durability.

The paper entitled "*Use of reclaimed asphalt pavement in conjunction with ground improvement: a case history*" describes the use of RAP and geosynthetic ground improvement in a design-built project for the reconstruction of an asphalt parking lot. The project was successfully completed at a cost significantly lower than the original cut and replace specification. The field observations during this project regarding drainage of the RAP aggregate base are in agreement with prior research findings in the literature and suggest that RAP aggregate base courses can be constructed with properties comparable to virgin stone aggregate base courses compacted with similar conditions. The paper also discusses contractual issues, such as the risk of adopting a less conventional method and materials to reduce construction costs and the efficiencies of the design-built approach in those cases.

Monica Prezzi
Paola Bandini
J. Antonio H. Carraro
Paulo J. M. Monteiro

Hindawi Publishing Corporation
Advances in Civil Engineering
Volume 2011, Article ID 567924, 6 pages
doi:10.1155/2011/567924

Review Article

Review of Research on and Implementation of Recycled Concrete Aggregate in the GCC

Akmal S. Abdelfatah and Sami W. Tabsh

Department of Civil Engineering, American University of Sharjah, P.O. Box 26666, Sharjah, UAE

Correspondence should be addressed to Akmal S. Abdelfatah, akmal@aus.edu

Received 28 February 2011; Revised 11 September 2011; Accepted 21 September 2011

Academic Editor: Paulo Monteiro

The goal of sustainable construction is to reduce the environmental impact of a constructed facility over its lifetime. Concrete is the main material used in construction in the Gulf Cooperation Council (GCC). Therefore, it makes economic and environmental sense to use recycled materials in the making of new concrete for different applications. The objectives of this study are to summarize published research on the use of recycled concrete aggregates in new concrete mixes and examine its implementation in construction and industry in the GCC region. The study showed that while there is reasonable research on recycled concrete, the practical implementation in the region greatly lacks behind, especially due to the lack of economic viability and awareness of such applications at the current time.

1. Introduction

Members of the GCC in the Middle-East include the Persian Gulf states of Bahrain, Kuwait, Oman, Qatar, Saudi Arabia and the United Arab Emirates. The GCC countries occupy the area within the Arabian Peninsula, which is located in the southwestern region of the Asian continent. The strength of GCC countries lies in having 24–40% of World's conventional oil reserves and about 23% of world's conventional natural gas reserves. The weakness is related to having an arid weather, shortage of fresh water, and limited farming areas [1]. The Arabian Peninsula is a harsh environment with temperatures ranging between 7° and 47°C, and an average annual rainfall being between 70 and 140 mm [2].

Apart from the oil and gas sector, economy of most of the GCC countries depends to a large extent on the construction industry and infrastructure activities. This is due to recent initiatives undertaken by the local governments to diversify from an oil- and gas- dependent economy. Published statistics in the Arab Construction World magazine [3] indicate that the total value of real estate projects currently under construction in the GCC stands over US$2.39 trillion. However, the limited natural resources in the GCC have a great impact on this industry. Key aspects of the construction industry in the Gulf which have considerable effect on the environment are limited useable natural aggregates for making concrete, scarcity of fresh water sources, and lack of iron ore for producing steel.

The Gulf is often seen as a region that lacks many of the natural resources required for concrete production. Concrete consists of 4 main ingredients: water, cement, sand, and aggregate. Water is locally available but is, for the most part, desalinated. While in some countries concrete batching plants recycle the water they use for cleaning, in the Gulf it is very limited. Although cement is produced locally, the raw materials are often imported from other countries. At peak market levels, demand had exceeded supply so some quantities of cement had to be imported to supplement local need. With the exception of Bahrain, sand is sourced from within the GCC countries, whereas most of the coarse aggregate is sourced from the mountains located in limited areas within the Arabian Peninsula.

2. Sustainable Construction in the GCC

Sustainability can be defined as providing today's need without compromising the capability of future generations

to meet their needs. Sustainable construction aspires to apply this concept to the construction industry. This is accomplished by using less natural materials, consuming less energy, causing lower levels of pollution, and reducing waste while gaining the same benefits that can be achieved through the use of tradition construction methods and materials.

The issue of sustainable buildings in the GCC has become an important topic in recent years, with the United Arab Emirates (UAE) being the leader in this track following the announcement of the green building initiative in January 2008 by Sheikh Mohammed bin Rashid Al Maktoum, Ruler of Dubai. This was shortly followed by the launching of the Estidama initiative in May 2008 by Abu Dhabi's Urban Planning Council, the agency which is responsible for the future of Abu Dhabi's urban environment.

Regional studies estimate that the GCC countries collectively produce more than 120 million tons of waste every year, of which 18.5 percent is related to solid construction waste [4]. For example, recent statistics from Dubai Municipality show that construction and demolition waste accounts for 75% of the 10,000 tons of general waste produced daily in the city, of which concrete demolition rubbles represent 70% of this quantity. Rapid urbanization, growth in the construction sector, high population increase rates, diversified cultures, and floating populations are believed to be the main reasons for such high waste production in the country.

Based on the above, recycling solid waste materials for construction purposes becomes an increasingly important waste management option, as it can lead to environmental and economic benefits. Conservation of natural resources, saving of energy in production and transportation, and reduction of pollution are also the advantages of recycling. In particular, concrete is a perfect construction material candidate for recycling. Some materials, such as plastic, can be recycled once or twice, and glass can only be done if it is properly sorted. However, concrete can be recycled continuously as long as the specification is right.

However, sustainability requires commitment and investment by all parties involved in the construction industry, both governmental and private. Lack of proper planning can lead to delays in implementation, as has happened in February 2011, when Abu Dhabi Municipality suspended the Estidama (meaning "sustainability" in Arabic) building requirements related to energy, but kept the other mandates, which represent 10% of all the requirements. The cited reason for the suspension was due to contractors' lack of preparation for meeting the strict requirements in their projects [5].

3. Objectives and Scope

The objectives of this paper are to review the published research and development studies on recycled concrete aggregate in the GCC region, examine the current use of such material in construction, and recommend suitable strategies for wider applications.

Several GCC researchers have addressed the use of recycled waste material in concrete and disseminated their work through publications. In addition, there have been some efforts to implement the results of research into practice. This paper provides a collective summary of the published technical studies by universities, research institutions, private entities, and governmental agencies that deal with recycled concrete aggregate. It also includes the current state of practice and implementation in the area of recycled concrete in the region.

4. Published Research

This section presents a review of published research on the utilization of recycled concrete aggregate in producing new concrete in the GCC countries.

4.1. Sustainability Issues in the GCC. Kartam et al. [6] discussed the current status of construction and demolition waste disposal system in Kuwait and identified the potential problems to the environment, people, and economy. They investigated alternative solutions to manage and control this waste in an economical, efficient, and safe way. They also described the feasibility and challenges of establishing a construction and demolition waste recycling facility in Kuwait.

The need for green buildings in Bahrain was investigated by Alnaser and Flanagan [7]. According to the authors, sustainable construction implementation is limited in the country due to the lack of awareness of the public in sustainable technology, lack of markets importing sustainable technologies, and client concerns about the profitability and pay-back period. The study revealed that local contractors were the most enthusiastic about implementing green building projects. As a followup to the previous study, Alnaser [8] discussed some of the current sustainable buildings in Bahrain, United Arab Emirate, and Kuwait. To encourage sustainable buildings projects in these countries, the author felt that it is necessary to create the conditions and incentives that would encourage stakeholders in the sector to actively pursue such projects, through governmental policies, economic incentives, rating systems, and coordination with key partners, such as the financing sector.

Kayali et al. [9] reviewed the available industrial waste products that can be used in making sustainable concrete and their relevance to the Middle East, with particular attention to the GCC. The feasibility of using various waste materials, including recycled concrete, is judged with reference to the relevant environment. The authors believe that the inclusion of recycled waste in the production of high-performance concrete can be a significant contribution to a sustainable industry. They concluded that it is the duty of the engineer to judge whether one or more of available waste materials should be used in the production of new concrete on a particular project.

In a paper by Galbraith [10] on structural sustainability, the author outlined the role of structural design in sustainable buildings and its implication within the Gulf region. He identified the available sustainable design techniques in the construction industry and categorized them according to their cost impact.

Lately, Bahrain took the initiative to hold a Green Building Forum in 2010 in Manama [11]. The forum's objective was to discuss the challenges facing the construction industry, with consideration of the environmental concerns, including sustainable building materials, smart buildings, and other topics related to sustainable construction. Another conference on concrete sustainability was recently held in Dubai, covering solutions for sustainable concrete manufacturing and construction [12]. During the conference, various experts addressed sustainable development initiatives, recycled materials, Carbon footprint and embodied energy, and performance-based concrete.

4.2. Recycled Concrete Aggregates. The literature search showed extensive research in the area of recycled concrete aggregates in many GCC countries. One of the earliest research on recycling concrete rubble as aggregate material for construction was carried out by Khan and Rasheeduzzafar in Saudi Arabia [13]. They utilized laboratory tests to investigate the strength, failure mechanism, and durability characteristics of the recycled aggregate concrete. Their study showed that for low W/C ratios the recycled aggregate concrete has 30% lower strength than conventional concrete with natural aggregate. Also, the recycled aggregate concrete showed lower modulus of elasticity and durability characteristics.

Al-Mutairi and Haque [14] used old demolished concrete in Kuwait to replace 50 and 100% of the coarse aggregate and seawater to replace 25, 50, and 100% of the tap water in a standard concrete mix having moderate target strength. The recycled concrete was cured in seawater for a period of 28 days. The results indicated that even with 100% usage of recycled concrete aggregate, design strength of 35 MPa was attainable. Highest concrete strength was obtained when the mixing water consisted of a blend of 25% seawater and 75% tap water.

Rahal [15, 16] tested the mechanical properties of recycled aggregate concrete with a compressive strength 20–50 MPa and compared the results to those of concrete made with natural aggregate. The results showed that the compressive strength, indirect shear strength, and modulus of elasticity of recycled aggregate concrete were all within 10% of those of natural aggregate concrete having the same mix proportions.

AlMutairi and AlKhaleefi [17] investigated the flexural behavior of plain concrete containing crushed old concrete as replacement for natural coarse aggregate. Plain concrete beams made with 0%, 50%, and 100% recycled coarse aggregate were tested as simple beams with third-point loading. When compared with the ACI standard, the obtained modul of rupture values were within the acceptable levels. Furthermore, statistical analyses of permeability tests indicated that the concrete was not greatly affected by the use of the recycled aggregates in the mix.

Al-Harthy et al. [18] conducted laboratory tests to examine the strength and durability of recycled aggregate concrete. The results showed that concrete strength is enhanced with the replacement of normal aggregates by recycled aggregate content of up to 30%, thereafter the strength decreases with further increase in recycled aggregate. However, replacement of natural aggregate by recycled aggregate was found to decrease the workability of the concrete due to the high absorption characteristics of the recycled aggregate.

Tabsh and Abdelfatah [19] studied the strength of concrete made with recycled concrete coarse aggregate. The toughness and soundness laboratory tests on the recycled coarse aggregate showed higher percentage loss than natural aggregate, but remained within acceptable limits. The compressive and splitting tensile strengths of concrete made with recycled coarse aggregate depend on the mix proportions. In general, the strength of recycled concrete was 10–25% lower than that of conventional concrete made with natural aggregate due to increase in water demand to maintain the specified slump. In a follow-up study, Abdelfatah et al. [20] utilized admixtures in concrete mixes containing demolished concrete as replacement for natural coarse aggregates to compensate for the need of additional water required to increase the workability. The results showed that the use of superplasticizers, instead of additional water, was able to increase the compressive strength of recycled aggregate concrete to a level around the same as that of the control mix containing natural aggregate. This finding is not in agreement with the results obtained by Gull [21] when testing low strength concrete utilizing recycled concrete aggregate.

Mirza and Saif [22] studied the effect of silica fume on recycled aggregate concrete characteristics. The percentages of recycled aggregate replacements of natural aggregate used by weight were 0, 50, and 100%, whereas the percentages of silica fume replacements of cement used by weight were 5, 10, and 15%. The results showed that the compressive and tensile strengths values of the recycled concrete aggregate increased as the recycled aggregate and the silica fume contents increased. The study also indicated that in order to accommodate 50% of recycled aggregate in structural concrete, the mix needs to incorporate 5% of silica fume.

Recently, Elchalakani [23] investigated the strength and durability of recycled concrete made from recycled aggregate and wastewater in the UAE. Experimental tests employing standard cubes and cylinders to assess the compressive strength and small beams to evaluate the flexural strength were utilized. The study showed that the effect of recycled aggregate and recycled water on axial and bending strength was found moderate but had a significant effect on durability. To enhance the durability of recycled concrete, the author recommended using ground granulated blast furnace slag and fly ash for any future building construction in the Gulf.

There have been some studies that considered the utilization of recycled concrete aggregate in different construction applications than in production of new concrete. For example, Al-Ali et al. [24, 25] investigated the suitability of using recycled concrete aggregates as subbase for pavement construction. A test model was built in the laboratory to assess the recycled material pavement performance under various loads and to comparatively measure its behavior against the natural aggregate layers. The experimental program considered ranges of pavement loads, material gradations, compositions, and layer thicknesses. The results

showed that the deflection of the pavement under load is generally less with the recycled concrete aggregate than that with the natural aggregate. Therefore, there is a good potential for using recycled concrete aggregate as a subbase layer in roadway pavement construction.

Another application of the use of recycled concrete aggregate is in the production of sand lime brick in Kuwait, which was considered by Al-Otaibi and El-Hawary [26] and Al-Otaibi [27]. The study evaluated the specific gravity, compressive strength, and absorption characteristics of the brick. It showed that the brick that is made from recycled concrete aggregate has properties that are within the specifications requirements.

5. Industry and Governmental Initiatives

Even though there is a considerable body of research related to using recycled concrete aggregate in the production of concrete mixes, the industrial implementation in the GCC countries of these technologies is still in its infancy. Some of the implementations are initiated by governmental agencies, and some other implementations are carried out by the industry.

The government of Kuwait has recognized the problems caused by the construction demolition waste. In order to reduce the area needed for landfills, the government of Kuwait approved the Environment Protection Industrial Co (EPIC) to start a construction waste recycling plant, with a daily capacity of about 7–20 thousand tones of construction waste [28]. Furthermore, the Arab International Industrial Projects company was established in 2005 with the objective of improving the environmental conditions in Kuwait. One of the projects for this company is concerned with cutting the production costs of new concrete and reducing the need for land fill space. For this purpose, concrete rubbles and old asphalt concrete are crushed to different sizes to be used as aggregate for some projects. The produced aggregate can be used in many projects, such as drainage and rain pipes packaging, base and subbase layers for road construction, asphalt concrete mixes for road paving, and ordinary nonreinforced concrete mixes [29].

In the process of producing sustainable concrete in Qatar, efforts towards using recycled aggregate and waste concrete are underway. In a report sponsored by Mobile-Baustoffe GmbH company, Blanco-Carrasco et al. [30] studied the benefits and potential implementation of using waste concrete and recycled aggregate. Among the cited applications by the authors is the use of crushed recycled concrete in nonstructural applications such as road base or subbase construction, core filling, embankments, backfills, and blinding slabs. Another effort to help Qatar in adopting green building design and construction is the establishment of the Qatar Green Building Council (QGBC), which is a private institution concerned with the promotion of environmentally sustainable practices [31]. One of the members of QGBC is the Khalid Cement Industries Company (KCIC), which is implementing an environment management system that allows the company to recycle water and concrete and apply a waste management plan [32]. A Domestic Solid Waste Management Center, which was initiated by Ministry of Municipal Affairs and Agriculture in Qatar, is under construction and will be opened in March 2011. The center is capable of recycling a total of 2,300 tons of mixed domestic waste and a total of 5,000 tons of construction waste per day [33].

In order to help the companies to interact and promote waste recycling, the Riyadh Exhibitions Co. Ltd has been organizing the International Recycling and Waste Management Exhibition, with the 3rd exhibition being organized in 2011 [34]. A recycling plant has been constructed in Jeddah, which has a sorting capacity of up to 1,200 tons/day; however, the plant does not recycle any construction material [35]. The limited implementation of recycled concrete in construction in Saudi Arabia has prompted some activists, such as Sultan Faden who is the head of the Founding Group of the Saudi Green Building Council, to call on municipalities in Jeddah and other cities to launch recycling factories, and to appeal for stronger regulations to protect mountains from crushers in the Kingdom [36].

The UAE seems to be one of the most active countries in the Gulf region when it comes to the application of concrete recycling. As part of the governmental efforts to promote recycling of construction materials, Dubai Central Laboratory has signed an agreement with Emirates Recycling and Dubai Municipality to study and evaluate construction demolition waste. Since this waste is usually ignored by contractors, the project aims at finding useful applications to use construction rubbles [37]. In Abu Dhabi, the city has supported several projects regarding green buildings and environmentally friendly construction material. For example, a new crushing plant in Al Dafra has been newly opened with the capability of crushing waste material and turning them into aggregate that can be used to replace natural aggregate in making concrete [38]. Unibeton Ready Mix is another company that supports the production of green concrete, which has been used in the Masdar City in Abu Dhabi. The company used 1.8 million tons of recycled aggregate in 20% of the needed concrete used in the City [39]. Another application is carried out by Al-Falah Ready Mix and Emirates Beton as they have capabilities to produce concrete that is environmentally friendly, by using recycled aggregate and other recycled waste materials aiming to zero waste from production and maximum usage of the waste material [40, 41].

The Emirate of Sharjah also has its share of activities in the sustainable construction field. Recently, a new waste recycling plant was opened in the industrial area of Sharjah. The plant receives concrete and other construction waste material from various places within the Emirate and processes them to be used again for construction purposes [42].

In Oman, the applications of concrete recycling are limited [43]. However, a royal decree has been issued in 2009 to appoint the Oman Environmental Services Holding Company to execute the task of implementing the government's policy with regard to the waste sector. In addition to the management of landfills allover Oman, the company has initiated several projects to develop facilities for the

management of medical waste, hazardous waste, electronic waste, and a tire recycling plant [44].

Generating about 3000 tons of waste in Bahrain each day has motivated the initiative to plan for a recycling factory that will process the majority of that waste, as announced in 2008 by Majeed Milad, the chairman of the Manama Municipal Council [45].

6. Conclusions

The study leads to the followings conclusions.

(1) There is an adequate body of research work on recycled concrete aggregate and its uses in the GCC, predominantly conducted by individuals in research and academic institutions.

(2) Most of the surveyed research considers the mechanical and strength characteristics of recycled aggregates with little focus on durability issues.

(3) There are few studies regarding the economic feasibility and financial implications of recycling and re-use of concrete rubbles in construction applications.

(4) Research on the environmental impacts of using such recycled material in construction has been rarely addressed in the region.

(5) Real-life applications of using recycled construction waste are still in their infancy and need some major efforts to attract investors to this industry.

(6) There are limited legislations and policies to encourage recycling and use of demolition waste in the GCC.

(7) No governmental standards and specifications for processing and use of recycled aggregate are currently available in the region.

Acknowledgments

The authors would like to acknowledge the financial support by the American University of Sharjah (AUS) through the Faculty Research Grant program and the contribution of students Bayan Kattan and Salam Yaghi, in compiling some of the information cited in the paper.

References

[1] M. Jefferson, "Energy for sustainable development: global context and rational options for the GCC," in *Proceedings of the 2nd Seminar on Potential of Alternative Energy in the GCC*, Arabian Gulf University, Manama, Bahrain, April 2007.

[2] M. F. Al-Rashed and M. M. Sherif, "Water resources in the GCC countries: an overview," *Water Resources Management*, vol. 14, no. 1, pp. 59–75, 2000.

[3] ACW, Arab Construction World, Vol. 27, Issue 4, April 2009, http://www.acwmag.com/index.aspx?all_lk_id=142&magazine_id=2#.

[4] The Gulf Today Newspaper, 19 May, 2010, http://p4papyrus.blogspot.com/2010/05/gulf-countries-generate-222-million.html.

[5] Al-Ittihad Newspaper, 3 February, 2011, http://www.alittihad.ae/details.php?id=12034&y=2011.

[6] N. Kartam, N. Al-Mutairi, I. Al-Ghusain, and J. Al-Humoud, "Environmental management of construction and demolition waste in Kuwait," *Waste Management*, vol. 24, no. 10, pp. 1049–1059, 2004.

[7] N. W. Alnaser and R. Flanagan, "The need of sustainable buildings construction in the Kingdom of Bahrain," *Building and Environment*, vol. 42, no. 1, pp. 495–506, 2007.

[8] N. AlNaser, "Towards sustainable buildings in Bahrain, Kuwait and United Arab Emirates," *The Open Construction and Building Technology Journal*, vol. 2, no. 1, pp. 30–45, 2008.

[9] O. Kayali, M. Haque, and J. Khatib, "Sustainability and emerging concrete materials and their relevance to the Middle East," *The Open Construction and Building Technology Journal*, vol. 2, no. 1, pp. 103–110, 2008.

[10] K. Galbraith, "Structural sustainability in the gulf—fact and fiction," in *Proceedings of the 8th World Congress, Council of Tall Buildings and Urban Habitat (CTBUH '08)*, Dubai, UAE, March 2008.

[11] Green Building Forum, Manama, Bahrain, May 2010, http://www.tradearabia.com/news/CONS_174322.html.

[12] Concrete Sustainability Conference, National Ready Mix Concrete Association, Dubai, UAE, December 2010, http://www.concretetechnologyforum.org/2010CSCDubaiProceedings.

[13] A. Khan and Rasheeduzzafar, "Recycled concrete—a source for new aggregate," *Journal of Cement, Concrete and Aggregates*, vol. 6, no. 1, pp. 17–26, 1984.

[14] N. Al-Mutairi and M. N. Haque, "Strength and durability of concrete made with crushed concrete as coarse aggregates," in *Proceedings of the International Symposium on Recycling and Reuse of Waste Materials*, pp. 499–506, Scotland, UK, September 2003.

[15] K. Rahal, "Mechanical properties of concrete with recycled coarse aggregate," *Building and Environment*, vol. 42, no. 1, pp. 407–415, 2007.

[16] K. Rahal, "Mechanical properties of recycled aggregate concrete," in *Proceedings of the Proceedings of the ACI-Kuwait Chapter 2nd International Conference on Design and Sustainability of Structural Concrete in the Middle East with Emphasis on High-Rise Buildings*, M. M. El-Hawary, N. Al-Mutairi, K. N. Rahal, and H. Kamal, Eds., 306, p. 299, Kuwait, March 2007.

[17] N. Z. AlMutairi and A. M. AlKhaleefi, "On flexural strength and permeability of recycled concrete as coarse aggregates," in *Proceedings of the ACI-Kuwait Chapter 2nd International Conference on Design and Sustainability of Structural Concrete in the Middle East with Emphasis on High-Rise Buildings*, M. M. El-Hawary, N. Al-Mutairi, K. N. Rahal, and H. Kamal, Eds., 162, p. 153, Kuwait, March 2007.

[18] A. Al-Harthy, R. Taha, A. Al-Saidy, and S. Al-Oraimi, "Properties of Recycled Aggregate Concrete," in *Proceedings of the ACI-Kuwait Chapter 2nd International Conference on Design and Sustainability of Structural Concrete in the Middle East with Emphasis on High-Rise Buildings*, M. M. El-Hawary, N. Al-Mutairi, K. N. Rahal, and H. Kamal, Eds., 318, p. 309, Kuwait, March 2007.

[19] S. W. Tabsh and A. S. Abdelfatah, "Influence of recycled concrete aggregates on strength properties of concrete," *Construction and Building Materials*, vol. 23, no. 2, pp. 1163–1167, 2009.

[20] A. Abdelfatah, S. W. Tabsh, and S. Yehia, "Alternative ways of making concrete with recycled coarse aggregate," in *Proceedings of the 4th International Conference on Applications of Traditional and High Performance Materials in Harsh*

Environments, Institute of Materials Systems, Sharjah, UAE, March 2010.

[21] I. Gull, "Testing of strength of recycled waste concrete and its applicability," *Journal of Construction Engineering and Management*, vol. 137, no. 1, pp. 1–5, 2011.

[22] F. A. Mirza and M. A. Saif, "Mechanical properties of recycled aggregate concrete incorporating silica fume," in *Proceedings of the 2nd International Conference on Sustainable Construction Materials and Technologies*, Coventry University and The University of Wisconsin Milwaukee Centre for By-products Utilization, Ancona, Italy, June 2010.

[23] M. Elchalakani, "Strength and durability of recycled concrete made from recycled aggregate and wastewater," in *Proceedings of the International Concrete Sustainability Conference*, The National Ready Mixed Concrete Association and Grey Matters Consultancy, Dubai, UAE, December 2010.

[24] A. Y. Al-Ali, A. M. Alshamsi, and Y. E. Hawas, "Structural performance of recycled concrete aggregates for road construction," in *Proceedings of the 1st International Conference on Quality Control and Quality Assurance of Construction Materials*, Dubai, UAE, October 2001.

[25] A. Y. Al-Ali, A. M. Alshamsi, and Y. E. Hawas, "Recycled concrete put on the test," *Gulf Construction Journal*, vol. 13, no. 2, pp. 15–22, 2002.

[26] S. Al-Otaibi and M. El-Hawary, "Potential for recycling demolished concrete and building rubble in Kuwait," in *Proceedings of the International Conference on Achieving Sustainability in Construction*, pp. 229–236, Scotland, UK, July 2005.

[27] S. Al-Otaibi, "Producing lime-silica bricks from crushed concrete fines," in *Proceedings of the International Conference on Sustainability in the Cement and Concrete Industry*, Lillehammer, Norway, September 2007.

[28] http://www.cleanmiddleeast.ae/articles/43/recycling-construction-waste-in-the-middle-east-commercial-operation-with-environmental-benefits.html.

[29] Arab International Industrial Projects K.S.C.C., 2011, http://www.best100.org/page.aspx?ID=682e327e-a9b6-428f-bd5a-a4091996b556.

[30] M. Blanco-Carrasco, F. Hornhung, and N. Ortner, *Qatar: Green Concrete Technology*, Mobile-Baustoffe GmbH Company, 2010.

[31] Arabian Business Magazine, 2009, http://www.arabianbusiness.com/qatar-green-building-council-on-way-79664.html.

[32] Khalid Cement Industries Company, 2011, http://www.kccqatar.com/en/news/latest-news/61-khalid-cement-marketing-manager-.html.

[33] Domestic Solid Waste Management Center, 2011, http://www.zawya.com/projects/project.cfm/pid150607090305?cc.

[34] Trade Shows Biz.com, 2011, http://www.tradeshows-biz.com/trade_event/recycling-waste-management-saudi-arabia.html.

[35] Jeddah Recycling Plant, 2011, http://www.recycleinme.com/rim-salum/home.aspx.

[36] Arab News, 2011, http://arabnews.com/saudiarabia/article98429.ece.

[37] Gulf News, 2011, http://gulfnews.com/news/gulf/uae/environment/sharjah-waste-treatment-plant-to-boost-recycling-1.105756.

[38] Arabian Business Magazine, 2011, http://www.arabianbusiness.com/rubble-turns-road-304142.html.

[39] Global Village Encyclopedia, 2011, http://www.gvpedia.com/Abu-Dhabi/Unibeton-Top-Ready-Mix-Company.aspx.

[40] Global Village Encyclopedia, 2011, http://www.gvpedia.com/Abu-Dhabi/Unibeton-Top-Ready-Mix-Company.aspx.

[41] Emirates Beton, 2011, http://emiratesbeton.com/achivements.php.

[42] Gulf News, 2011, http://gulfnews.com/news/gulf/uae/environment/sharjah-waste-treatment-plant-to-boost-recycling-1.105756.

[43] R. Taha, A. Al-Rawas, K. Al-Jabri, A. Al-Harthy, H. Hassan, and S. Al-Oraimi, "An overview of waste materials recycling in the Sultanate of Oman," *Resources, Conservation and Recycling*, vol. 41, no. 4, pp. 293–306, 2004.

[44] Oman Environmental Services Holding Company, 2011, http://www.oeshc.co.om/.

[45] Bahraini TV, 2011, http://bahraini.tv/2008/08/29/waste-management/.

[46] British Standards Institution, BS 8500-1, *Concrete-Complimentary British Standard to BS EN 206-1. Part 2: Specification for Constituent Materials and Concrete*, London, UK, 2006.

[47] AASHTO MP 16, *Standard Specification for Reclaimed Concrete Aggregate for Use as Coarse Aggregate in Hydraulic Cement Concrete*, American Association of State and Highway Transportation Officials, Washington, DC, US, 2010.

[48] CSIRO, *Guide for Specification of Recycled Concrete Aggregates (RCA) for Concrete Production*, Ecorecycle, Victoria, Australia, 1998.

[49] RILEM, "Specifications for concrete with recycled aggregates," *Materials and Structures*, vol. 27, no. 173, pp. 557–559, 1994.

Hindawi Publishing Corporation
Advances in Civil Engineering
Volume 2011, Article ID 283984, 6 pages
doi:10.1155/2011/283984

Research Article

Structural Concrete Prepared with Coarse Recycled Concrete Aggregate: From Investigation to Design

Valeria Corinaldesi

Engineering Faculty, Universitá Politecnica delle Marche, Brecce Bianche Street, 60131 Ancona, Italy

Correspondence should be addressed to Valeria Corinaldesi, v.corinaldesi@univpm.it

Received 28 February 2011; Accepted 24 August 2011

Academic Editor: Paulo Monteiro

An investigation of mechanical behaviour and elastic properties of recycled aggregate concrete (RAC) is presented. RACs were prepared by using a coarse aggregate fraction made of recycled concrete coming from a recycling plant in which rubble from concrete structure demolition is collected and suitably treated. Several concrete mixtures were prepared by using either the only virgin aggregates (as reference) or 30% coarse recycled aggregate replacing gravel and by using two different kinds of cement. Different water-to-cement ratios were adopted ranging from 0.40 to 0.60. Concrete workability was always in the range 190–200 mm. Concrete compressive strength, elastic modulus, and drying shrinkage were evaluated. Results obtained showed that structural concrete up to C32/40 strength class can be manufactured with RAC. Moreover, results obtained from experimentation were discussed in order to obtain useful information for RAC structure design, particularly in terms of elastic modulus and drying shrinkage prediction.

1. Introduction

Crushing concrete to produce coarse aggregate for the production of new concrete is one common means for achieving a more environmentally friendly concrete. Recycling concrete wastes will lead to reduction in valuable landfill space and savings in natural resources. In fact, the use of recycled aggregate concrete (RAC) is acquiring particular interest in civil construction as regards to sustainable development.

Many studies demonstrate the feasibility of the use of crushed concrete as coarse aggregates [1–10], its use being already accounted for in the regulations of many countries. In Italy, the use of 30% recycled concrete instead of virgin aggregate is definitively allowed for producing structural concretes (up to C 30/37 strength class) since July 2009 [11]. Nevertheless, in the Italian regulations no indication about predictions of RAC elastic modulus and drying shrinkage is reported. The study of the elastic behaviour of concretes made of 30% recycled-concrete aggregates, discussed here, just had the aim to provide useful information.

2. Experimental Program

2.1. Materials. Two commercial portland-limestone blended cements were alternatively used, type CEM II/A-L 42.5 R and type CEM II/B-L 32.5 R according to EN-197/1 [12] (the main difference is the content of calcium carbonate that in the first case is less than 20% and in the second case is included in the range 21–35% according to EN-197/1). The Blaine fineness of cements were 0.42 m^2/g and 0.40 m^2/g, respectively, and their specific gravity were 3.05 kg/m^3. The first kind of cement (i.e., CEM II/A-L 42.5 R) due to its composition and its higher fineness is expected to perform more than the other.

Quartz sand (0–5 mm), fine gravel (6–12 mm), and gravel (11–22 mm) were used, suitably combined, for preparing the reference mixtures. Their main physical properties were evaluated according to EN 1097-6 [13] and reported in Table 1 and their gradations evaluated according to EN 933-1 [14] are shown in Figure 1.

In addition, a coarse recycled aggregate fraction (11–22 mm) was used, coming from a recycling plant in which

Table 1: Main physical properties of the aggregate fractions.

Aggregate fractions	Quartz sand	Fine gravel	Gravel	Coarse recycled fraction
Relative specific gravity (SSD)	2.540	2.560	2.570	2.420
Water absorption (%)	3.5	3.0	3.0	6.8

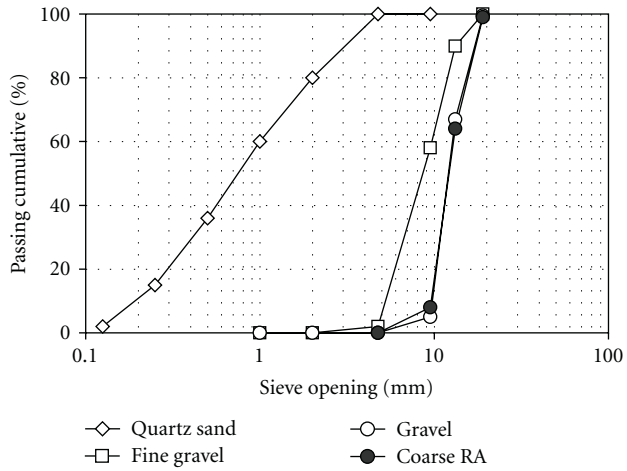

Figure 1: Grain size distribution curves of the aggregate fractions.

rubble from concrete structure demolition is suitably treated. Its composition is 100% recycled concrete; the original concrete strength class was unknown and likely different for waste concrete coming from different sources. The main physical properties of the recycled aggregate fraction are reported in Table 1, and its gradation is shown in Figure 1. The content in recycled concrete fraction of chlorides, sulphates, and organic materials were evaluated according to the methods recommended by UNI EN 1744-1 (part 7, 11, 12, 14, and 15) [15] and the presence of alkali-silica reactive materials according to the method recommended by UNI EN 8520-22 [16]. No organic or alkali-silica reactive materials were detected; concerning the amount of chlorides and sulphates they were below the threshold value of 0.04% (by weight) and 0.15% (by weight), respectively.

As a-water-reducing admixture, a 30% aqueous solution of carboxylic acrylic ester polymer was added to the mixtures.

2.2. Concrete Mixture Proportions. The concrete mixture proportions of the reference mixtures (REF) made of 100% virgin aggregates and of the mixtures made of 30% coarse recycled aggregate replacing gravel (CRA) are reported in Tables 2 and 3, respectively. The recycled-aggregate fraction was added to the mixture after water soaking, in a condition very close to that defined as saturated surface dried. In fact, on the basis of the results obtained in a previous work [17], it seems that presoaked aggregates can be more effective in order to create an internal water supply able to reduce drying shrinkage as well as to avoid water absorption of aggregate during mixing and, consequently, to maintain concrete workability for enough time to be cast.

Five different water-to-cement ratios were adopted when the cement type CEM II/A-L 42.5 R was used: 0.40, 0.45, 0.50, 0.55, and 0.60. On the other hand, the study was limited to three water-to-cement ratios when the cement type CEM II/B-L 32.5 R was used: 0.40, 0.50, and 0.60.

All the concrete mixtures showed the same fluidity level (S5, slump in the range 190–200 mm), evaluated according to EN 12350-2 [18].

In order to optimize the grain size distribution of the solid particles in the concrete, the aggregate fractions were suitably combined according to the Bolomey particle size distribution curve [19].

A water-reducing admixture was always added to the mixtures but at different dosages, ranging from 1.2% to 0.4% by weight of cement in order to adjust cement dosage (always kept under 350 kg/m^3 and gradually decreased for increasing water to cement ratios). In fact, in the current practice concretes with water/cement of 0.40 are typically prepared with about 350 kg/m^3 of cement and concretes with water/cement of 0.60 with roughly 300 kg/m^3 of cement.

2.3. Preparation and Curing of Specimens. Thirty cubic specimens, 100 mm in size, were cast in steel forms for each concrete mixture for compression tests, according to UNI EN 12390-1 [20] and wet cured at 20°C.

In addition, three prismatic specimens (100 by 100 by 500 mm) were prepared for each concrete mixture according to UNI 6555 [21]. After one day of wet curing, the specimens were stored at constant temperature (20 ± 2°C) and constant relative humidity (50 ± 2%) while measuring drying shrinkage at different curing times.

Finally, three cylindric specimens, 250 mm high with a diameter of 100 mm, for each concrete mixture were manufactured for evaluating static modulus of elasticity in compression according to UNI 6556 [22].

3. Results and Discussion

3.1. Compression Test. Compressive strength was evaluated after 3 and 28 days of wet curing according to UNI EN 12390-3 [23] on cubic specimens, which were tested at right angles to the position of casting. The mean values obtained from fifteen specimens as well as the standard deviation values are reported in Table 4.

On the basis of the data reported in Table 4, whichever the kind of cement used, the substitution of 30% virgin aggregate with coarse recycled concrete aggregate produced a loss of strength of about 20% after 28 days of wet curing.

Concerning the standard deviation values, they were practically independent on the type of aggregate used, showing that the same degree of homogeneity of the concrete

Table 2: Mixture proportions of concretes made of 100% virgin aggregates.

Mixture	REF-I-0.40	REF-II-0.40	REF-I-0.45	REF-I-0.50	REF-II-0.50	REF-I-0.55	REF-I-0.60	REF-II-0.60
Water/cement	0.40	0.40	0.45	0.50	0.50	0.55	0.60	0.60
Water, kg	140	140	153	165	165	176	186	186
Cement 42.5R, kg	350	—	340	330	—	320	310	—
Cement 32.5R, kg	—	350	—	—	330	—	—	310
Quartz sand, kg (% in volume)	732 (40)	732 (40)	723 (40)	715 (40)	715 (40)	708 (40)	702 (40)	702 (40)
Fine gravel, kg (% in volume)	553 (30)	553 (30)	547 (30)	541 (30)	541 (30)	535 (30)	531 (30)	531 (30)
Gravel, kg (% in volume)	556 (30)	556 (30)	549 (30)	543 (30)	543 (30)	537 (30)	533 (30)	533 (30)
Superplasticizer, % by weight of cement	1.2	1.2	1.0	0.8	0.8	0.6	0.4	0.4

Table 3: Mixture proportions of concretes made of 30% coarse recycled aggregates.

Mixture	CRA-I-0.40	CRA-II-0.40	CRA-I-0.45	CRA-I-0.50	CRA-II-0.50	CRA-I-0.55	CRA-I-0.60	CRA-II-0.60
Water/cement	0.40	0.40	0.45	0.50	0.50	0.55	0.60	0.60
Water, kg	140	140	153	165	165	176	186	186
Cement 42.5R, kg	350	—	340	330	—	320	310	—
Cement 32.5R, kg	—	350	—	—	330	—	—	310
Quartz sand, kg (% in volume)	732 (40)	732 (40)	723 (40)	715 (40)	715 (40)	708 (40)	702 (40)	702 (40)
Fine gravel, kg (% in volume)	553 (30)	553 (30)	547 (30)	541 (30)	541 (30)	535 (30)	531 (30)	531 (30)
Coarse recycled aggregate, kg (% in volume)	523 (30)	523 (30)	517 (30)	511 (30)	511 (30)	506 (30)	501 (30)	501 (30)
Superplasticizer, % by weight of cement	1.2	1.2	1.0	0.8	0.8	0.6	0.4	0.4

Table 4: Compressive strengths (MPa) after 3 and 28 days.

Curing times	3 days		28 days	
Mixtures	Mean values	Standard deviations	Mean values	Standard deviations
REF-I-0.40	37.0	2.4	58.6	3.4
REF-I-0.45	28.5	1.8	56.1	2.5
REF-I-0.50	28.7	2.6	51.2	3.1
REF-I-0.55	24.7	2.4	47.1	2.6
REF-I-0.60	20.1	2.8	43.9	1.3
REF-II-0.40	32.1	2.2	52.2	1.7
REF-II-0.50	19.8	2.1	43.3	2.0
REF-II-0.60	15.3	1.9	36.1	1.8
CRA-I-0.40	29.7	1.3	46.1	3.2
CRA-I-0.45	26.2	1.7	45.8	2.9
CRA-I-0.50	22.2	2.3	39.9	3.7
CRA-I-0.55	21.7	1.7	36.3	2.7
CRA-I-0.60	15.5	1.8	34.7	1.6
CRA-II-0.40	26.1	1.6	41.8	1.8
CRA-II-0.50	16.4	1.9	35.1	1.8
CRA-II-0.60	12.9	1.7	29.2	1.9

mixtures could be achieved by using recycled aggregates instead of ordinary aggregates.

However, whichever the kind of cement used, RAC strength classes C 25/30 and C 28/35 can be confidently achieved, by keeping the water/cement under 0.60 and 0.50, respectively, with cement type 42.5 R, and under 0.50 and 0.40, respectively, with cement type 32.5 R.

On the other hand, RAC strength class C 32/40 can be achieved only by using cement type 42.5 R, by keeping the water/cement under 0.45.

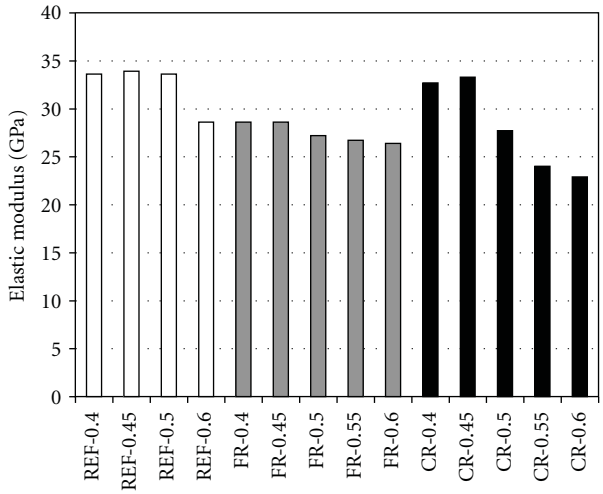

Figure 2: Static elastic modulus after 28 days of wet curing.

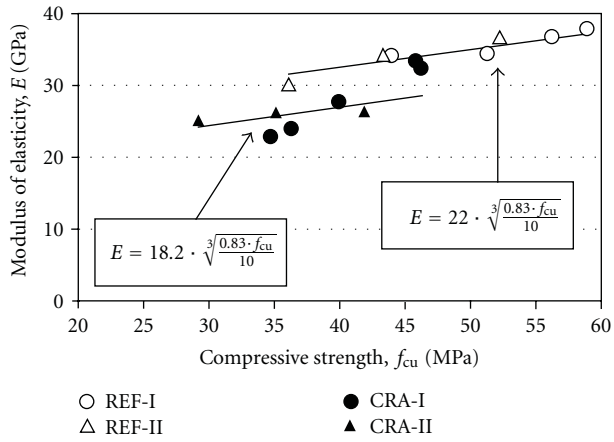

Figure 3: Static elastic modulus versus compressive strength after 28-days of wet curing.

3.2. Static Elastic Modulus Evaluation. Static modulus of elasticity was determined according to the procedure described in the Italian Standards UNI 6556 [22]. The mean values obtained after 28 days are shown in Figure 2 and plotted also in Figure 3 as a function of the concrete compressive strength after 28 days.

In Figure 3 two equations are reported:

$$E = 22.0 \cdot \sqrt[3]{\frac{0.83 \cdot f_{cu}}{10}}, \quad (1)$$

$$E = 18.2 \cdot \sqrt[3]{\frac{0.83 \cdot f_{cu}}{10}}. \quad (2)$$

The first one (1) is the formula proposed by the Italian Standard [11] for regular concrete. Results obtained in this work on ordinary concretes showed to be in good agreement with (1).

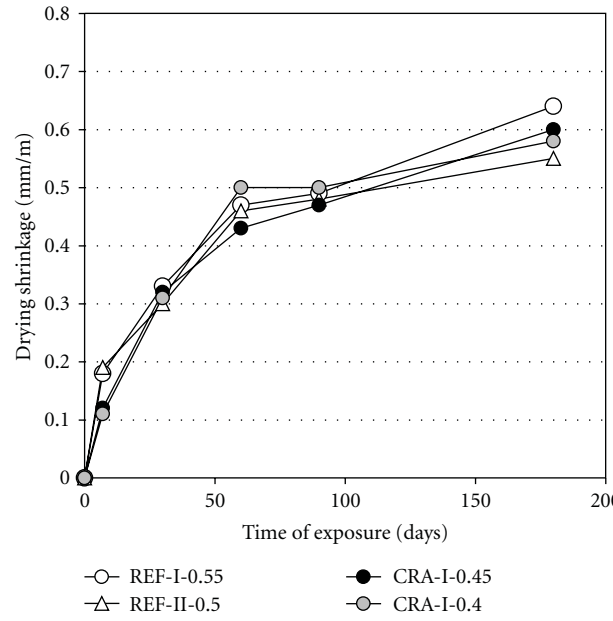

Figure 4: Drying shrinkage versus time of exposure for C 32/40 strength class concretes.

On the other hand, the second formula (2) was obtained by fitting experimental data obtained for the concrete mixtures prepared with 30% coarse recycled concrete aggregate, whichever the type of cement used.

In practice, it means that, for equal compressive strength, 17% lower elastic modulus is achieved by using 30% coarse recycled aggregates. A similar result was obtained by the author in a previous work [10], in which a coefficient of 18.8 instead of 18.2 was found when the fine gravel (6–12 mm), instead of gravel (11–22 mm), was completely replaced by recycled concrete aggregate fraction (6–12 mm), also in that case the percentage of substitution was 30%. This slight difference can signify a certain dependence of the RAC elastic modulus on the grain size of the recycled concrete aggregate used: the higher is the aggregate size the higher is the decrease with respect to the reference mixtures.

However, for practical uses a common coefficient equal to 18.5 can be suggested, independently on the recycled aggregate particle size, corresponding to 16% reduction of elastic modulus with respect to conventional concrete.

3.3. Drying Shrinkage Test. Drying shrinkage was evaluated according to UNI 6555 [21], results obtained up to 180 days of exposure are reported in Table 5.

In Figures 4, 5, and 6, three comparisons of the drying shrinkage strains of equal strength class concretes are shown. The compared mixtures were "REF-I-0.55," "REF-II-0.50," "CRA-I-0.40," and "CRA-II-0.45" for the strength class (see Table 4); "REF-I-0.60," "CRA-I-0.50," and "CRA-II-0.40" for the strength class (see Table 4) and "REF-II-0.60", "CRA-I-0.55" and "CRA-II-0.50" for the strength class (see Table 4). Results obtained on C 32/40, C 28/35, and C 25/30

Table 5: Drying shrinkage measurements (mm/m).

Mixture	Days of exposure to 50% R.H., 20°C temperature				
	7	30	60	90	180
REF-I-0.40	0.09	0.26	0.34	0.4	0.44
REF-I-0.45	0.11	0.3	0.37	0.4	0.48
REF-I-0.50	0.19	0.27	0.43	0.45	0.5
REF-I-0.55	0.18	0.33	0.47	0.49	0.64
REF-I-0.60	0.24	0.34	0.48	0.58	0.7
REF-II-0.40	0.1	0.28	0.38	0.43	0.46
REF-II-0.50	0.19	0.3	0.46	0.48	0.55
REF-II-0.60	0.25	0.37	0.5	0.62	0.68
CRA-I-0.40	0.11	0.31	0.5	0.5	0.58
CRA-I-0.45	0.12	0.32	0.43	0.47	0.6
CRA-I-0.50	0.14	0.38	0.52	0.54	0.58
CRA-I-0.55	0.17	0.28	0.43	0.53	0.63
CRA-I-0.60	0.18	0.4	0.62	0.66	0.68
CRA-II-0.40	0.12	0.32	0.49	0.52	0.59
CRA-II-0.50	0.15	0.4	0.54	0.56	0.61
CRA-II-0.60	0.18	0.42	0.61	0.67	0.69

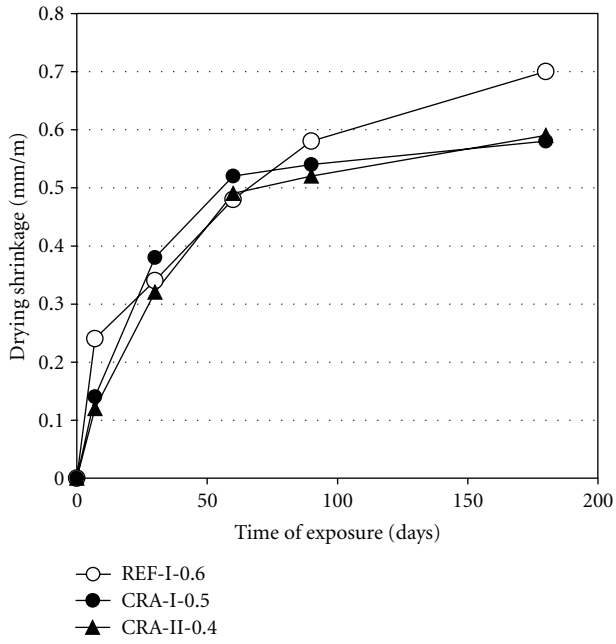

Figure 5: Drying shrinkage versus time of exposure for C 28/35 strength class concretes.

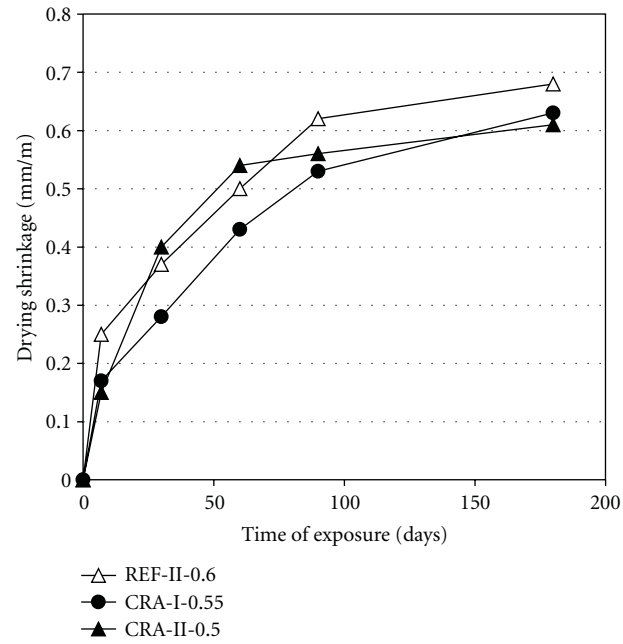

Figure 6: Drying shrinkage versus time of exposure for C 25/30 strength class concretes.

strength class concretes are reported in Figures 4, 5, and 6, respectively.

It can be noticed that, by using 30% coarse recycled aggregate, the values of the measured strains on RACs are similar (Figure 4), if not lower (Figures 5 and 6), to those obtained for the reference mixtures of the same strength class. Indeed, by comparing equal-strength concretes, the different kind of cement used seems to affect the drying shrinkage behavior of concrete more than the kind of aggregate used (see Figure 4), due to the different water-to-cement ratios required to gain the same 28-day compressive strength.

4. Conclusions

Results obtained show that structural concrete up to C32/40 strength class can be manufactured by replacing 30% virgin aggregate with coarse recycled-concrete aggregate.

Moreover, a correlation between elastic modulus and compressive strength of recycled-aggregate concrete was found showing that, in general, 16% lower elastic modulus is achieved by using 30% coarse recycled aggregates, whatever the recycled aggregate grain size distribution.

Finally, on the basis of the results obtained by free drying shrinkage measurements, similar shrinkage behaviours are detected for equal-strength concretes, not depending on the kind of aggregate used. This last aspect, when considered together with a lower elastic modulus, predicts a lower tendency to crack appearance in RACs rather than in conventional concretes.

References

[1] "RILEM recommendation. 121-DRG guidance for demolition and reuse of concrete and masonry. Specifications for concrete with recycled aggregates," *Materials and structures*, vol. 27, pp. 557–559, 1994.

[2] ACI Committee 555, "Removal and reuse of hardened concrete," *ACI Materials Journal*, vol. 99, no. 3, pp. 300–325, 2002.

[3] K. Rahal, "Mechanical properties of concrete with recycled coarse aggregate," *Building and Environment*, vol. 42, no. 1, pp. 407–415, 2007.

[4] M. C. Limbachiya, E. Marrocchino, and A. Koulouris, "Chemical-mineralogical characterisation of coarse recycled concrete aggregate," *Waste Management*, vol. 27, no. 2, pp. 201–208, 2007.

[5] V. W. Y. Tam, K. Wang, and C. M. Tam, "Assessing relationships among properties of demolished concrete, recycled aggregate and recycled aggregate concrete using regression analysis," *Journal of Hazardous Materials*, vol. 152, no. 2, pp. 703–714, 2008.

[6] A. K. Padmini, K. Ramamurthy, and M. S. Mathews, "Influence of parent concrete on the properties of recycled aggregate concrete," *Construction and Building Materials*, vol. 23, no. 2, pp. 829–836, 2009.

[7] S. W. Tabsh and A. S. Abdelfatah, "Influence of recycled concrete aggregates on strength properties of concrete," *Construction and Building Materials*, vol. 23, no. 2, pp. 1163–1167, 2009.

[8] M. L. Berndt, "Properties of sustainable concrete containing fly ash, slag and recycled concrete aggregate," *Construction and Building Materials*, vol. 23, no. 7, pp. 2606–2613, 2009.

[9] M. Chakradhara Rao, S. K. Bhattacharyya, and S. V. Barai, "Influence of field recycled coarse aggregate on properties of concrete," *Materials and Structures*, vol. 44, pp. 205–220, 2011.

[10] V. Corinaldesi, "Mechanical and elastic behaviour of concretes made of recycled-concrete coarse aggregates," *Construction and Building Materials*, vol. 24, no. 9, pp. 1616–1620, 2010.

[11] NTC 2008, "Norme Tecniche per le costruzioni," D.M. 14/01/2008.

[12] EN 197-1, "Cement—part 1: composition, specifications and conformity criteria for common cements," , 2000.

[13] EN 1097-6, "Tests for mechanical and physical properties of aggregates—determination of particle density and water absorption," , 2000.

[14] EN 933-1, "Tests for geometrical properties of aggregates—determination of particle size distribution—sieving method," , 1997.

[15] UNI EN 1744-1, "Tests for chemical properties of aggregates—chemical analysis," , 1999.

[16] UNI 8520-22, "Aggregati per confezione di calcestruzzi—determinazione della potenziale reattività degli aggregati in presenza di alcali (Aggregates for concretes—determination of potential alkali reactivity)," , 2002.

[17] V. Corinaldesi and G. Moriconi, "Recycling of rubble from building demolition for low-shrinkage concretes," *Waste Management*, vol. 30, no. 4, pp. 655–659, 2010.

[18] EN 12350-2, "Testing fresh concrete—slump test," , 1999.

[19] J. Bolomey, "The grading of aggregate and its influence on the characteristics of concrete," *Revue des Matériaux de Construction et Travaux Publiques*, pp. 147–149, 1947.

[20] EN 12390-1, "Testing hardened concrete. Shape, dimensions and other requirements for specimens and moulds," , 2000.

[21] UNI 6555, "Concrete made with aggregate maximum size 30 mm," Hydraulic Shrinkage Determination, 1973.

[22] UNI 6556, "Tests of concretes—determination of static modulus of elasticity in compression," , 1976.

[23] EN 12390-3, "Testing hardened concrete. Part 3: compressive strength of test specimens," , 2003.

Hindawi Publishing Corporation
Advances in Civil Engineering
Volume 2011, Article ID 463638, 13 pages
doi:10.1155/2011/463638

Research Article

Chemical, Mineralogical, and Morphological Properties of Steel Slag

Irem Zeynep Yildirim[1] and Monica Prezzi[2]

[1] *Fugro Consultants, Inc., 6100 Hillcroft Avenue (77081), Houston, TX, 77274, USA*
[2] *School of Civil Engineering, Purdue University, 550 Stadium Mall Drive, West Lafayette, IN, 47907, USA*

Correspondence should be addressed to Irem Zeynep Yildirim, iremzeynep@gmail.com

Received 2 February 2011; Accepted 27 July 2011

Academic Editor: J. Antonio H. Carraro

Steel slag is a byproduct of the steelmaking and steel refining processes. This paper provides an overview of the different types of steel slag that are generated from basic-oxygen-furnace (BOF) steelmaking, electric-arc-furnace (EAF) steelmaking, and ladle-furnace steel refining processes. The mineralogical and morphological properties of BOF and electric-arc-furnace-ladle [EAF(L)] slag samples generated from two steel plants in Indiana were determined through X-Ray Diffraction (XRD) analyses and Scanning Electron Microscopy (SEM) studies. The XRD patterns of both BOF and EAF(L) slag samples were very complex, with several overlapping peaks resulting from the many minerals present in these samples. The XRD analyses indicated the presence of free MgO and CaO in both the BOF and EAF(L) slag samples. SEM micrographs showed that the majority of the sand-size steel slag particles had subangular to angular shapes. Very rough surface textures with distinct crystal structures were observed on the sand-size particles of BOF and EAF(L) slag samples under SEM. The characteristics of the steel slag samples considered in this study are discussed in the context of a detailed review of steel slag properties.

1. Introduction

The steelmaking industries in the US generate 10–15 million tons of steel slag every year. Approximately 15 to 40% of the steel slag output is initially stockpiled in the steel plants and, eventually, sent to slag disposal sites. Utilization of steel slag in civil engineering applications can alleviate the need for their disposal and reduce the use of natural resources. A better understanding of the properties of steel slag is required for large volumes of this material to be utilized in a technically sound manner in civil engineering applications.

Knowledge of the chemical, mineralogical, and morphological properties of steel slags is essential because their cementitious and mechanical properties, which play a key role in their utilization, are closely linked to these properties. As an example, the frictional properties of steel slag are influenced by its morphology and mineralogy. Similarly, the volumetric stability of steel slag is a function of its chemistry and mineralogy. The chemical, mineralogical, and morphological characteristics of steel slag are determined by the processes that generate this material. Therefore, knowledge of the different types of steelmaking and refining operations that produce steel slag as a byproduct is also required. This paper provides an overview of steel slag generation and a literature review on the chemical and mineralogical properties of steel slags. Moreover, the mineralogical and morphological characteristics of steel slag samples generated from two steel plants in Indiana were evaluated through XRD analyses and SEM studies.

2. Overview

Slags are named based on the furnaces from which they are generated. Figure 1 shows a flow chart for the iron and steelmaking processes and the types of slag generated from each process [1, 2].

The main types of slags that are generated from the iron and steelmaking industries are classified as follow:

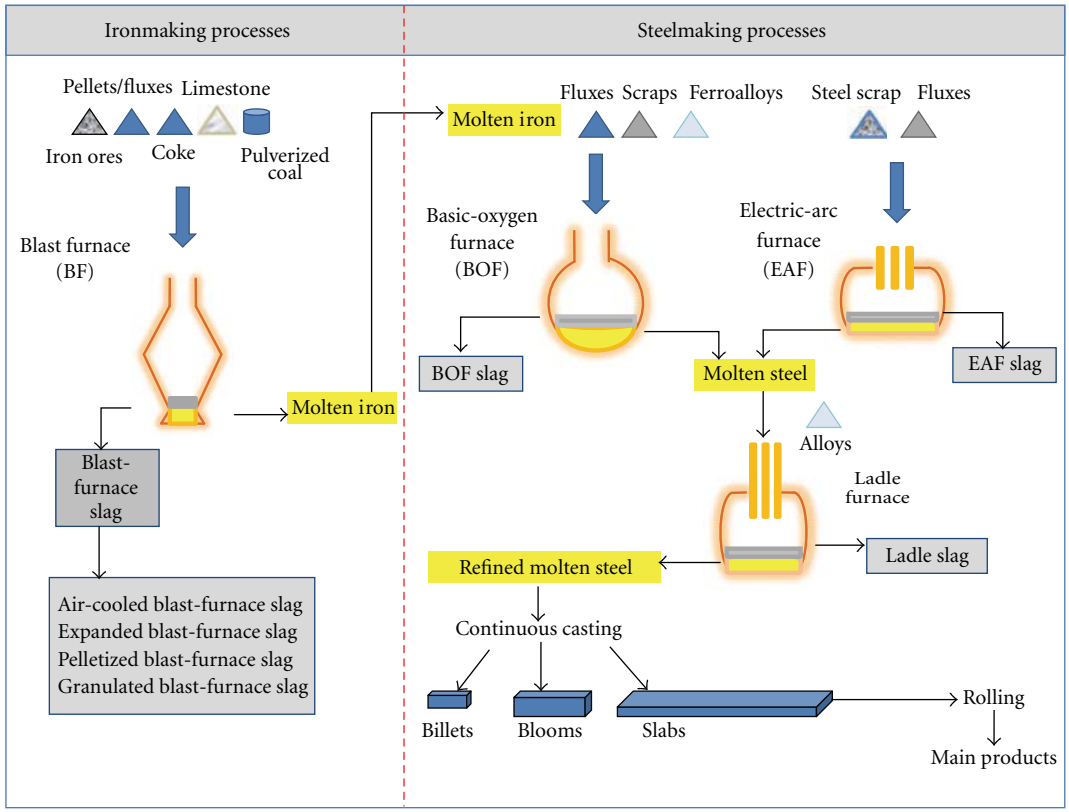

Figure 1: Flowchart of iron and steelmaking processes [1, 2].

(i) blast-furnace slag (ironmaking slag),

(ii) steel-furnace slag,

(a) basic-oxygen-furnace (BOF) slag,

(b) electric-arc-furnace (EAF) slag,

(c) ladle slag.

2.1. Basic-Oxygen-Furnace Process of Steelmaking and Slag Generation. Basic-oxygen furnaces, which are located at integrated steel mills in association with a blast furnace, are charged with the molten iron produced in the blast furnace and steel scraps. Typically, the proper basic-oxygen furnace charge consists of approximately 10–20% of steel scrap and 80–90% of molten iron [1, 3]. The presence of steel scraps in the basic-oxygen furnace charge plays an important role in cooling down the furnace and maintaining the temperature at approximately 1600°C–1650°C for the required chemical reactions to take place.

Figure 2 shows a schematic representation of a basic-oxygen furnace [1, 4]. First, steel scrap is charged to the furnace and, immediately after this charge, a ladle of molten iron (~200 tons) is poured on top of it with the help of a crane. Then an oxygen lance, lowered into the furnace, blows 99% pure oxygen on the charge at supersonic speeds. During the blowing cycle, which lasts approximately 20–25 minutes, intense oxidation reactions remove the impurities of the charge. Carbon dissolved in the steel is burned to form carbon monoxide, causing the temperature to rise to 1600–1700°C (the temperature in the furnace is carefully monitored throughout the oxygen blowing period). The scrap is thereby melted, and the carbon content of the molten iron

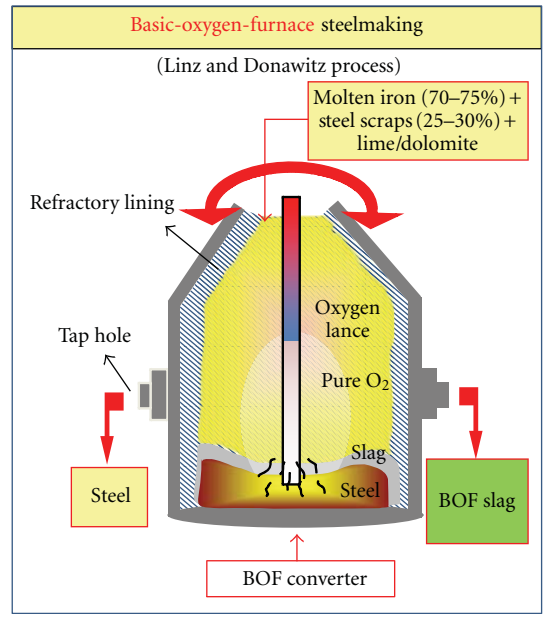

Figure 2: Schematic representation of the basic-oxygen furnace process [1, 4].

is lowered [1, 3]. In order to remove the unwanted chemical elements of the melt, the furnace is also charged with fluxing agents, such as lime (CaO) or dolomite ($MgCa(CO_3)_2$), during the oxygen blowing cycles. The impurities combine with the burnt lime or dolomite forming slag and reducing the amount of undesirable substances in the melt. Samples of the molten metal are collected near the end of the blowing cycle and tested for their chemical composition. Once the desired chemical composition is achieved, the oxygen lance is pulled up from the furnace.

Slag resulting from the steelmaking process floats on top of the molten steel. The basic-oxygen furnace is tilted in one direction in order to tap the steel into ladles. The steel produced in the basic-oxygen furnace can either undergo further refining in a secondary refining unit or be sent directly to a continuous caster where semifinished shapes (blooms, billets, or slabs) are solidified in integrated steel mills. After all the steel is removed from the basic-oxygen furnace, it is tilted again in the opposite direction to pour the liquid slag into ladles. The slag generated from a steelmaking cycle is later processed, and the final product after processing is referred to as *basic-oxygen-furnace slag* (BOF slag). The chemical reactions occurring during the removal of impurities determine the chemical composition of the basic-oxygen-furnace slag [1, 3, 5].

2.2. Electric-Arc-Furnace (EAF) Process of Steelmaking and Slag Generation. Electric-arc furnaces (mini mills) use high-power electric arcs, instead of gaseous fuels, to produce the heat necessary to melt recycled steel scrap and to convert it into high quality steel. The electric-arc furnace steelmaking process is not dependent on the production from a blast furnace since the main feed for it is steel scrap with some pig iron. Electric-arc furnaces are equipped with graphite electrodes and resemble giant kettles with a spout or an eccentric notch on one side. The roof of the electric-arc furnaces can pivot and swing to facilitate the loading of raw materials. Steel scraps, either as heavy melt (large slabs and beams) or in shredded form are separated, graded, and sorted into different classes of steel in scrap yards. Scrap baskets are loaded carefully with different types of scrap according to their size and density to ensure that both the melting conditions in the furnace and the chemistry of the finished steel are within the targeted range [1–3].

The electric-arc furnace steelmaking process starts with the charging of various types of steel scrap to the furnace using steel scrap baskets. Next, graphite electrodes are lowered into the furnace. Then, an arc is struck, which causes electricity to travel through the electrodes and the metal itself. The electric arc and the resistance of the metal to this flow of electricity generate the heat. As the scrap melts, the electrodes are driven deeper through the layers of scrap. In some steel plants, during this process, oxygen is also injected through a lance to cut the scrap into smaller sizes. As the melting process progresses, a pool of liquid steel is generated at the bottom of the furnace. CaO, in the form of burnt lime or dolomite, is either introduced to the furnace together with the scrap or is blown into the furnace during melting. After several baskets of scraps have melted, the refining metallurgical operations (e.g., decarburization and dephosphorization) are performed. During the steel refining period, oxygen is injected into the molten steel through an oxygen lance. Some iron, together with other impurities in the hot metal, including aluminum, silicon, manganese, phosphorus, and carbon, are oxidized during the oxygen injections. These oxidized components combine with lime (CaO) to form slag. As the steel is refined, carbon powder is also injected through the slag phase floating on the surface of the molten steel, leading to the formation of carbon monoxide. The carbon monoxide gas formed causes the slag to foam, thereby increasing the efficiency of the thermal energy transfer. Once the desired chemical composition of the steel is achieved, the electric-arc furnace is tilted, and the slag and steel are tapped out of the furnace into separate ladles. Steel is poured into a ladle and transferred to a secondary steelmaking station for further refining. The molten slag is carried to a slag-processing unit with ladles or slag pot carriers [1–3, 5].

In electric-arc furnaces, up to 300 tons of steel can be manufactured per cycle (a cycle takes one to three hours to complete). Initially, the EAF steelmaking process was more expensive than the BOF process and, hence, it was only used for production of high quality steels. However, as the size of the electric-arc furnaces increased over the years, the EAF steelmaking process has become competitive in the production of different grades of steel and has started to dominate the US steel industry with a 55% share of the total steel output in 2006, according to USGS [6].

2.3. Ladle Furnace Refining and Slag Generation. After completion of the primary steelmaking operations, steel produced by the BOF or EAF processes can be further refined to obtain the desired chemical composition. These refining processes are called secondary steelmaking operations. Refining processes are common in the production of high-grade steels. The most important functions of secondary refining processes are final desulfurization, degassing of oxygen, nitrogen, and hydrogen, removal of impurities, and final decarburization (done for ultralow carbon steels). Depending on the quality of the desired steel, molten steel produced in the EAF and BOF process goes through some or all of the above mentioned refining processes [1, 2]. Most of the mini mills and integrated steel mills have ladle-furnace refining stations for secondary metallurgical processes. Figure 3 shows a schematic representation of an electric-arc-furnace and a ladle-refining unit associated with it [2, 4].

Ladle furnaces, which look like smaller versions of EAF furnaces, also have three graphite electrodes connected to an arc transformer used to heat the steel. Typically, the bottom of the ladle furnace has a pipeline through which argon gas is injected for stirring and homogenization of the liquid steel in the furnace. By injecting desulfurizing agents (such as Ca, Mg, CaSi, CaC_2) through a lance, the sulfur concentration in the steel can be lowered to 0.0002% [1]. The addition of silicon and aluminum during deoxidation forms silica (SiO_2) and alumina (Al_2O_3); these oxides are later absorbed by the slag generated by the refining process. In addition,

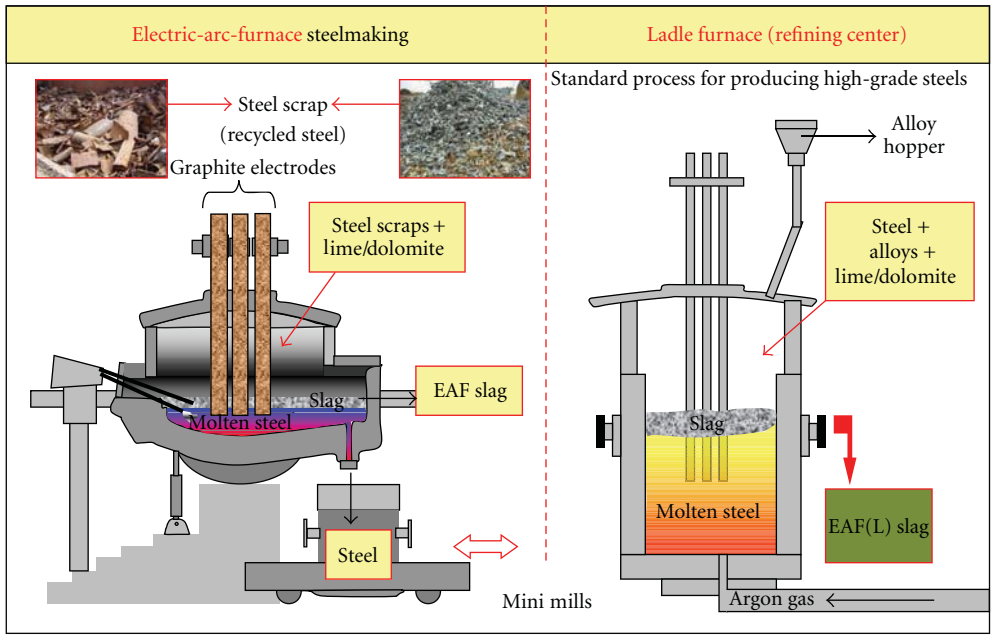

Figure 3: Schematic representation of the electric-arc-furnace steelmaking and ladle refining process [2, 4].

in order to adjust precisely the chemical composition of the steel to produce different grades of steel, the desired alloys are added to the molten steel through an alloy hopper that is connected to the ladle furnace. Ladle furnaces also function as a storage unit for the steel before the initiation of casting operations. Therefore, ladle furnaces reduce the cost of high-grade steel production and allow flexibility in the steelmaking operations [1, 2].

3. Chemical Composition of Steel Slags

Both BOF and EAF slags are formed during basic steelmaking operations, as explained above. Therefore, in general, the chemical and mineralogical compositions of BOF and EAF slags are similar. Calcium oxide and iron oxide are the two major chemical constituents of both EAF and BOF slags. Ladle slag is generated during the steel refining processes in which several alloys are added to the ladle furnace to produce different grades of steel. For this reason, the chemical constituents of ladle slag differ from those of BOF and EAF slags. Table 1 provides the chemical composition of basic-oxygen-furnace (BOF), electric-arc-furnace (EAF), and ladle slags from various sources [7–22].

The main chemical constituents of the basic-oxygen-furnace slag are CaO, FeO, and SiO_2. During the conversion of molten iron into steel, a percentage of the iron (Fe) in the hot metal cannot be recovered into the steel produced. This oxidized iron is observed in the chemical composition of the BOF slag. Depending on the efficiency of the furnace, the iron oxide (FeO/Fe_2O_3) content of BOF slag can be as high as 38% (refer to Table 1); this is the amount of oxidized iron that cannot be recovered during the conversion of molten iron into steel. The silica (SiO_2) content of BOF slag ranges from 7 to 18%. The Al_2O_3 and MgO contents are in the 0.5–4% and 0.4–14% ranges, respectively. The free lime content can be as high as 12%. Large quantities of lime or dolomotic lime are used during the process of conversion from iron to steel and, hence, the CaO content of BOF slag is typically very high (CaO >35%) [1, 8, 12, 23].

EAF slag has a chemical composition similar to that of BOF slag (refer to Table 1). The EAF steelmaking process is essentially a steel scrap recycling process. Therefore, the chemical composition of EAF slag depends significantly on the properties of the recycled steel. Compared to BOF slags, the main chemical constituents of EAF slags can vary widely. Typically, the FeO, CaO, SiO_2, Al_2O_3, and MgO contents of EAF slags are in the 10–40%, 22–60%, 6–34%, 3–14%, and 3–13% ranges, respectively. Other minor components include other oxidized impurities, such as MgO, MnO, and SO_3. EAF slags also contain free CaO and MgO along with other complex minerals and solid solutions of CaO, FeO, and MgO. The FeO content of EAF slags generated from stainless steel production processes can be as low as 2% [24].

Information on the chemical composition of ladle slags (LS) is limited in the literature. During the steel refining process, different alloys are fed into the ladle furnace in order to obtain the desired steel grade. Hence, the chemical composition of ladle slag is highly dependent on the grade of steel produced. As a result, compared to BOF and EAF slags, the chemical composition of ladle slag is highly variable. Typically, the FeO content of ladle slag is much lower (<10%) than that of EAF and BOF slags. On the other hand, the Al_2O_3 and CaO contents are typically higher for ladle slags (refer to Table 1).

Table 1: Chemical composition of BOF, EAF, and Ladle Slags.

		Oxide composition (%)											
Reference	Slag type	CaO	SiO_2	Al_2O_3	MgO	FeO	Fe_2O_3	Fe_{total}	SO_3	MnO	TiO_2	P_2O_5	Free CaO
Das et al. [7]	BOF	47.9	12.2	1.2	0.8	26.3	—	—	0.3	0.3	—	3.3	—
Juckes [8][a]	BOF	36.4–45.8	10.7–15.2	1–3.4	4.1–7.8	—	—	19–24	0.1–0.2	2.7–4.3	—	1–1.5	2.5–12
Mahieux et al. [9]	BOF	47.5	11.8	2.0	6.3	—	22.6	—	—	1.9	0.5	2.7	—
Poh et al. [10]	BOF	52.2	10.8	1.3	5.04	17.2	10.1	—	—	2.5	0.6	1.3	10.2
Shen et al. [11]	BOF	39.3	7.8	0.98	8.56	—	38.06	—	0.0	4.2	0.9	—	—
Shi [12]	BOF	30–55	8–20	1–6	5–15	10–35	—	—	0.1–0.2	2–8	0.4–2	0.2–2	—
Tossavainen et al. [13]	BOF	45.0	11.1	1.9	9.6	10.7	10.9	—	—	3.1	—	—	—
Waligora et al. [14]	BOF	47.7	13.3	3.0	6.4	—	24.4			2.6	0.7	1.5	9.2
Xuequan et al. [15][b]	BOF	45–60	10–15	1–5	3–13	7–20	3–9	—	—	—	—	1–4	—
Barra et al. [16]	EAF	29.5	16.1	7.6	5.0	—	32.56	—	0.6	4.5	0.78	0.6	—
Luxán et al. [17]	EAF	24.4	15.4	12.2	2.9	34.4	—	—	—	5.6	0.56	1.2	—
Manso et al. [18]	EAF	23.9	15.3	7.4	5.1	—	—	42.5	0.1	4.5	—	—	0.5
Shi [12]	EAF	35–60	9–20	2–9	5–15	15–30	—	—	0.1–0.2	3–8	—	0.0–0.3	—
Tossavainen et al. [13]	EAF	38.8	14.1	6.7	3.9	5.6	20.3	—	—	5	—	—	—
Tsakiridis et al. [19]	EAF	35.7	17.5	6.3	6.5	—	26.4	—	—	2.5	0.8	—	—
Nicolae et al. [20]	Ladle	49.6	14.7	25.6	7.9	0.44	0.22	0.17	0.8	0.4	—	0.2	—
Shi [12]	Ladle	30–60	2–35	5–35	1–10	0–15	—	—	0.1–1	0–5.0	—	0.1–0.4	—
Qian et al. [21]	Ladle	49.5	19.59	12.3	7.4	—	0.9	—	—	1.4	—	0.4	2.5
Setién et al. [22]	Ladle	50.5–57.5	12.6–19.8	4.3–18.6	7.5–11.9	—	1.6–3.3	—		0.4–0.5	0.3–0.9	0–0.01	3.5–19
Tossavainen et al. [13]	Ladle	42.5	14.2	22.9	12.6	0.5	1.1	0.4	—	0.2	—	—	—

[a] The range of values are compiled based on the chemical composition data from 4 different sources in Great Britain provided by Juckes [8].
[b] Xuequan et al. [15] report chemical composition of steel slag from refining process (not specified as BOF).
— = data not available.

4. Mineralogical Properties of Steel Slag

Crystal formation is a function of both the chemical composition of the melt and its cooling rate. Silica rich blast-furnace slag vitrifies (forms a glassy phase) easily when it is rapidly cooled. Steel slag has a lower silica content than blast-furnace slag and, hence, steel slag seldom vitrifies even when rapidly cooled. Tossavainen et al. [13] studied the effect of the cooling rate on the mineralogy of BOF, EAF, and ladle slag samples with different proportions of major chemical constituents and showed that ladle slag rapidly cooled using the water granulation technique becomes almost completely amorphous, with the exception of the crystalline phase of periclase (MgO). On the other hand, the rapidly cooled (granulated) BOF and EAF slag samples showed very complex crystalline structures similar to those of slowly cooled BOF and EAF slag samples. Reddy et al. [25] also identified a very crystalline structure in quenched BOF slag using XRD analysis. These studies indicate that even when rapidly cooled, in general, steel slag tends to crystallize due to its chemical composition.

Several researchers studied the mineralogical composition of steel slags. X-ray diffraction analysis of steel slag samples shows a complex structure with many overlapping peaks reflecting the crystalline phases present in steel slag. These crystalline phases appear to be mainly due to the chemical composition of steel slag and the slow cooling rate applied during processing [1, 26–28]. The feed (charge) into the furnaces vary from one steelmaking plant to another, so variations in the chemical constituents of steel slags produced at different steelmaking plants are expected. A variety of mineral phases were identified and reported in the literature for EAF, BOF, and ladle slags. Table 2 presents the minerals identified in steel slags, as reported in the literature [8, 13, 16, 17, 20, 21, 25, 28–30].

The common mineral phases present in steel slags include merwinite ($3CaO{\cdot}MgO{\cdot}2SiO_2$), olivine ($2MgO{\cdot}2FeO{\cdot}SiO_2$), β-C_2S ($2CaO{\cdot}SiO_2$), α-C_2S, C_4AF ($4CaO{\cdot}Al_2O_3{\cdot}FeO_3$), C_2F ($2CaO{\cdot}Fe_2O_3$), CaO (free lime), MgO, FeO and C_3S ($3CaO{\cdot}SiO_2$), and the RO phase (a solid solution of CaO-FeO-MnO-MgO) [21, 24, 31], as can be seen in Table 2. Since BOF and EAF slags both have high iron oxide contents, solid solutions of FeO (wustite) are typically observed as one of the main mineral phases. Ladle slag has a lower FeO content, and polymorphs of C_2S are therefore frequently observed as the main phase [19, 24, 27, 29].

Due to the presence of unstable phases in its mineralogy, steel slags can show volumetric instability, caused mainly by the presence of free CaO. In the presence of water, free lime hydrates and forms portlandite ($Ca(OH)_2$). Portlandite has a lower density than CaO and, hence, hydration of free CaO results in volume increase. Ramachandran et al. [32] studied the hydration mechanism of CaO and proved that when it is immersed in water, compacted CaO can hydrate almost completely in a few days with a volume increase as high as 100%. Their study also demonstrated that hydration of lime by exposure to water vapor causes more expansion than hydration caused by exposure to water due to the effect of temperature. The fact that limes hydrates quickly suggests that the majority of the free lime in steel slag will hydrate in a few days if it is given access to water. However, residual lime can be embedded in small pockets in gravel-size steel slag particles. Figure 4 depicts a gravel-size BOF slag particle with a lime pocket (seen in white). Lime pockets may not hydrate at all if they are not given access to water through the fractures extending to them. If there are fractures in the slag particles extending to these lime pockets, then hydration can progress [8, 12, 33].

Figure 4: Gravel-size steel slag particle with a lime pocket (photograph taken at Mittal Steel, Indiana Harbor West Plant).

Other expansive compounds, such as free MgO, may also be present in steel slag. Unlike CaO, free MgO hydrates at a much slower rate, causing significant volume changes for months or even years. In general, slags generated from modern steelmaking technologies have low MgO content. However, if dolomite ($CaMg(CO_3)_2$) is used as a fluxing agent instead of lime, the free MgO content in steel slag increases and, therefore, the possibility of volumetric expansion due to hydration of MgO increases as well [8, 34–37].

Another reaction that causes volumetric expansion involves the dicalcium silicate (C_2S) phase. The C_2S phase is commonly present in all types of steel slags and, in particular, is abundant typically as the main phase in ladle slags. C_2S exists in four well-defined polymorphs: α, α', β, and γ. α-C_2S is stable at high temperatures (>630°C). At temperatures below 500°C, β-C_2S starts transforming into γ-C_2S. This transformation produces volumetric expansion of up to 10%. If the steel slag cooling process is slow, crystals break, resulting in a significant amount of dust. This phase conversion and the associated dusting are typical for ladle slags. For this reason, ladle slags are commonly called "self-dusting" or "falling" slags [8, 27].

5. Characterization of Steel Slag from Indiana Steel Plants

5.1. Materials. The chemical composition, mineralogy, and morphology of steel slag particles can influence both the cementitious characteristics and mechanical properties of steel slag. Two different types of steel slag (BOF and EAF ladle slags) generated from Indiana steel plants were considered in this study.

Table 2: Mineralogical phases of BOF, EAF, and ladle slags.

Reference	Slag	Mineralogical phases
Barra et al. [16]	EAF	$CaCO_3$, FeO, MgO, Fe_2O_3, $Ca_2Al(AlSiO_7)$, Ca_2SiO_4
Geiseler [29]	—	$2CaO\cdot SiO_2$, $3CaO\cdot SiO_2$, $2CaO\cdot Fe_2O_3$, FeO, (Ca, Fe)O (calciowustite), (Mg, Fe)O (magnesiowustite), free MgO, CaO
Juckes [8]	BOF	C_3S, C_2S, C_2F, RO phase (FeO-MgO-CaO-FeO), MgO, CaO
Luxán et al. [17]	EAF	Ca_2SiO_5, $Ca_2Al(AlSiO_7)$, Fe_2O_3, $Ca_{14}Mg_2(SiO_4)_8$, $MgFe_2O_4$, Mn_3O_4, MnO_2
Manso et al. [28]	Ladle	Al_2O_4Mg, $Ca(OH)_2$, Si_2O_6CaMg, MgO, Ca_3SiO_5, β-Ca_2SiO_4, γ-Ca_2SiO_4, SO_4Ca
Nicolae et al. [20]	BOF	$2CaO\cdot Al_2O_3\cdot SiO_2$, Fe_2O_3, CaO, FeO
Nicolae et al. [20]	EAF	MnO_2, MnO, Fe_2SiO_4, Fe_7SiO_{10}
Nicolae et al. [20]	Ladle	$CaO\cdot SiO_2$, $CaOAl_2O_3\cdot 2SiO_2$, CaS, Al_2O_3
Qian et al. [21]	EAF	γ-Ca_2SiO_4, C_3MS_2, CFMS, FeO-MnO-MgO solid solution
Qian et al. [21]	Ladle	γ-Ca_2SiO_4, C_3MS_2, MgO
Reddy et al. [25]	BOF	$2CaO\cdot Fe_2O_3$, $2CaO\cdot P_2O_5$, $2CaO\cdot SiO_2$, CaO
Reddy et al. [25]	BOF[q]	$2CaO\cdot Fe_2O_3$, $3CaO\cdot SiO_2$, $2CaO\cdot SiO_2$, Fe_2O_3
Tossavainen et al. [13]	Ladle	$Ca_{12}Al_{14}O_{33}$, $MgO\cdot\beta$-Ca_2SiO_4, γ-Ca_2SiO_4, $Ca_2Al_2SiO_7$
Tossavainen et al. [13]	BOF	β-Ca_2SiO_4, FeO-MnO-MgO solid solution, MgO
Tossavainen et al. [13]	EAF	$Ca_3Mg(SiO_4)_2$, β-Ca_2SiO_4, Spinel solid solution (Mg, Mn)(Cr, Al)$_2O_4$, wustite-type solid solution ((Fe, Mg, Mn)O), $Ca_2(Al, Fe)_2O_5$
Tsakiridis et al. [19]	EAF	Ca_2SiO_4, $4CaO\cdot Al_2O_3\cdot Fe_2O_3$, $Ca_2Al(AlSiO_7)$, Ca_3SiO_5, $2CaO\cdot Al_2O_3\cdot SiO_2$, FeO, Fe_3O_4, MgO, SiO_2
Wachsmuth et al. [30]	BOF	Ca_2SiO_4, Ca_3SiO_5, FeO, $2CaO\cdot Fe_2O_3$

[q] quenched; — = type of slag not provided.

Mittal Steel, Indiana Harbor Works West Plant, which is located in Highland, Indiana, was the source plant for the BOF slag. Multiserv Ltd., Harsco Corporation, which performs slag processing operations at the Mittal Steel Plant, supplied representative samples of BOF slag consisting of particles smaller than 15 mm. The Whitesville Steel Mill at Nucor Steel, which is located in Crawfordsville, Indiana, was the source for the EAF ladle (L) slag. The Edward C. Levy Co., which operates at the Whitesville Steel Mill, supplied The EAF(L) slag. This slag is referred to as EAF(L) slag, as it is the ladle slag generated from the refining of the steel from the electric-arc furnace. Edward C. Levy Co. provided representative samples of EAF(L) slag consisting of particles smaller than 9.5 mm.

5.2. Testing Methods. The oxide composition of both the BOF slag and EAF(L) samples was determined by the slag processing companies (Multiserv and Edward C. Levy Co.) using X-ray fluorescence (XRF) analysis. In order to determine the mineralogical phases present in the steel slag samples, X-ray diffraction analyses were carried out on both BOF slag and on EAF(L) slag samples with a Siemens D-500 diffractometer using copper radiation. Representative oven-dried steel slag samples (with both gravel-size and finer particles) were crushed until a powder passing the No. 200 (0.075 mm opening) sieve was attained. The powder samples were step-scanned from 5 to 65° (2θ) in 0.02° increments and 1 s count time. The X-ray diffraction patterns of the steel slag samples were analyzed by comparing the peaks present in the XRD patterns with those provided in The Joint Committee for Powder Diffraction Standards, Hanawalt System for identification of inorganic compounds (JCPDS). The software program Jade was also used to help identify the minerals present in the samples. Only qualitative analyses were performed due to the presence of overlapping peaks in the XRD patterns and to the complexity of the crystalline phases in the slag samples tested. The main, minor, and probable phases were determined for each slag sample tested.

Table 3: Chemical composition of BOF slag.

Oxides	% (by weight)
CaO	39.40
FeO	30.23
SiO_2	11.97
MgO	9.69
MnO	2.74
Al_2O_3	2.16
P_2O_5	1.00
TiO_2	0.40
Na_2O	0.25
Cr_2O_3	0.20
K_2O	0.05
Cl	0.01
SO_3	0.12
L.O.I.[a]	1.80

[a] L.O.I: Loss on ignition.

Table 4: Mineralogical phases identified in BOF slag based on XRD analyses.

Mineral type	Formula	BOF slag
Portlandite	$Ca(OH)_2$	major
Srebrodol'skite	$Ca_2Fe_2O_5$	major
Merwinite	$Ca_3Mg(SiO_4)_2$	major
Larnite	Ca_2SiO_4	minor
Calcite (manganoan)	$(Ca, Mn)CO_3$	minor
Lime	CaO	minor
Dolomite	$CaMg(CO_3)_2$	minor
Wollastonite	$CaSiO_3$	probable
Periclase	MgO	probable
Pentahydrite	$MgSO_4 \cdot 5H_2O$	probable
Monticellite	$CaMgSiO_4$	probable
Hematite	Fe_2O_3	probable
Magnesite	$MgCO_3$	probable

Table 5: Chemical composition of EAF(L) slag.

Oxides	% (by weight)
CaO	47.52
Al_2O_3	22.59
FeO	7.61
MgO	7.35
SiO_2	4.64
SO_3	2.28
MnO	1.00
Cr_2O_3	0.37
TiO_2	0.33
P_2O_5	0.09
Na_2O	0.06
K_2O	0.02
Zn	0.01
L.O.I[a]	6.20

[a] L.O.I: Loss on ignition.

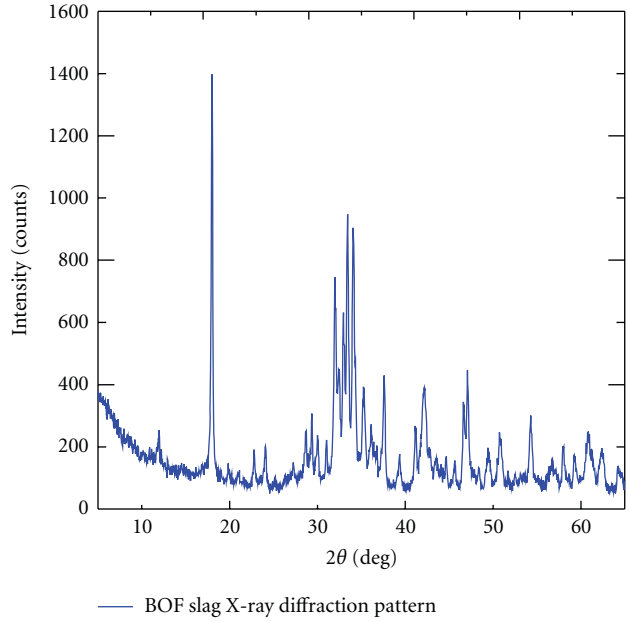

Figure 5: X-ray diffraction pattern for BOF slag.

Figure 6: Gravel-size BOF slag particles.

Steel slag particles were subjected to microscopic examination to characterize their shape, angularity, and surface texture. The examination was performed with a scanning electron microscope (manufactured by ASPEX, Model Personal SEM) and a light microscope (manufactured by Nikon). The shape and surface texture of the gravel-size particles were visible to the naked eye. The medium sand-size particles were examined under the light microscope. Finer sand and silt-size particles were examined under the SEM. To prevent charging of the steel slag particles, they were coated with palladium with the Hummer 6.2 sputtering system. The coated steel slag particles were examined on a two-sided copper tape. The SEM images were captured on both photomicrographs and digital files.

6. Chemical Composition and Particle Mineralogy of BOF Slag

Table 3 gives the oxide composition of the BOF slag samples. The percentages of most of the oxides present in the BOF slag samples tested in this study are within the ranges reported by other researchers [8, 10, 13, 38, 39]. However, the FeO content of the tested BOF slag samples is slightly higher than that of most of the BOF slags reported in the literature.

The XRD patterns of the BOF slag samples were very complex, with several overlapping peaks resulting from the many minerals present in the samples (see Figure 5). BOF slag is cooled slowly in slag pits thereby allowing enough time for formation of well-defined crystals. Several other researchers have reported similar, complex XRD patterns for BOF slag [13, 20, 25].

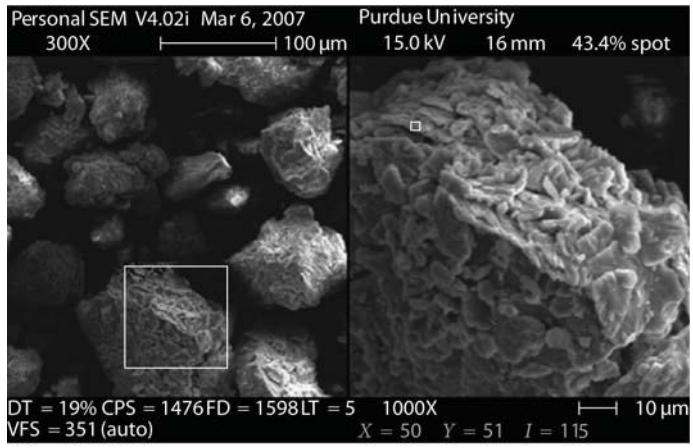

(a)

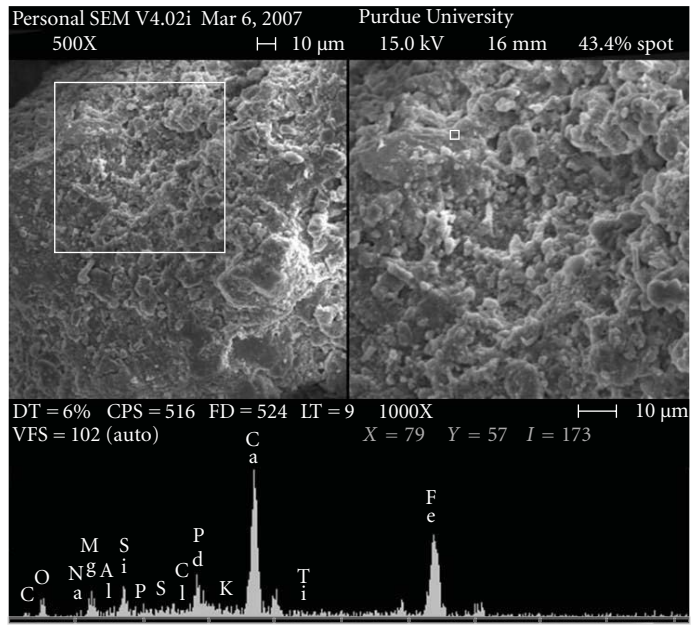

(b)

Figure 7: SEM micrographs of BOF slag sample. (a) Particle shape and (b) surface texture and elemental analysis.

Table 4 summarizes all of the mineral phases that were identified in the BOF slag samples. The mineral phases identified in the BOF slag samples were determined as major or minor phases depending on the intensity of the peaks, which is an indication of the quantity of the minerals present in the samples. It is important to note that the very complex mineralogical composition of BOF slag, with many overlapping peaks and different solid solutions of oxides (FeO and MgO), makes the identification of the phases very difficult. Therefore, some of the overlapping mineral phases that could not be determined with certainty were identified as probable. The most abundant mineral phase present in BOF slag is portlandite ($Ca(OH)_2$). The presence of this mineral is expected since BOF slag contains 39% lime (CaO), which in the presence of moisture, converts to $Ca(OH)_2$. The other major phases included merwinite ($Ca_3Mg(SiO_4)_2$), and srebrodol'skite ($Ca_2Fe_2O_5$). The presence of free lime (CaO) and the probable presence of free magnesia (MgO) in the samples are an indication of the potential for volumetric instability of the tested BOF slag.

7. BOF Slag Particle Morphology

Figure 6 shows the gravel-size particles of BOF slag. The gravel-size particles of BOF slag had shapes varying from subrounded to subangular. Distinct asperities and edges were visible in subangular, bulky particles. Most of the gravel-size particles had a high sphericity and a solid structure. A heterogeneous porous structure was also observed on the surface of a few particles.

Figures 7(a) and 7(b) are SEM micrographs showing the shape and surface texture of BOF slag particles, respectively. The SEM studies showed that the sand- and silt-size BOF slag

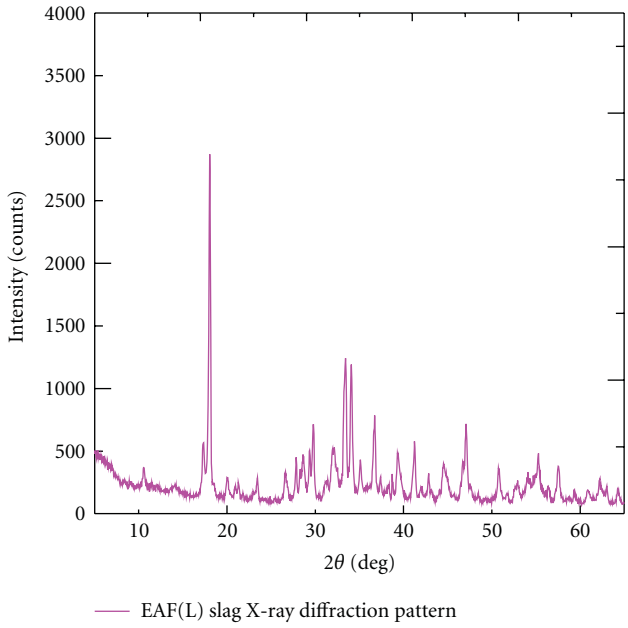

Figure 8: X-ray diffraction patterns for EAF(L) slag.

Figure 9: Gravel-size EAF(L) slag particles.

Table 6: Mineralogical phases identified in EAF(L) slag based on XRD analyses.

Mineral type	Formula	EAF(L) slag
Portlandite	$Ca(OH)_2$	major
Mayenite	$Ca_{12}Al_{14}O_{33}$	major
Larnite	Ca_2SiO_4	minor
Lime	CaO	minor
Uvavorite	$Ca_3 \cdot Cr_2(SiO_4)_3$	minor
Wollastonite[f]	$(Ca, Fe)SiO_3$	minor
Periclase	MgO	minor
Calcite	$CaCO_3$	probable
Merwinite	$Ca_3Mg(SiO_4)_2$	probable

[f] ferroan.

particles had subrounded to angular shapes. Distinct asperities and edges were visible in angular, bulky particles. Most of the sand- and silt-size particles examined under the SEM had rough surface textures.

8. Chemical Composition and Particle Mineralogy of EAF(L) Slag

Table 5 shows the oxide composition of the tested EAF(L) slag sample.

Shi [12] reported that the CaO, SiO_2, Al_2O_3, MgO, and FeO contents of ladle slag are in the ranges of 30–60%, 2–35%, 5–35%, 1–10%, and 0.1–15%, respectively. The SiO_2 content of the EAF(L) slag used in this study was slightly higher than the lower limit of the range reported by Shi [12]. The EAF(L) slag used in this research is cooled very slowly in the pits under ambient atmospheric conditions. These slow cooling conditions allow the formation of various crystalline phases; these are reflected in the very complex XRD patterns shown in Figure 8. Mineral phases with distinct peaks of high intensities and some overlapping peaks of low intensities were detected. Several other researchers have reported similar XRD patterns for EAF(L) slag [13, 20, 28].

Table 6 summarizes all the mineral phases that were identified in the EAF(L) slag samples. As done for BOF slag, the mineral phases identified in the EAF(L) slag samples were determined as major or minor depending on the intensity of the peaks. Some of the overlapping mineral phases that could not be determined with certainty were identified as probable. The two major mineral phases present in the EAF(L) slag samples were portlandite ($Ca(OH_2)$) and mayenite ($Ca_{12}Al_{14}O_{33}$). The highest peak in the XRD pattern of the EAF(L) slag samples was observed for portlandite (see Table 5). Other minor phases identified were lime (CaO), larnite (Ca_2SiO_4), uvavorite ($Ca_3 \cdot Cr_2(SiO_4)_3$), wollastonite $(Ca, Fe)SiO_3$), and periclase (MgO).

9. EAF(L) Slag Particle Morphology

Figure 9 shows the gravel-size particles of EAF(L) slag. The gravel-size particles of the EAF(L) slag sample had shapes varying from subrounded to subangular. Both bulky and platy gravel-size particles were observed. Distinct asperities and edges were also visible in subangular, bulky particles. Most of the platy particles had irregular shapes with very low sphericity and sharp edges. Figures 10(a) and 10(b) show the EAF(L) slag sand- and silt-size particles. The EAF(L) slag sand- and silt-size particles had subrounded to subangular shapes. Some very irregularly shaped platy particles were also observed. Most of the EAF(L) slag sand-size particles examined under SEM had extremely rough surface textures with platy, crystalline structures (see Figure 10). Some of the SEM micrographs of the EAF(L) slag sand-size particles indicated the presence of a porous structure.

10. Conclusions

The mineralogical and morphological properties of BOF and EAF(L) slag samples generated from two steel plants in

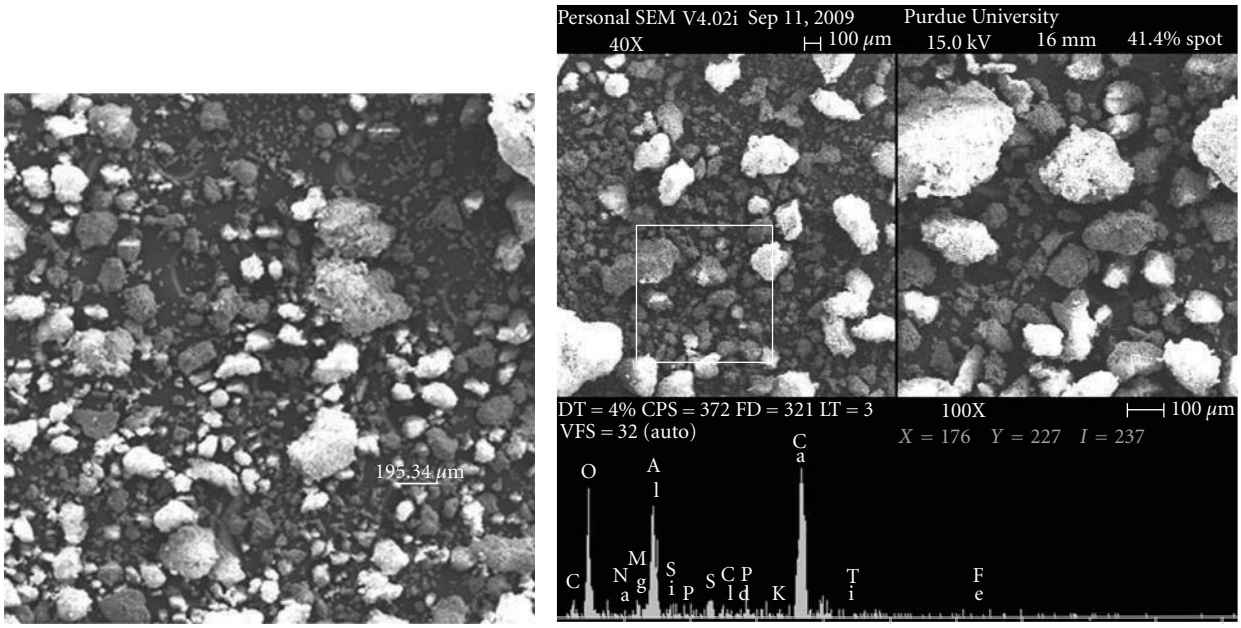

(a) (b)

Figure 10: SEM micrographs of EAF(L) slag. (a) sand- and silt-size particle shapes (magnification = 50X) and (b) particles with their elemental analysis.

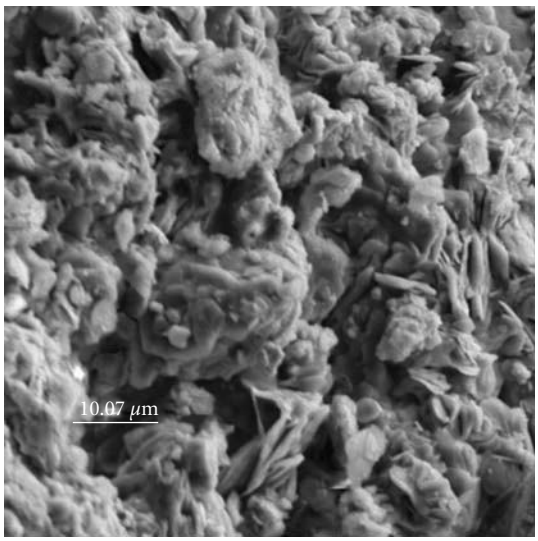

Figure 11: SEM micrograph showing the surface texture of a sand-size EAF slag particle (magnification = 1200X).

Indiana were investigated through XRD analyses and SEM studies. The following conclusions were reached.

(1) The main mineral phases identified in the BOF slag samples were Portlandite, srebrodol'skite, and merwinite.

(2) Most of the BOF slag gravel-size particles had a high sphericity and a solid structure. Sand- and silt-size BOF slag particles had subrounded to angular shapes and rough surface textures under SEM.

(3) The main mineral phases identified in the EAF(L) slag samples were portlandite, mayenite, and malenterite.

(4) Both bulky and platy gravel-size particles with very low sphericity and sharp edges were observed in the EAF(L) slag samples. Sand- and silt-size particles of EAF(L) slag samples showed subrounded to subangular shapes. SEM micrographs showed that the majority of the sand-size particles had extremely rough surface textures with distinct crystal structures.

(5) The morphological studies suggest that both the BOF and EAF(L) slag samples tested in this study have favorable frictional characteristics.

(6) The complex XRD patterns of the tested BOF and EAF(L) slag samples were a result of their chemical composition and the very slow cooling conditions applied during their processing. The XRD analyses of both the BOF and EAF(L) slag samples indicated the presence of free MgO and CaO. Since these compounds expand when hydrated, the volumetric instability of the tested steel slags needs to be assessed for their use in civil engineering applications.

Acknowledgments

This work was supported by the Joint Transportation Research Program administered by the Indiana Department of Transportation (INDOT) and Purdue University, Edw. C. Levy Co., and Multiserv Ltd., Harsco Corporation. The contents of this paper reflect the views of the writers, who are responsible for the facts and the accuracy of the data

presented herein. The contents neither necessarily reflect the official views or policies of the Indiana Department of Transportation, nor do the contents constitute a standard, specification or regulation. The writers are thankful to John Yzenas of Levy Co., and Nayyar Siddiki of INDOT for their support during this project.

References

[1] H. Schoenberger, "Final draft: best available techniques reference document on the production of iron and steel," Publications of EC: European Commission, Joint Research Centre, IPTS, European IPPC Bureau, 2001.

[2] Energy Manager Training (EMT), "Iron and steel process," July 2008, http://www.energymanagertraining.com/.

[3] D. Brandt and J. C. Warner, *Metallurgy Fundamentals*, Goodheart-Willcox, Tinley Park, Ill, USA, 3rd edition, 2005.

[4] American Iron and Steel Institute (AISI), "How Steel is Made," October 2011, http://www.steel.org/.

[5] S. Seetharaman, *Fundamentals of Metallurgy*, Woodhead Publishing and CRC Press, Boca Raton, Fla, USA, 2005.

[6] United Stated Geological Survey (USGS), "Slag-iron and steel," Annual Review, Mineral Industry Surveys, U.S. Geological Survey, Minerals Yearbook, Reston, Va, USA, 1993–2006.

[7] B. Das, S. Prakash, P. S. R. Reddy, and V. N. Misra, "An overview of utilization of slag and sludge from steel industries," *Resources, Conservation and Recycling*, vol. 50, no. 1, pp. 40–57, 2007.

[8] L. M. Juckes, "The volume stability of modern steelmaking slags," *Mineral Processing and Extractive Metallurgy*, vol. 112, no. 3, pp. 177–197, 2003.

[9] P. Y. Mahieux, J. E. Aubert, and G. Escadeillas, "Utilization of weathered basic oxygen furnace slag in the production of hydraulic road binders," *Construction and Building Materials*, vol. 23, no. 2, pp. 742–747, 2009.

[10] H. Y. Poh, G. S. Ghataora, and N. Ghazireh, "Soil stabilization using basic oxygen steel slag fines," *Journal of Materials in Civil Engineering*, vol. 18, no. 2, pp. 229–240, 2006.

[11] D. H. Shen, C. M. Wu, and J. C. Du, "Laboratory investigation of basic oxygen furnace slag for substitution of aggregate in porous asphalt mixture," *Construction and Building Materials*, vol. 23, no. 1, pp. 453–461, 2009.

[12] C. Shi, "Steel slag—its production, processing, characteristics, and cementitious properties," *Journal of Materials in Civil Engineering*, vol. 16, no. 3, pp. 230–236, 2004.

[13] M. Tossavainen, F. Engstrom, Q. Yang, N. Menad, M. L. Larsson, and B. Bjorkman, "Characteristics of steel slag under different cooling conditions," *Waste Management*, vol. 27, no. 10, pp. 1335–1344, 2007.

[14] J. Waligora, D. Bulteel, P. Degrugilliers, D. Damidot, J. L. Potdevin, and M. Measson, "Chemical and mineralogical characterizations of LD converter steel slags: a multi-analytical techniques approach," *Materials Characterization*, vol. 61, no. 1, pp. 39–48, 2010.

[15] W. Xuequan, Z. Hong, H. Xinkai, and L. Husen, "Study on steel slag and fly ash composite Portland cement," *Cement and Concrete Research*, vol. 29, no. 7, pp. 1103–1106, 1999.

[16] M. Barra, E. V. Ramonich, and M. A. Munoz, "Stabilization of soils with steel slag and cement for application in rural and low traffic roads," in *Proceedings of the Beneficial Use of Recycled Materials in Transportation Application*, pp. 423–432, RMCR University of Durham, Arlington, Va, November 2001.

[17] M. P. Luxán, R. Sotolongo, F. Dorrego, and E. Herrero, "Characteristics of the slags produced in the fusion of scrap steel by electric arc furnace," *Cement and Concrete Research*, vol. 30, no. 4, pp. 517–519, 2000.

[18] J. M. Manso, J. A. Polanco, M. Losañez, and J. J. González, "Durability of concrete made with EAF slag as aggregate," *Cement and Concrete Composites*, vol. 28, no. 6, pp. 528–534, 2006.

[19] P. E. Tsakiridis, G. D. Papadimitriou, S. Tsivilis, and C. Koroneos, "Utilization of steel slag for Portland cement clinker production," *Journal of Hazardous Materials*, vol. 152, no. 2, pp. 805–811, 2008.

[20] M. Nicolae, I. Vîlciu, and F. Zăman, "X-ray diffraction analysis of steel slag and blast furnace slag viewing their use for road construction," *UPB Scientific Bulletin Series B*, vol. 69, no. 2, pp. 99–108, 2007.

[21] G. R. Qian, D. D. Sun, J. H. Tay, and Z. Y. Lai, "Hydrothermal reaction and autoclave stability of Mg bearing RO phase in steel slag," *British Ceramic Transactions*, vol. 101, no. 4, pp. 159–164, 2002.

[22] J. Setién, D. Hernández, and J. J. González, "Characterization of ladle furnace basic slag for use as a construction material," *Construction and Building Materials*, vol. 23, no. 5, pp. 1788–1794, 2009.

[23] H. L. Robinson, "The utilization of blastfurnace and steel making slags as aggregates for construction," in *Proceedings of the 11th Extractive Industry Geology Conference*, pp. 327–330, The Geological Society of London, 2000, 36th forum on the Geology of Industrial Minerals, Industrial Minerals and Extractive Industry Geology.

[24] H. Shen, E. Forssberg, and U. Nordström, "Physicochemical and mineralogical properties of stainless steel slags oriented to metal recovery," *Resources, Conservation and Recycling*, vol. 40, no. 3, pp. 245–271, 2004.

[25] A. S. Reddy, R. K. Pradhan, and S. Chandra, "Utilization of Basic Oxygen Furnace (BOF) slag in the production of a hydraulic cement binder," *International Journal of Mineral Processing*, vol. 79, no. 2, pp. 98–105, 2006.

[26] A. Monaco and W. K. Wu, "The effect of cooling conditions on the characterization of steel slag," in *Proceedings of the International Symposium on Resource Conservation and Environmental Technologies in Metallurgical Industry*, pp. 107–116, Toronto, Canada, August 1994.

[27] C. Shi, "Characteristics and cementitious properties of ladle slag fines from steel production," *Cement and Concrete Research*, vol. 32, no. 3, pp. 459–462, 2002.

[28] J. M. Manso, M. Losañez, J. A. Polanco, and J. J. Gonzalez, "Ladle furnace slag in construction," *Journal of Materials in Civil Engineering*, vol. 17, no. 5, pp. 513–518, 2005.

[29] J. Geiseler, "Use of steelworks slag in Europe," *Waste Management*, vol. 16, no. 1–3, pp. 59–63, 1996.

[30] F. Wachsmuth, J. Geiseler, W. Fix, K. Koch, and K. Schwerdtfeger, "Contribution to the structure of BOF-slags and its influence on their volume stability," *Canadian Metallurgical Quarterly*, vol. 20, no. 3, pp. 279–284, 1981.

[31] G. Qian, D. D. Sun, J. H. Tay, Z. Lai, and G. Xu, "Autoclave properties of kirschsteinite-based steel slag," *Cement and Concrete Research*, vol. 32, no. 9, pp. 1377–1382, 2002.

[32] V. S. Ramachandran, P. J. Sereda, and R. F. Feldman, "Mechanism of hydration of calcium oxide," *Nature*, vol. 201, no. 4916, pp. 288–299, 1964.

[33] A. W. Kneller, J. Gupta, L. M. Borkowski, and D. Dollimore, "Determination of original free lime content of weathered iron and steel slags by thermogravimetric analysis," Transportation

Research Record 1434, Transportation Research Board, National Research Council, Washington, DC, USA, 1994.

[34] C. B. Crawford and K. N. Burn, "Building damage from expansive steel slag backfill," *Journal of the Soil Mechanics and Foundations Division*, vol. 95, no. 6, pp. 1325–1334, 1969.

[35] A. Verhasselt and F. Choquet, "Steel slags as unbound aggregate in road construction: problems and recommendations," in *Proceedings of the International Symposium on Unbound Aggregates in Roads*, pp. 204–211, London, UK, 1989.

[36] J. Geiseler, "Steel slag-generation, processing and utilization," in *Proceedings of the International Symposium on Resource Conservation and Environmental Technologies in Metallurgical Industry*, pp. 87–97, Toronto, Canada, August 1994.

[37] H. Motz and J. Geiseler, "Products of steel slags an opportunity to save natural resources," *Waste Management*, vol. 21, no. 3, pp. 285–293, 2001.

[38] I. A. Altun and I. Yilmaz, "Study on steel furnace slags with high MgO as additive in Portland cement," *Cement and Concrete Research*, vol. 32, no. 8, pp. 1247–1249, 2002.

[39] P. Chaurand, J. Rose, V. Briois et al., "Environmental impacts of steel slag reused in road construction: a crystallographic and molecular (XANES) approach," *Journal of Hazardous Materials*, vol. 139, no. 3, pp. 537–542, 2007.

Hindawi Publishing Corporation
Advances in Civil Engineering
Volume 2011, Article ID 594270, 8 pages
doi:10.1155/2011/594270

Research Article

Development of a Lightweight Low-Carbon Footprint Concrete Containing Recycled Waste Materials

S. Talukdar, S. T. Islam, and N. Banthia

Department of Civil Engineering, University of British Columbia, 1012J-6250 Applied Science Lane, Vancouver, BC, Canada V6T 1Z4

Correspondence should be addressed to S. Talukdar, sudip@civil.ubc.ca

Received 4 April 2011; Revised 27 July 2011; Accepted 27 July 2011

Academic Editor: Monica Prezzi

Use of any recycled material helps to maintain a greener environment by keeping waste materials out of the landfills. Recycling practices also can decrease the environmental and economical impact of manufacturing the materials from virgin resources, which reduces the overall carbon footprint of industrial materials and processes. This study examined the use of waste materials such as crushed glass, ground tire rubber, and recycled aggregate in concrete. Compressive strength and elastic modulus were the primary parameters of interest. Results demonstrated that ground tire rubber introduced significant amounts of air into the mix and adversely affected the strength. The introduction of a defoamer was able to successfully remove part of the excess air from the mix, but the proportional strength improvements were not noted implying that air left in the defoamed mixture had undesirable characteristics. Freeze-thaw tests were next performed to understand the nature of air in the defoamed mixtures, and results demonstrated that this air is not helpful in resisting freeze-thaw resistance either. Overall, while lightweight, low-carbon footprint concrete materials seem possible from recycled materials, significant further optimization remains possible.

1. Introduction

Construction materials are increasingly judged by their ecological impact. Presently, the industry is concentrating on reducing the ecological footprint of concrete by looking at ways of making it "greener" [1]. Consequently, the use of recycled materials for coarse and fine aggregate is being actively encouraged.

Construction and demolition waste constitutes a major portion of all generated solid waste, with 200–300 million tons generated annually in the United States alone. The traditional disposal of these large amounts of waste in landfills is no longer an acceptable option. Coupled with the increasing scarcity of suitable aggregate, the pressure is severe to find an acceptable replacement for virgin aggregate. Use of recycled concrete aggregate (RCA) from the demolition of old structures could be an acceptable solution [2]. There are some well-known technical problems of incorporating RCA into mixes, such as the presence of contaminants and deleterious materials which affect the strength and durability of the final mix. There is also the possibility of cement reacting with the aggregate itself. For example, if crushed glass is used as a substitute for fine aggregate, then there is the possibility of an alkali silica reaction between the paste and the glass. However, experience shows that if the recycled aggregate is cleaned, sorted, and selected properly, then it can be used as an acceptable substitute for virgin coarse aggregate.

Fine and coarse aggregates traditionally account for a very small amount of CO_2 emissions during production of concrete even though they usually constitute more than 2/3 of the concrete volume. Manufacturing of fine and coarse aggregates have less emissions than production of cementitious binders despite quarrying that entails blasting, crushing, screening, haulage, and stockpiling of aggregates. Therefore, the most effective way of lowering the carbon footprint of concrete is to reduce the cement concrete in the mix. However, CO_2 emissions due to demolition and reuse are a fraction of those compared to the production of virgin aggregate [3]. Furthermore, the stockpiles of recycled aggregate are generally closer to the construction site than that of virgin aggregate, which generally is quarried and

transported from long distances [2]. In this respect, use of recycled aggregates to reduce carbon footprint should be encouraged.

The United States generates approximately 242 million scrap tires per year, and the US Environmental Protection Agency estimates that 2-3 billion scrap tires have already accumulated in illegal stockpiles or uncontrolled tire dumps throughout the country, with millions more scattered around in the natural environment [4]. It is essential that innovative solutions be developed to deal with this excess material to prevent it from becoming an environmental nuisance.

A sustainable proposition is to use scrap tires in concrete mixtures. Such a study was undertaken in the research reported here. Coarse aggregate was replaced with a high fraction of ground tire rubber, and the role of a defoaming agent was examined. Next, ground tire rubber was combined with crushed glass and recycled aggregate to further reduce the carbon footprint.

2. Previous Work

There have been countless number of studies which have looked at the properties of concrete containing various types and quantities of recycled coarse and fine aggregate. Properties such as chemical stability [5], physical durability [6], workability [7], strength [8], permeability [9], and shrinkage resistance [10] have been examined. A general consensus between these studies is that concrete containing recycled coarse aggregate which are properly cleaned, and in quantities no more than 50% replacement of virgin aggregate would have adequate durability, workability, and strength when compared with concrete containing 100% virgin aggregate. Concrete containing recycled aggregate is expected to display slightly more shrinkage than that containing virgin aggregate only [10]. Permeability of concrete containing recycled aggregate at w/c ratios same as that of concrete containing only virgin aggregate is also expected to increase [9]. With regards to chemical stability, it is important that waste aggregates being used do not contain reactive silica in order to avoid alkali-silica reaction (ASR) in the final product.

Waste glass constitutes a problem for solid waste disposal in many municipalities. The current practice is still to landfill most of it. Since glass is usually not biodegradable, landfills do not provide an environment-friendly solution. Consequently, there is a strong need to utilize/recycle waste glasses. One option is to crush and grade it and use it as a replacement for fine aggregate in a concrete mix.

As with waste recycled aggregates, it is very important that the glass used be silica-free in order to avoid ASR in the final composite. If this basic criterion is met, past studies indicate that recycled waste glass is an acceptable material to be used in concrete. There tends to be a slight decrease in compressive strength as the fraction of recycled glass is increased in a mix, and other properties such as air content and mix are dependent on the shape of the individual grains of the crushed glass [5, 11, 12].

The idea of using recycled scrap tires in concrete has been around for some time. Earlier, research on the use of worn out tires was concentrated in asphalt mix design. However, it soon became apparent that the asphalt industry can only absorb 30%–40% of scrap tires generated [13], and so, emphasis has been slowly shifting to Portland cement concrete mix designs. Properties, testing and design of rubber as an engineering material in Portland Cement concrete were investigated as early as 1960 [14]. A comprehensive summary of the properties and application of concrete containing scrap tire rubber was presented by Siddique and Naik [15] and Nehdi and Khan [16].

Hernández-Olivares et al. [17], Huang et al. [18], Li et al. [4], Ganjian et al. [19], Toutanji [20], Batayneh et al. [21], Kahloo et al. [22], and Mohammed [23] conducted studies which included observation and modeling of the mechanical properties of recycled shredded tire concrete composites. The general trend observed was that as the percent content of tire rubber increases, the strength of the mix decreases. This is most likely due to the increase in the entrapped air in the concrete mix due to the tire. It was also noted that such composites exhibit large displacement and deformations, thereby generally increasing toughness, which is most likely due to the fact the rubber aggregate has the ability to withstand large deformations. Savas et al. [24] reported that the freeze-thaw durability of concrete with ground waste tire rubber deteriorated as the percent of ground rubber increases.

Many studies have reported that scrap tires increase the amount of entrapped air in concrete [25, 26]. The reasons often cited are the rough rubber surfaces that entrap air, the nonpolar nature of rubber itself and its tendency to be hydrophobic. Several attempts have been made to improve the hydrophilicity of rubber, and the most promising one thus far appears to be soaking the rubber in an NaOH solution for short periods of time [15].

3. Material and Methods

Given that scrap tire entraps excessive amounts of air, the primary objectives of the study was to investigate the effectiveness of using a defoamer to reduce the air in mixes containing ground tire rubber. Having successfully achieved a reduction in the air content, ground tire rubber was then combined with other recycled materials such as recycled aggregate and crushed glass to further reduce the carbon footprint. The four concrete mixtures investigated (M0, M1, M2, and M3) are given in Table 1. Their fresh properties are also listed therein.

CSA Type 10 Portland Cement, saturated surface dry river sand as fine aggregate, gravel with a maximum nominal size of 9.5 mm as coarse aggregate, and potable tap water were used in all mixes. Slump was maintained at 150 mm for all mixes. Where ground tire rubber was used, it was used as a 15% replacement of the coarse aggregate by mass which produce 25% more fresh concrete by volume. This meant that the mass % of ground rubber in the mix relative to cement was of 47%. The ground tire rubber had a specific gravity of 1.1 and a maximum nominal size of 9.5 mm (Figure 1). Its gradation curve is given in Figure 3. The size of the recycled glass materials was between 297–840 micron

Table 1: Mix proportions and fresh properties.

Material	Mixture proportions			
	Control Mix M0 (m^3)	RMC Mix M1 ($1.25\ m^3$)	RMC Mix M2 ($1.25\ m^3$)	RMC Mix M3 ($1.25\ m^3$)
Cement (kg)	360	360	360	360
Coarse aggregate (kg)	1130	960.5	960.5	565
Fine aggregate (kg)	580	580	580	290
Water (kg)	180	180	180	180
Defoaming agent (mL)	0	0	360	360
Air entrainment agent (mL)	90	0	0	0
Ground tire rubber (kg)	0	169.5	169.5	169.5
Recycled concrete (kg)	0	0	0	395.5
Crushed glass (kg)	0	0	0	290
Superplasticizer (mL)	0	0	0	300
Fresh properties				
Slump (mm)	150	150	150	150
Air content (%)	4.5	16.0	5.5	9
Measured density (kg/m^3)	2350	2100	2300	2050

(Figure 2). The defoaming agent used was Rhodoline 1010 manufactured by Brenntag Industries. The air entrainment admixture used was Darex II manufactured by Grace Construction Products. The recycled coarse aggregate used in the study had a maximum nominal size of 9.5 mm, and it had been washed and brought to SSD conditions before mixing. Batches were prepared as per ASTM C192.

Slump tests (ASTM C143) and air content tests (ASTM C173) were carried out on fresh mixture and the values are reported in Table 1. The mixes containing ground tire rubber were more difficult to work with and showed slightly more segregation in the fresh state.

From each mix, ten standard 100 mm × 200 mm cylinders were cast for a total of 40 cylinders. Cylinders were moist cured for at least 28 days following which compressive strength tests were performed as per ASTM C69. An 890 kN capacity Forney Compressive Testing Machine was used. From each batch, five specimens were tested at an age of 7 days, and the remaining five were tested at an age of 28 days. For the tests at 28 days, elastic modulus values were also determined using a deformation cage as per ASTM C469.

Air content values in Table 1 indicated that while the air content was reduced as a result of defoamer addition, one needed to further characterize the nature of air that was left behind. To gain this understanding, six 75 mm × 100 mm × 405 mm prismatic beams were cast from each mix, for a total of 24 such beams, for freeze-thaw testing. For Mixes M1 and M2 following a cyclic exposure to freezing and thawing in an automated freeze-thaw chamber, damage was quantified using ultrasonic pulse velocity (UPV) measurements (ASTM C597) and compared with the Control Mix M0. For Mix M3, ASTM C666 was followed, and the damage was quantified using the Resonant Frequency Test (ASTM C215). The change in the resonant frequency of each specimen was monitored at regular intervals of every 35 cycles using a Sonometer. The dynamic modulus of elasticity was determined by measuring the fundamental transverse frequency of the sample at each test interval. The relative dynamic modulus of elasticity and the Durability Factors were calculated according to ASTM C666.

Finally, one 300 mm × 100 mm round panel was cast for control Mix M0 and RMC Mix M3 for a total of two such panels, on which torrent permeability tests were performed [27]. Torrent is a surface permeability test which determines the ease with which concrete surface can get saturated.

4. Results

4.1. Strength. The strengths measured at 7 and 28 days are given, respectively, in Figures 4 and 5(a). In Figure 5(b), the 28-day elastic moduli are also plotted.

When mixes M0 and M1 are compared, a steep reduction in the compressive strength at both ages is apparent. This has been reported often by others and is most likely related to the increased air content (from 4.5% to 16.0%) and an apparent lack of bond between the tire rubber and the paste. The addition of a defoaming agent does bring down the air significantly from 16% to 5.5% (almost to the level of control concrete), but the compressive strength in the defoamed mixture (M2) increased only marginally. It seems likely that the loss of strength in mixtures with scrap tires is not only due to the increased air but also due to poor bond between scrap tire and cement paste. It is also conceivable that the 5.5% air left in Mix M2 is of a different nature. To try and determine the type and nature of the voids present in concrete containing ground rubber, we turn to fracture mechanics.

Assuming that linear elastic fracture mechanics applies to concrete, the condition determining unstable tensile fracture in Mode I when an internal flaw of size $2a$ is present is given by

$$K_{IC} = Y\sigma_c\sqrt{\pi a}, \tag{1}$$

where K_{IC} is Plain Strain Fracture Toughness (i.e., Critical Stress Intensity Factor) in Mode I, Y is a dimensionless

Figure 1: Recycled ground rubber.

Figure 2: Recycled glass.

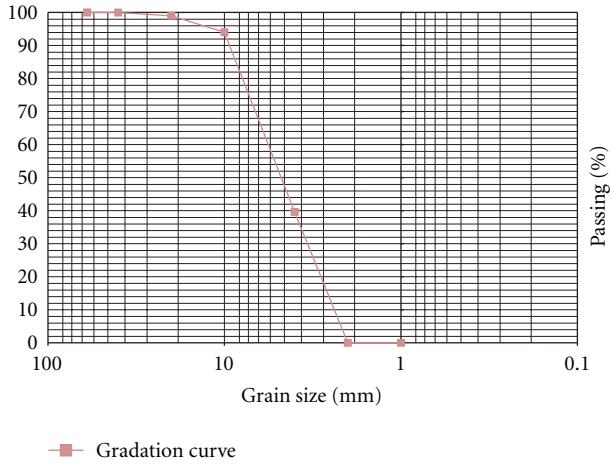

Figure 3: Ground tire gradation curve.

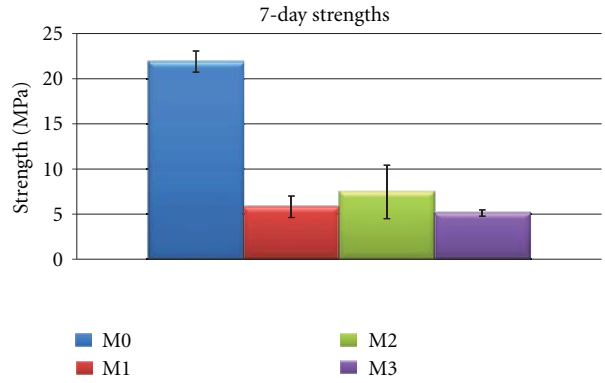

Figure 4: 7-day compressive strengths.

parameter that depends on the specimen and crack geometries, and σ_c is the failure stress.

Equation (1) can also be written in the form of maximum allowable flaw size (a_c) that will trigger an unstable fracture as

$$a_c = \frac{1}{\pi}\left(\frac{K_{IC}}{\sigma_c Y}\right)^2. \quad (2)$$

For concrete, K_{IC} can be taken as 0.2 MPa m$^{1/2}$ [28]. For a finite cylinder with a flaw much smaller than the cylinder width, Y can be taken as 1.0 [29].

Finally, the tensile strength of concrete (σ_c) can be estimated from its compressive strength (f_c') as [30]

$$\sigma_c = 0.94\sqrt{f_c'}. \quad (3)$$

Substituting the appropriate values into (2), we find that for

(a) M0, $a_c = 0.48$ mm, or the allowable flaw size = $2a_c$ = 0.96 mm,

(b) M1, $a_c = 2.05$ mm, or the allowable flaw size = $2a_c$ = 4.10 mm.

Interestingly, approximately 40% of the ground rubber in the mix has a nominal length of around 4 mm (Figure 3) which corresponds to the approximate predicted flaw size in M1. It implies, therefore, that most of the air in the mixes containing ground rubber is trapped at the interfaces between rubber and concrete and not entrained in the cement-paste. This entrapment of air would lead to poor bond between rubber and concrete and a dramatic reduction in the compressive strength. Even for mixes where defoaming agent was added although there was an overall reduction in the air content down to the level of Control concrete, the remaining air still gathered at the rubber-concrete interface and continued to weaken the bond and persistently lowered the strength. The concept is illustrated in Figure 6. Notice that the Mix M1 in Figures 6(b) entrapped significantly greater amounts of air over Mix M0 in Figure 6(a). While the Mixes M2 and M3 saw improvements and air contents over M1, the remaining air still persistently congregated at the interfaces, and no appreciable strength gains over M0 were achievable. Air in M1, M2, and M3 continued to reside in flocculated, continuous and elongated voids causing large stress concentration and drop of strength. This also conceivably increased the permeability to water and the ease with which M1, M2, and M3 became saturated and depicted lower resistance to freezing and thawing as will be seen later.

Bringing other recycled materials in the mix (recycled aggregate and crushed glass) further increases the air from 5.5% to 9%. This is expected as recycled aggregate do entrap air by themselves. This increase in air is also accompanied

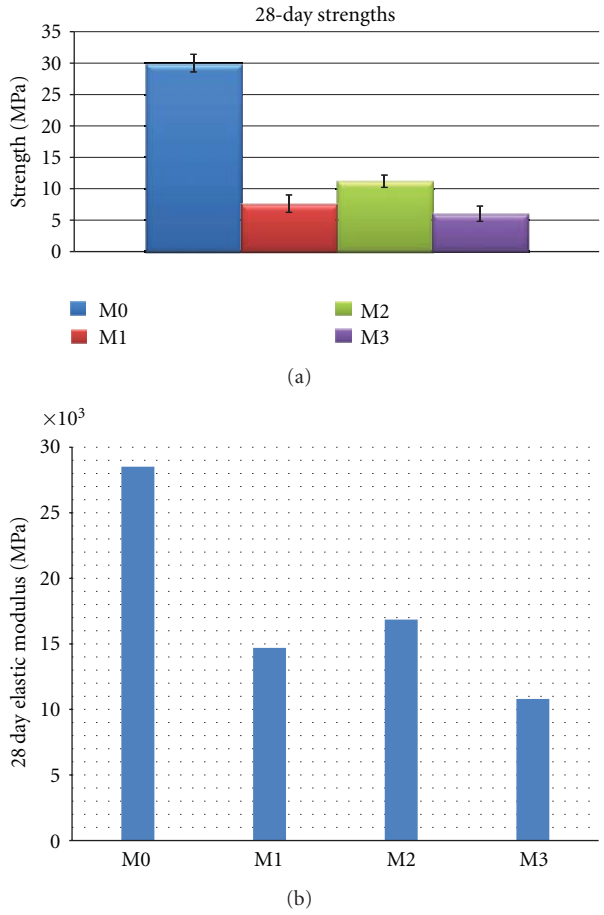

Figure 5: (a) 28-day compressive strengths, (b) 28-day elastic moduli.

by a corresponding drop in the compressive strength (and modulus of Mix M3) at both ages.

Based on the data obtained, the following empirical equation (4) is proposed to try and estimate the Elastic Modulus of Ground Rubber Concrete based on its strength and density:

$$E = 0.001\sigma^{0.5}\gamma^{2}, \tag{4}$$

where E is the elastic modulus of concrete with ground rubber (MPa), σ is the compressive strength of ground rubber concrete (MPa), and γ is the density of concrete (kg/m^3).

ACI 318 has established an empirical relationship, between Elastic Modulus, Strength, and Density as:

$$E = 0.043\gamma^{1.5}\sigma^{0.5}. \tag{5}$$

Using these two equations, the predicted results versus the actual results are shown in Figure 7.

Therefore, although the data set with which (4) was derived is quite limited, it compares quite well with not only measured results, but also with predictions from ACI 318 which is based on a large amount of empirical data. Therefore, we believe it still may be used as a basis for future work to try and formulate the relationship between strength, density, and elastic modulus for concrete containing ground rubber.

4.2. Freeze Thaw Resistance. In order to further understand the nature of air voids in concrete carrying scrap tire and other recycled materials, freeze-thaw tests were performed as per ASTM C666. Freeze thaw resistance was assessed using ultrasonic pulse velocity measurements for Mixes M0, M1 and M2, while the Resonant Frequency measurements were carried out on Mixes M0 and M3. Photographs of specimens after 210 cycles of freezing and thawing are given in Figure 8.

Notice that Mixes M1 and M2 both containing rubber show a significantly lower initial UPV reading compared to the control, a difference that persists over the entire duration of the freeze-thaw test. This finding is reasonable, as the addition of rubber is believed to have a damping effect on wave propagation, mainly due to the provision of extra air voids [31, 32]. M2 initially does not have as much of a decrease in UPV readings compared to the control, as the air content is almost the same as that of mix M0.

Notice in Figure 9 that while the control concrete was able to sustain 300 cycles of freezing and thawing without any drop in the ultrasonic pulse velocity reading, the addition of the rubber (Mix M1) had adverse consequences on UPV starting at a very low number of freeze-thaw cycles. Additionally these samples exhibited severe scaling (Figure 8). The mix with defoaming agent fared marginally better in comparison to the nondefoamed concrete, but ultimately still showed a marked decrease in UPV in a freeze-thaw environment. The result of the UPV decrease will be correlated later with a drop in dynamic modulus as determined in ASTM C666 that were performed on Mixes M0 and M3. Such a correlation has been previously attempted by Mirmiran and Wei [33] and by Yildiz and Ugur [34]. More specifically, UPV measurement were carried out on ASTM C666 at failure for Mix M3 and that value of UPV was used to determine freeze-thaw failure cycle for Mixes M1 and M2. This was considered to be an acceptable approach as Mixes M1, M2, and M3 all had very similar 28-day strength.

In Figure 10, the freeze-thaw durability of Mix M3 is compared with control Mix M0 using the ASTM C666 specified criteria of resonant frequency (and thereby the dynamic modulus) and the resulting durability factor (Figure 11). Notice that Mix M3 sustained far greater number of cycles than Mixes M1 and M2 but still did not approach the performance of the control and did not sustain the required 300 cycles.

For Mix 3 the specimen failed after 210 cycles according to ASTM C666 since the durability factor dropped below 60 percent. The UPV value was recorded at this point as being 3050 m/s (Figure 12). In comparison, Mix 1 reached this failure point after 116 cycles and Mix 2 failed after 171 cycles. Defoamer appears to have a positive effect, as it increases the time to failure by to 32.2% compared to the defoamer-free mix.

One of the reasons why a particular concrete mix would perform poorly under freeze-thaw cycling is its void structure. Concrete which contains entrained air will be more

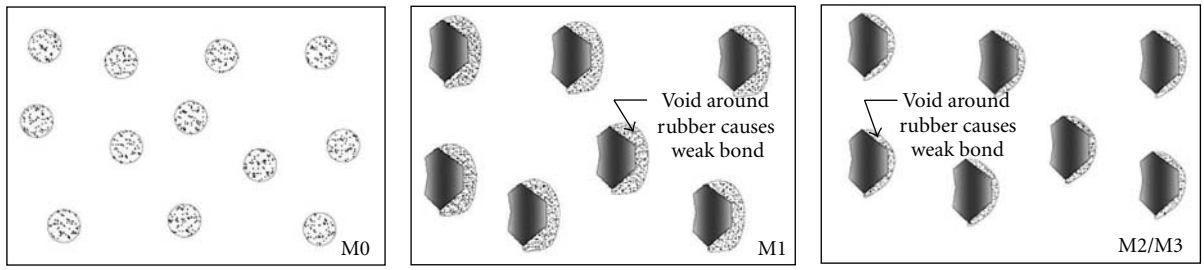

Figure 6: Comparison different shapes of voids in concrete.

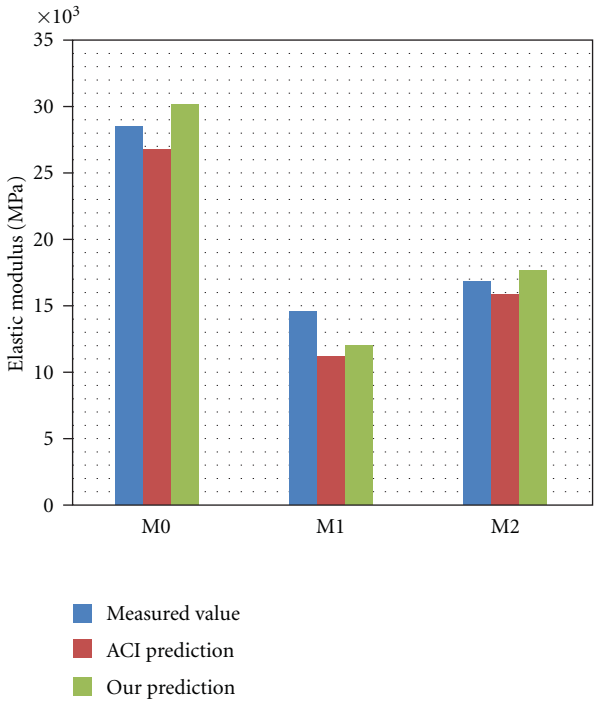

Figure 7: Predicted results versus actual results using (4) and (5).

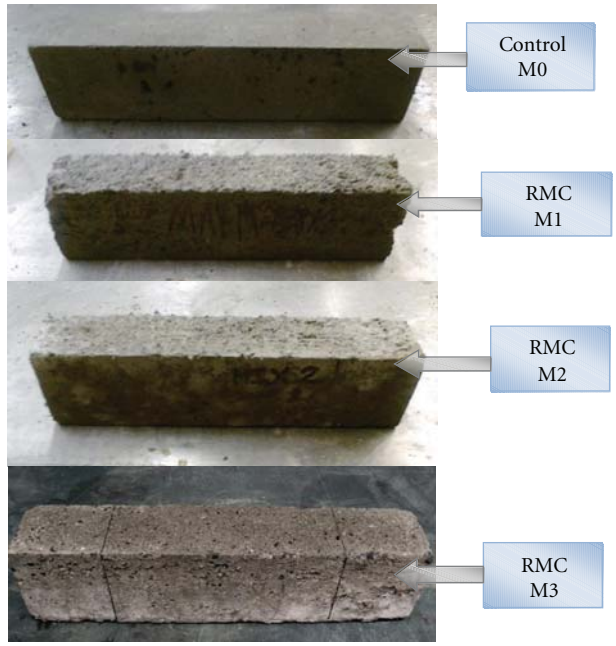

Figure 8: Beam samples after 210 freeze-thaw cycles.

durable and have more freeze-thaw resistance. Entrained air produces discrete, nearly spherical bubbles in the cement paste so that no channels for the flow of water are formed and the permeability of the concrete is not increased [35]. Excess water is able to escape into these air filled voids and damage of concrete due to freeze thaw conditions will not occur. Entrapped air will form larger, interconnected voids, may lower concrete strength, and subsequently lower freeze-thaw resistance.

To assess the possibility, torrent permeability tests were performed and the results are given in Table 2. Notice that Mix M3 was far more permeable compared to control Mix M0. The increase in permeability is further evidence that the additional air voids formed due to the inclusion of ground rubber in the mix is of the nonentrained nature and coagulating at the rubber-concrete interface as proposed earlier in this paper.

Table 2: Torrent permeability measurements.

	Control Mix M0	RMC Mix M3
Permeability coefficient (kT) (m^2)	0.063×10^{-16}	0.157×10^{-16}

5. Conclusions and Recommendations

(1) Addition of ground tire rubber into a concrete mix greatly increases the air content of the mix, but it seems possible to reduce the air content to acceptable levels by using a defoamer.

(2) When recycled aggregates and glass are brought into a mix containing ground tire rubber, air contents move up again, and the defoamer is less effective.

(3) In concrete mixtures containing ground tire rubber, while a defoaming agent may reduce the air appreciably, a proportional increase in the compressive strength is not noticed. This implies that the remaining air in the defoamed mixture is of poor quality. Specifically, the voids appear to be less dispersed,

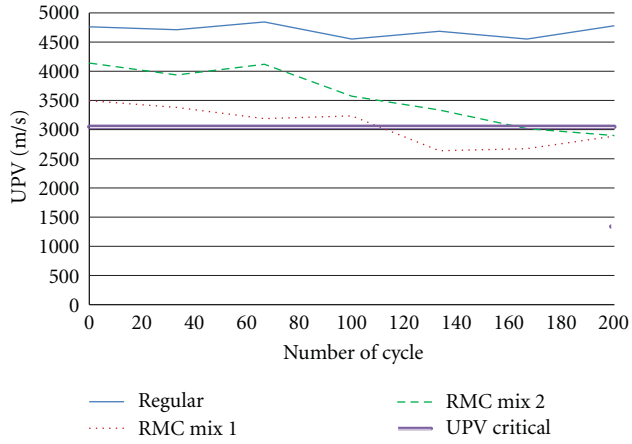

Figure 9: Freeze-thaw resistance using UPV values as a function of cycles.

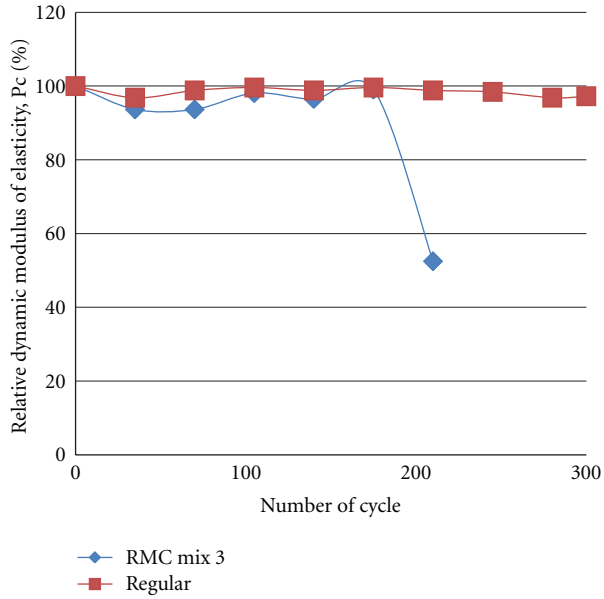

Figure 10: Average relative dynamic modulus of elasticity versus freeze-thaw cycles.

elongated, and coagulate at the rubber-concrete interface, thereby affecting the bond and reducing overall strength. These observations were further supported by freeze-thaw and permeability testing.

(4) Freeze-thaw testing indicated that concrete carrying ground tire rubber fares poorly under freeze-thaw, but the performance can be marginally improved using a defoamer. The freeze-thaw performance stabilizes when other recycled materials such as recycled aggregate and crushed glass are added to the mix.

(5) While it is probably not possible to use the concrete mixtures developed here for structural elements where high strength and durability under loads are required, they may still be used in nonstructural applications such as partition walls, road barriers, pavements, or low-strength foundations.

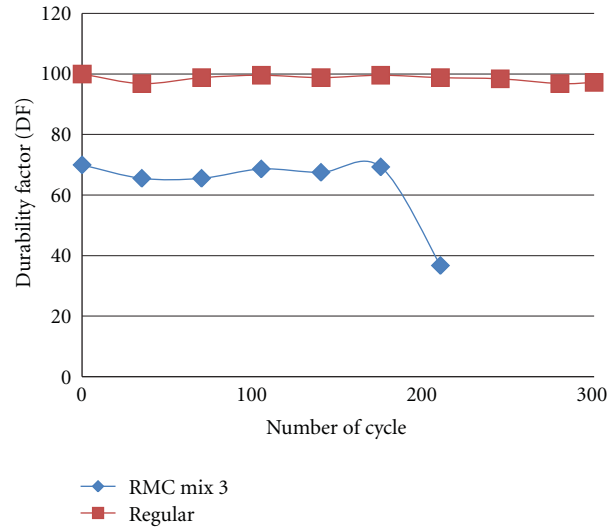

Figure 11: Average durability factor versus no freeze-thaw cycles.

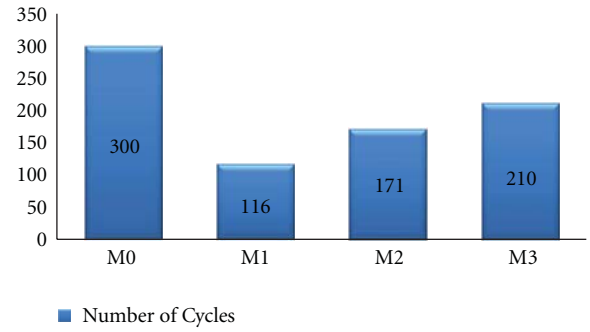

Figure 12: Number of freeze-thaw cycles survived (N_f) by various mixes.

Acknowledgments

The authors wish to acknowledge the help of Mr. Patrick McConnell for supplying the recycled materials used in this study. Also, they would like to thank Mr. Adrien Drochon, Mr. Sylvian Lioux, Ms. Saakshi Mahajan, and Ms. Roxanna Mousavi for their assistance in the lab with specimen preparation and testing.

References

[1] L. Lemay, "Concrete and climate change: how does concrete stack up against other building materials," *Concrete Infocus*, vol. 7, no. 2, pp. 38–43, 2008.

[2] C. Meyer, "The greening of the concrete industry," *Cement and Concrete Composites*, vol. 31, no. 8, pp. 601–605, 2009.

[3] F. Collins, "Inclusion of carbonation during the life cycle of built and recycled concrete: influence on their carbon footprint," *International Journal of Life Cycle Assessment*, vol. 15, no. 6, pp. 549–556, 2010.

[4] G. Li, M. A. Stubblefield, G. Garrick, J. Eggers, C. Abadie, and B. Huang, "Development of waste tire modified concrete," *Cement and Concrete Research*, vol. 34, no. 12, pp. 2283–2289, 2004.

[5] I. B. Topçu and M. Canbaz, "Properties of concrete containing waste glass," *Cement and Concrete Research*, vol. 34, no. 2, pp. 267–274, 2004.

[6] S. M. Levy and P. Helene, "Durability of recycled aggregates concrete: a safe way to sustainable development," *Cement and Concrete Research*, vol. 34, no. 11, pp. 1975–1980, 2004.

[7] C. S. Poon, Z. H. Shui, L. Lam, H. Fok, and S. C. Kou, "Influence of moisture states of natural and recycled aggregates on the slump and compressive strength of concrete," *Cement and Concrete Research*, vol. 34, no. 1, pp. 31–36, 2004.

[8] T. C. Hansen and H. Narud, "Strength of recycled concrete made from crushed concrete coarse aggregate," *Concrete International*, vol. 5, no. 1, pp. 79–83, 1983.

[9] T. C. Hansen, "Recycled aggregates and recycled aggregate concrete second state-of-the-art report developments 1945–1985," *Materials and Structures*, vol. 19, no. 3, pp. 201–246, 1986.

[10] J. M. Khatib, "Properties of concrete incorporating fine recycled aggregate," *Cement and Concrete Research*, vol. 35, no. 4, pp. 763–769, 2005.

[11] S. B. Park, B. C. Lee, and J. H. Kim, "Studies on mechanical properties of concrete containing waste glass aggregate," *Cement and Concrete Research*, vol. 34, no. 12, pp. 2181–2189, 2004.

[12] T. R. Naik and Z. Wu, "Crushed post-consumer glass as a partial replacement of sand in concrete," in *Proceedings of the 5th CANMET/ACI International Conference on Recent Advances of Concrete Technology, SP-200*, V. M. Malhotra, Ed., pp. 553–568, American Concrete Institute, Farmington Hills, Mich, USA, 2001.

[13] A. I. Isayev, K. Khait, and S. K. De, *Rubber Recycling*, CRC Press, Boca Raton, Fla, USA, 2005.

[14] N. N. Eldin and A. B. Senouci, "Rubber-tire particles as concrete aggregate," *Journal of Materials in Civil Engineering*, vol. 5, no. 4, pp. 478–496, 1993.

[15] R. Siddique and T. R. Naik, "Properties of concrete containing scrap-tire rubber—an overview," *Waste Management*, vol. 24, no. 6, pp. 563–569, 2004.

[16] M. Nehdi and A. Khan, "Cementitious composites containing recycled tire rubber: overview of engineering properties and potential applications," *Journal of Cement, Concrete and Aggregates*, vol. 23, no. 1, pp. 3–10, 2001.

[17] F. Hernández-Olivares, G. Barluenga, M. Bollati, and B. Witoszek, "Static and dynamic behaviour of recycled tyre rubber-filled concrete," *Cement and Concrete Research*, vol. 32, no. 10, pp. 1587–1596, 2002.

[18] B. Huang, G. Li, S. S. Pang, and J. Eggers, "Investigation into waste tire rubber-filled concrete," *Journal of Materials in Civil Engineering*, vol. 16, no. 3, pp. 187–194, 2004.

[19] E. Ganjian, M. Khorami, and A. A. Maghsoudi, "Scrap-tyre-rubber replacement for aggregate and filler in concrete," *Construction and Building Materials*, vol. 23, no. 5, pp. 1828–1836, 2009.

[20] H. A. Toutanji, "The use of rubber tire particles in concrete to replace mineral aggregates," *Cement and Concrete Composites*, vol. 18, no. 2, pp. 135–139, 1996.

[21] M. K. Batayneh, I. Marie, and I. Asi, "Promoting the use of crumb rubber concrete in developing countries," *Waste Management*, vol. 28, no. 11, pp. 2171–2176, 2008.

[22] A. R. Khaloo, M. Dehestani, and P. Rahmatabadi, "Mechanical properties of concrete containing a high volume of tire-rubber particles," *Waste Management*, vol. 28, no. 12, pp. 2472–2482, 2008.

[23] B. S. Mohammed, "Structural behavior and m-k value of composite slab utilizing concrete containing crumb rubber," *Construction and Building Materials*, vol. 24, no. 7, pp. 1214–1221, 2010.

[24] B. Z. Savas, S. Ahmad, and D. Fedroff, "Freeze-thaw durability of concrete with ground waste tire rubber," *Transportation Research Record*, no. 1574, pp. 80–88, 1997.

[25] D. Fedroff, S. Ahmad, and B. Z. Savas, "Mechanical properties of concrete with ground waste tire rubber," *Transportation Research Board*, no. 1532, pp. 66–72, 1996.

[26] Z. K. Khatib and F. M. Bayomy, "Rubberized Portland cement concrete," *Journal of Materials in Civil Engineering*, vol. 11, no. 3, pp. 206–213, 1999.

[27] M. Romer, "Effect of moisture and concrete composition on the Torrent permeability measurement," *Materials and Structures*, vol. 38, no. 5, pp. 541–547, 2005.

[28] W. D. Callister, *Materials Science and Engineering: An Introduction*, John Wiley & Sons, New York, NY, USA, 5th edition, 2000.

[29] D. P. Rooke and D. J. Cartwright, *Compendium of Stress Intensity Factors*, Hillingdon Press, Uxbridge, UK, 1976.

[30] S. Mindess, J. F. Young, and D. Darwin, *Concrete*, Prentice Hall, Upper Saddle River, NJ, USA, 2nd edition, 2002.

[31] K. B. Najim and M. R. Hall, "A review of the fresh/hardened properties and applications for plain- (PRC) and self-compacting rubberised concrete (SCRC)," *Construction and Building Materials*, vol. 24, no. 11, pp. 2043–2051, 2010.

[32] B. S. Mohammed, N. J. Azmi, and M. Abdullahi, "Evaluation of rubbercrete based on ultrasonic pulse velocity and rebound hammer tests," *Construction and Building Materials*, vol. 25, no. 3, pp. 1388–1397, 2011.

[33] A. Mirmiran and Y. Wei, "Damage assessment of FRP-encased concrete using ultrasonic pulse velocity," *Journal of Engineering Mechanics*, vol. 127, no. 2, pp. 126–135, 2001.

[34] K. Yildiz and L. O. Ugur, "Examination of durability of high performance concrete that has been subjected to $MgSO_4$ and NaCl corrosion against freezing and thawing," *Scientific Research and Essay*, vol. 4, no. 9, pp. 929–935, 2009.

[35] A. M. Neville, *Properties of Concrete*, Pearson Education, New Delhi, India, 4th edition, 1995.

Hindawi Publishing Corporation
Advances in Civil Engineering
Volume 2011, Article ID 478475, 12 pages
doi:10.1155/2011/478475

Research Article

Seismic Performance Comparison of a High-Content SDA Frame and Standard RC Frame

John W. van de Lindt[1] and R. Karthik Rechan[2]

[1] *Department of Civil, Construction, and Environmental Engineering, The University of Alabama, Tuscaloosa, AL 35487, USA*
[2] *Department of Civil and Environmental Engineering, Colorado State University, Campus Delivery 1372, Fort Collins, CO 80523-1372, USA*

Correspondence should be addressed to John W. van de Lindt, jwvandelindt@eng.ua.edu

Received 3 November 2010; Accepted 24 June 2011

Academic Editor: J. Antonio H. Carraro

This study presents the method and results of an experiment to study the seismic behavior of a concrete portal frame with fifty percent of its cement content replaced with a spray dryer ash (SDA). Based on multiple-shake-table tests, the high content SDA frame was found to perform as well as the standard concrete frame for two earthquakes exceeding design-level intensity earthquakes. Hence, from a purely seismic/structural standpoint, it may be possible to replace approximately fifty percent of cement in a concrete mix with SDA for the construction of structural members in high seismic zones. This would help significantly redirect spray dryer ash away from landfills, thus, providing a sustainable greener alternative to concrete that uses only Portland cement, or only a small percentage of SDA or fly ash.

1. Introduction

Ash is a byproduct obtained during the combustion of coal. Fly ash is generally obtained from the chimneys of coal-fired power plants. Depending on the amount of calcium, silica, iron, and alumina content of the ash there are two classes of fly ash as defined by ASTM C618, specifically Class C and Class F fly ash. Class C fly ash has high-calcium content, and its carbon content is usually less than two percent, while Class F fly ash has a low-calcium content with a carbon content usually less than five percent. Fly Ash, due to its pozzolanic properties is often used as an additive to Portland cement in concrete production. The use of fly ash in concrete increases the strength and durability of the concrete and also decreases the heat of hydration and permeability of the concrete. The use of fly ash in concrete helps to reduce environmental pollution, because for every ton of fly ash used to replace Portland cement in the manufacture of concrete, there is a reduction of carbon dioxide emissions which is, for example, equal to the amount of carbon dioxide generated from the average automobile during a two-month period [1]. Since the majority of SO_2 emissions into the atmosphere are due to coal fired power plants, many coal fired power plants in the United States are now utilizing spray dry absorbers for the reduction of these SO_2 gas emissions. The result is SDA which has material and behavioral properties similar to fly ash, but a different chemical makeup. In this process alkali sorbents such as lime (CaO) or calcium hydroxide ($Ca(OH)_2$) are mixed with water to form an aqueous slurry [2]. This slurry is sprayed into the flue gas in a cloud of fine droplets. SO_2 is then captured with this sorbent and is dried by the heat of the flue gases. The dried mix of the sorbent and SO_2 is collected. The ash utilized in the project described in this paper was from the Platte River Power Authority's Rawhide Power Plant (RPP) which uses the SDA system. The ash obtained from RPP power plant has a unit mass of 2.1 g/cc, and, due to its high sulphur content its chemical properties and mineralogical properties [3] are slightly different, and, therefore, it cannot be classified as Class C ash.

There have been numerous studies conducted on the use of ash in concrete. Swamy et al. [4] conducted tests

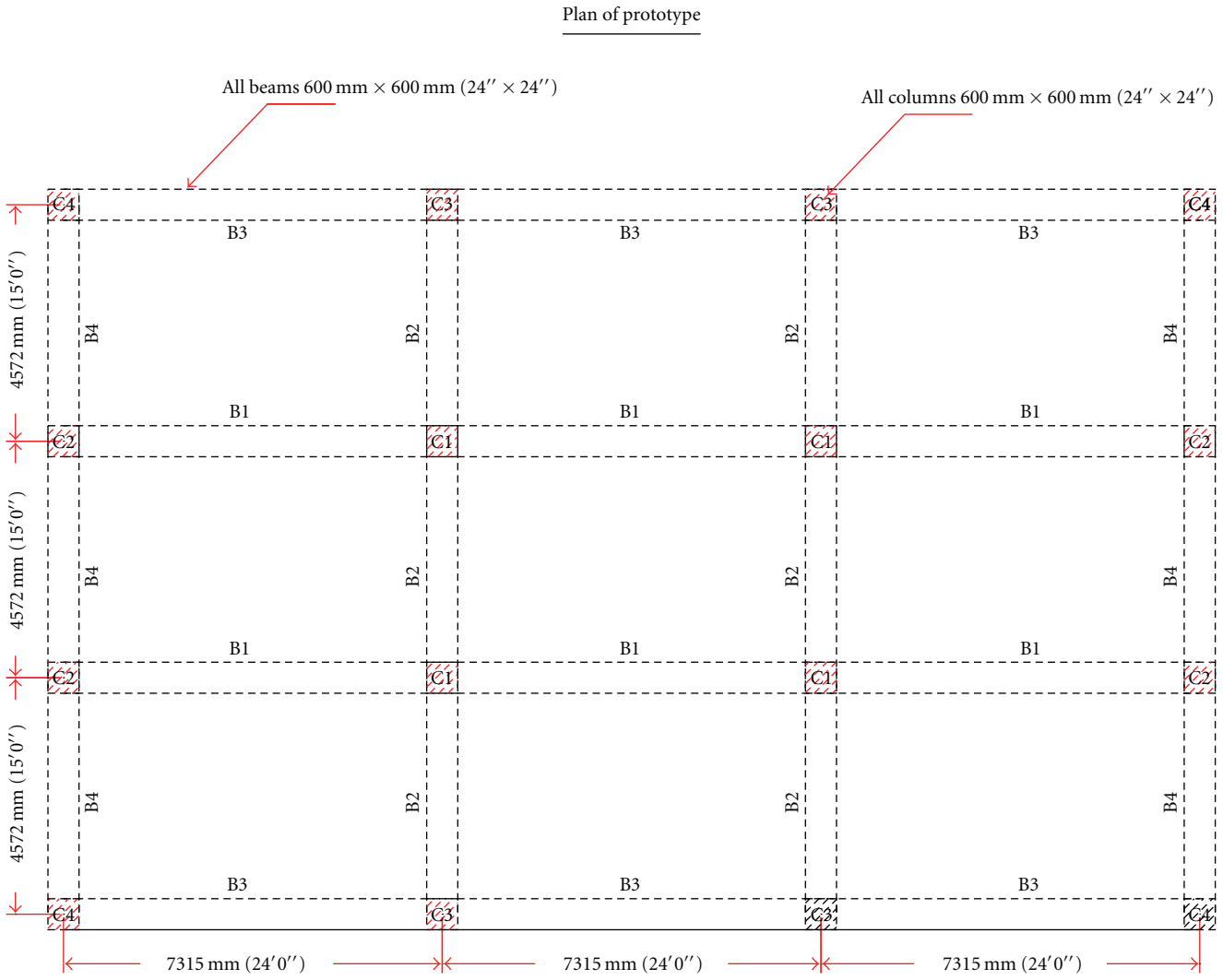

Figure 1: Plan of the prototype structure.

Figure 2: Experimental setup of the model on the shake table.

on reinforced concrete fly ash concrete beams and slabs containing normal weight aggregates and light weight aggregates. The results of their tests showed that concrete with fly ash can exhibit structural performance similar to that of conventional concrete with adequate safety factors used in existing design codes at the time. The results of their study also showed that structural concrete components can be designed to incorporate fly ash at quantities as high as 30 percent cement replacement, by weight.

Joshi et al. [5] studied the engineering properties of non-air-entrained concrete. Laboratory tests were conducted on both fly ash concrete and ordinary Portland cement concrete specimens. Based on properties such as compressive, flexural, indirect tensile strengths, and additional nondestructive tests, it was concluded that fly ash concrete could be used as a construction material for the core of a gravity dam and for pavement subbase. Hussain and Rasheeduzzafar [6] conducted accelerated corrosion tests on reinforced concrete specimens made of plain cement concrete and fly ash blended cement concrete. The results of the test showed superior corrosion resistance of fly ash concrete when compared to plain cement concrete. Pigeon and Malhotra [7] designed four high-volume fly ash-compacted concrete mixes by fixing

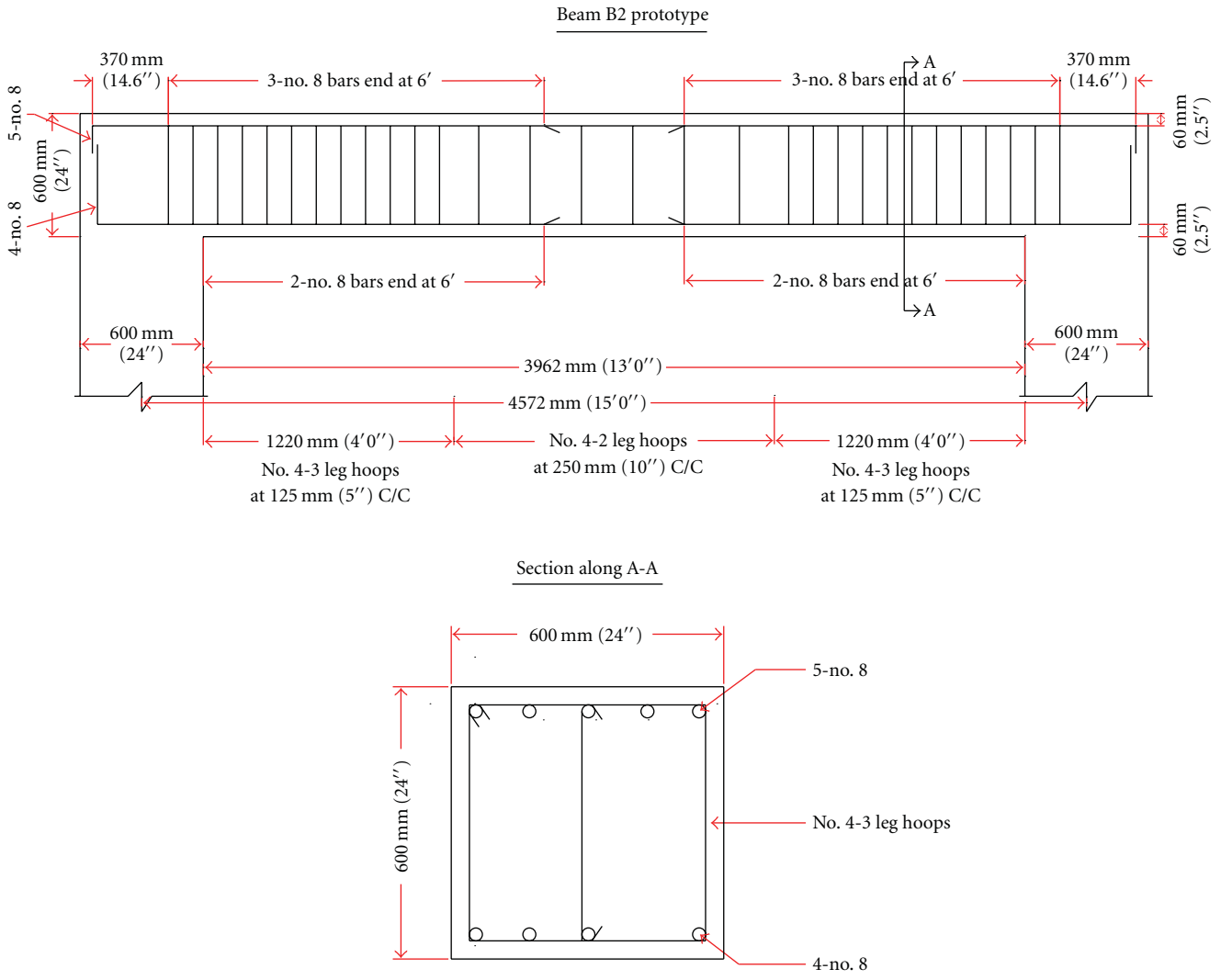

Figure 3: Reinforcement detail of prototype beam B2.

the amount of fly ash to the total cementitious material content. Laboratory investigations were carried out on air-entrained and non-air-entrained concrete mixes, and the results showed that frost resistance of air-entrained concrete mixes was slightly more than that of non-air-entrained concrete mixes. The results of this study recommended the use of air entrainment for roller-compacted high-volume fly ash concretes.

Dinelli et al. [9] conducted experiments to find the possibility of partial or complete substitution of traditional aggregates in light weight concrete with aggregates made of fly ash. The results of their experiments demonstrated that traditional aggregate could be substituted with aggregate made of fly ash. Fernandez-Jimenez et al. [10] studied the durability of alkali-activated fly ash (AAFA) cement under different conditions and in a number of aggressive environments such as deionized water, ASTM sea water, sodium sulphate, and acidic solutions. Studies were also made with respect to alkali-silica reaction-induced expansion. Weight loss, compressive strength, variations in volume, presence of the products of degradation, and microstructural changes were the chief parameters which were studied. The results of the study showed that AAFA cement pastes performed satisfactorily in aggressive environments, and the degradation of the materials resulting from such processes was distinctly different from that of the ordinary Portland cement paste. The AAFA mortars were found to be compliant with the 16-day expansion limit stipulated in ASTM standard C 1260-94 on potential alkali-silica reactivity.

Van de Lindt et al. [11] carried out a study to investigate the possibility of increasing the thermal efficiency of a light frame residential structure through the addition of fly ash-scrap tire fiber composite to traditional fiberglass insulation in light-frame wood residential construction. They found that the fly ash-scrap tire composite not only provided a sustainable supplement to traditional insulation but also helped to significantly reduce the environmental issues associated with the disposal of these materials by diverting

Table 1: Details of beam B1.

Case	Location	Sway direction	Mu, KN-m (k-ft)	Reinforcement provided	As, mm^2 (in^2)	pi Mn, KN-m (k-ft)	Mpr, KN-m (k-ft)
1	Exterior end Negative moment	Left	−591.27 (−436.1)	7-No 8	3,567.73 (5.53)	−656.80 (−484.43)	−888.41 (−655.26)
2	Exterior end Negative moment	Right	−591.27 (−436.1)	7-No 8	3,567.73 (5.53)	−656.80 (−484.43)	-888.41 (−655.26)
3	Exterior end Positive moment	Right	295.64 (218.05)	4-No 8	2,038.71 (3.16)	392.12 (289.21)	536.82 (395.94)
4	Exterior end Positive moment	Left	295.64 (218.05)	4-No 8	2,038.71 (3.16)	392.12 (289.21)	536.82 (395.94)
5	Midspan Positive moment		147.81 (109.02)	1-No 9			

Table 2: Details of beam B2.

Case	Location	Sway direction	Mu, KN-m (k-ft)	Reinforcement provided	As, mm^2 (in^2)	pi Mn, KN-m (k-ft)	Mpr, KN-m (k-ft)
1	Exterior end Negative moment	Left	−448.02 (−330.44)	5-No 8	2,548.38 (3.95)	−483.175 (−356.35)	−658.93 (−485.97)
2	Exterior end Negative moment	Right	−448.02 (−330.44)	5-No 8	2,548.38 (3.95)	−483.175 (−356.35)	−658.93 (−485.97)
3	Exterior end Positive moment	Right	295.64 (218.05)	4-No 8	2,038.71 (3.16)	323.23 (238.38)	443.75 (327.27)
4	Exterior end Positive moment	Left	295.64 (218.05)	4-No 8	2,038.71 (3.16)	323.23 (238.38)	443.75 (327.27)
5	Midspan Positive moment		83.91 (61.89)	2-No 8			

Table 3: Scale factors used for modeling.

Quantity	General case	Same material and acceleration (Model)	
		Required	Provided
Geometric length, l	$S_l = 3.0$	$S_l = 3.0$	$S_l = 3.0$
Elastic modulus, E	$S_E = 1.0$	$S_E = 1.0$	$S_E = 1.0$
Acceleration, a	$S_a = (= 1/S_l * S_E/S_\rho)$	$S_a = 1.0$	$S_a = 1.0$
Density, ρ	$S_\rho = S_E/(S_l S_a)$	$S_\rho = .33$	$S_\rho = 1.0$
Velocity, v	$S_v = \sqrt{(S_l S_a)}$	$S_v = 1.73$	$S_v = 1.73$
Forces, f	$S_f = S_E S_l^2$	$S_f = 9.0$	$S_f = 9.0$
Stress, σ	$S_\sigma = S_E$	$S_\sigma = 1.0$	$S_\sigma = 1.0$
Strain, ε	$S_\varepsilon = 1.0$	$S_\varepsilon = 1.0$	$S_\varepsilon = 1.0$
Area, A	$S_A = S_l^2$	$S_A = 9.0$	$S_A = 9.0$
Volume, V	$S_V = S_l^3$	$S_V = 27$	$S_V = 27.0$
Second moment of area, I	$S_I = S_l^4$	$S_I = 81$	$S_I = 81.0$
Mass, m	$S_m = S_\rho S_l^3$	$S_m = 9$	$S_m = 27$
Impulse, i	$S_i = S_l^3\sqrt{(S_\rho S_E)}$	$S_i = 15.59$	$S_i = 27$
Energy, e	$S_e = S_e S_l^3$	$S_e = 27.0$	$S_e = 27.0$
Frequency, ω	$S_\omega = 1/S_s\sqrt{(S_E/S_\rho)}$	$S_\omega = 0.58$	$S_\omega = 0.33$
Time (Period), t	$S_t = \sqrt{S_l/S_a}$	$S_t = 1.73$	$S_t = 1.73$
Gravitational acceleration, g	$S_g = 1.0$	$S_g = 1.0$	$S_g = 1.0$
Gravitational force, fg	$S_{\text{fg}} = S_\rho S_l^3$	$S_{\text{fg}} = 9.0$	$S_{\text{fg}} = 27.0$
Critical damping, ξ	$S_\xi = 1.0$	$S_\xi = 1.0$	$S_\xi = 1.0$

All the scale factors are obtained from [8].

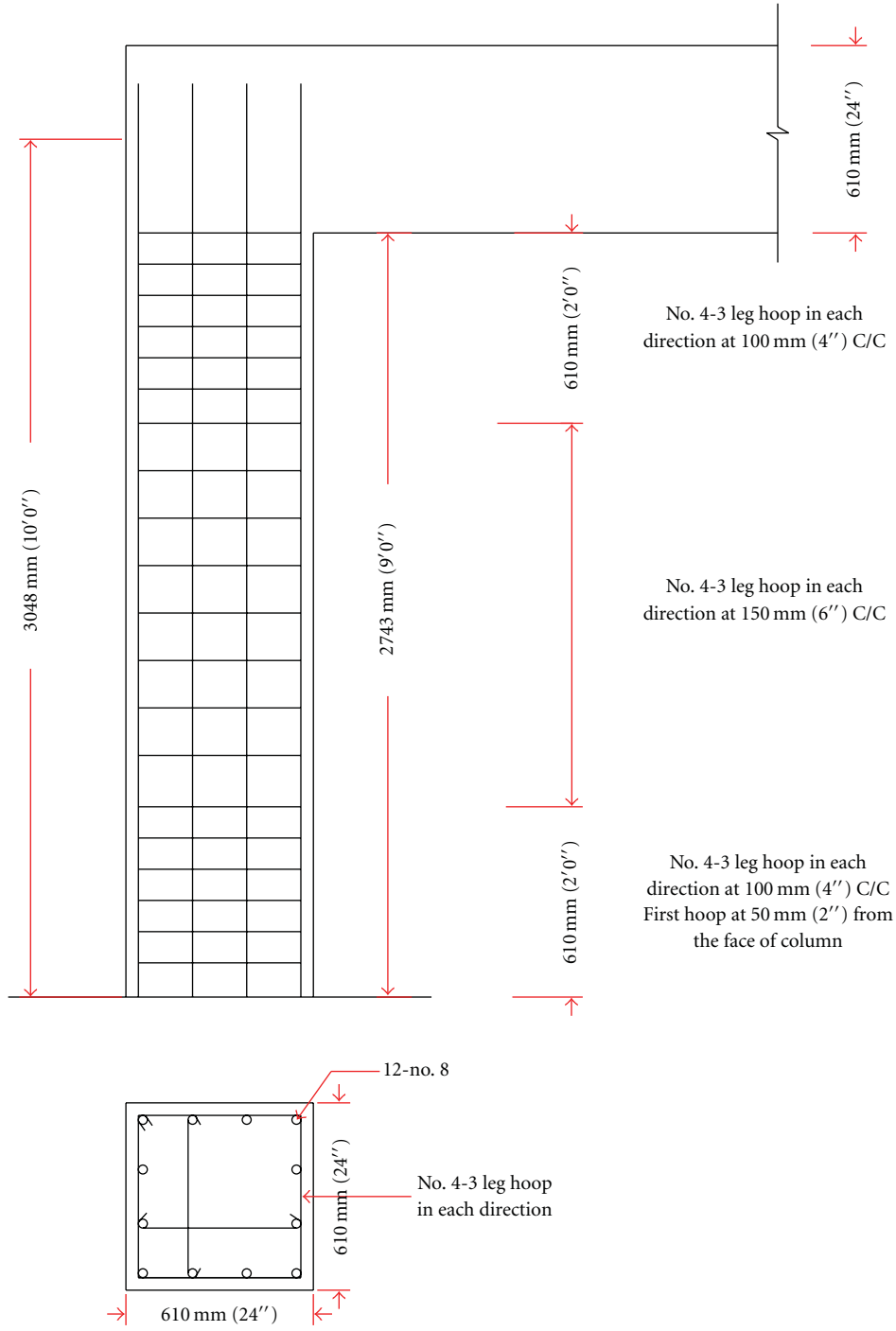

Figure 4: Reinforcement detail of the prototype column.

them from a landfill. Other numerous studies have been conducted over the past decades with most of them focusing on fly ash concrete and its use as a concrete additive.

The objective of this study was to evaluate the seismic behavior of concrete portal frames when replacing fifty percent of their cement content with spray dryer ash (SDA) and comparing that with the seismic behavior of ordinary Portland cement concrete frames when subjected to the same ground motions. Figure 1 shows the plan view of the three storey office building that served as the example building for this study. The building was designed for seismic load conditions per ASCE 7-05 [12] and seismic detailing according to ACI 318-05 [13] as if it were situated in Los Angeles, California. A mid bay portal frame was selected as the prototype frame, and, in total, four similar 1/3 scale models of this frame were constructed for testing. Two

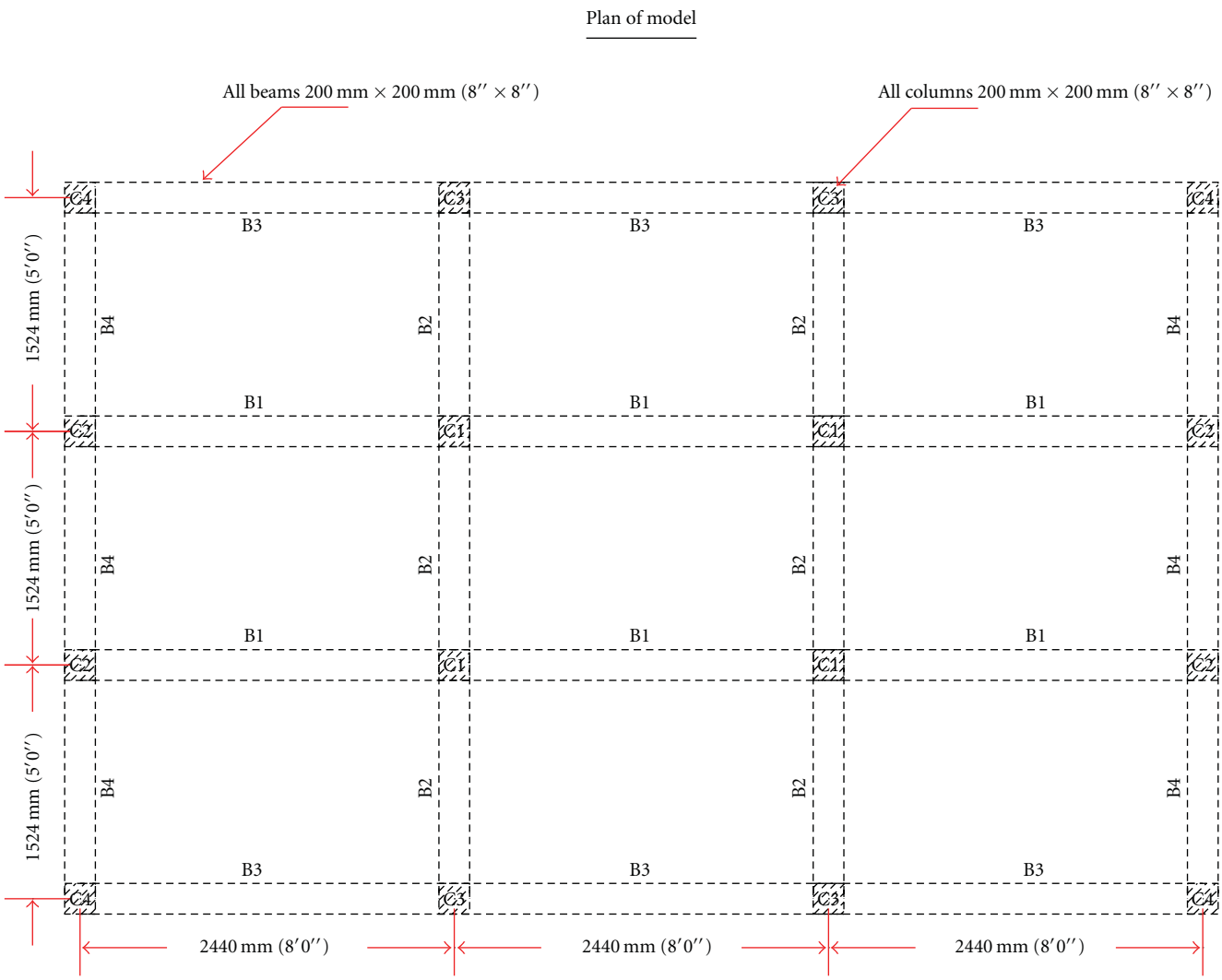

Figure 5: Plan of the 1/3rd scaled model.

Table 4: SDA concrete mix Design weights for 0.093 cubic meter (1 cubic foot) of 50% SDA concrete.

Type II Portland cement	5.07 kg (11.17 lb)
Spray dryer ash	5.07 kg (11.17 lb)
Sand	24.21 kg (53.38 lb)
19 mm (3/4″ coarse aggregate)	32.49 kg (71.62 lb)
Water	3.38 kg (7.46 lb)
High-range water reducer	3.3 mL
W/CM ratio	0.33
Compressive strength	MPa (psi)
7 days	20.04 (2907)
21 days	37.79 (5482)
28 days	46.91 (6803)

frames were constructed with fifty percent SDA concrete and the other two frames were constructed with ordinary Portland cement concrete.

Table 5: Type II Portland cement concrete mix design weights for 0.093 cubic meter (1 cubic foot) of concrete.

	kg (lb)
Water	6.44 (14.19)
Cement	14.94 (32.93)
19 mm (3/4″) coarse aggregate	22.68 (50.00)
Fine aggregate	90.72 (200)

2. Design and Construction

2.1. Frame Design. The frame tested on the shake table was selected from the center bay of a three story office building having three bays in both the X and Y directions as shown in Figure 1. The office building was selected such that there were no plan irregularities or vertical irregularities. A 200 mm (8 inch) thick reinforced concrete slab was assumed for the load calculations on beams. Design loads and load factors were selected as per the seismic load combinations from ASCE 7-05 [12]. The prototype frames were selected for

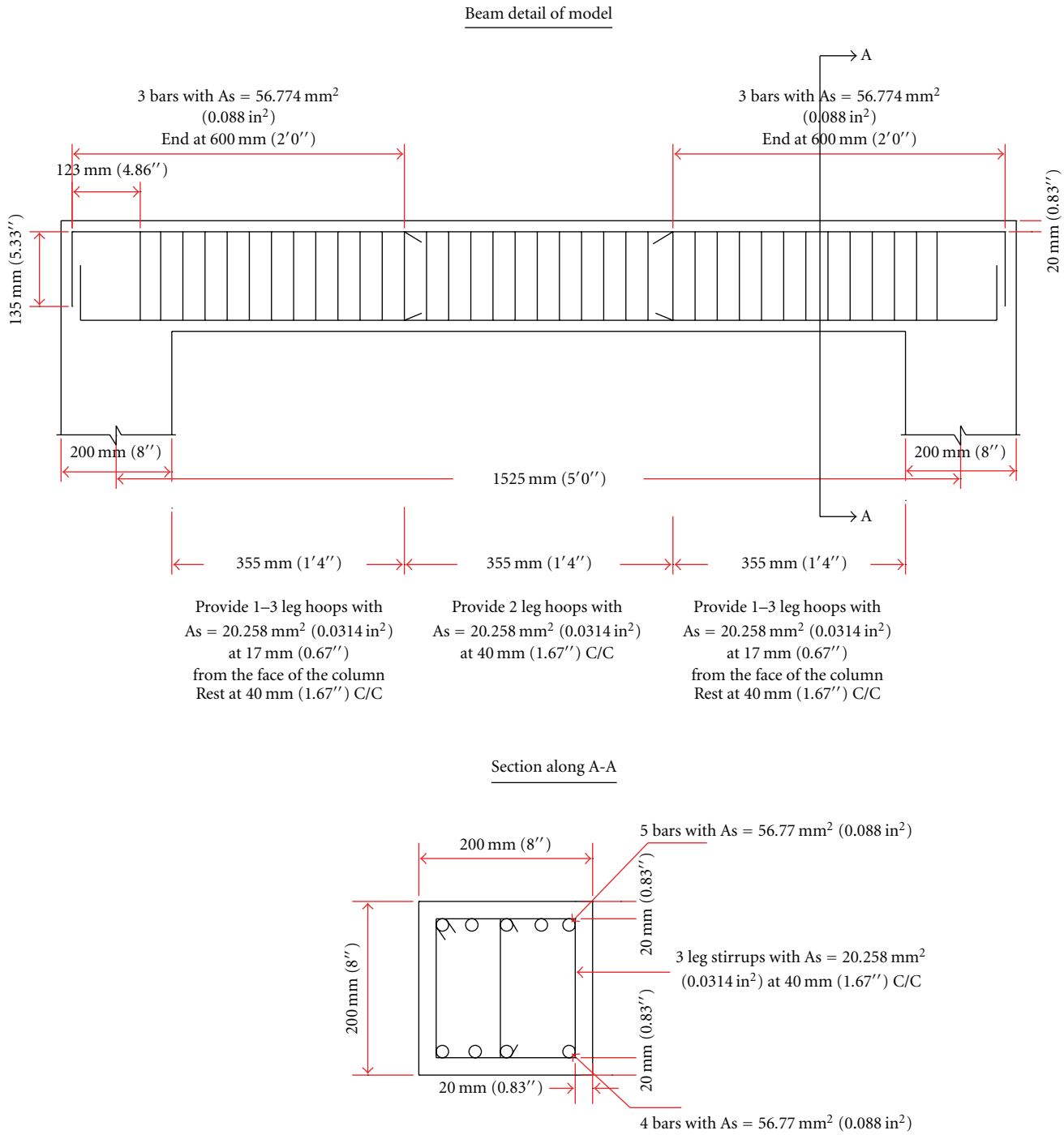

Figure 6: Reinforcement details of the 1/3rd scaled beam B2.

the design such that two 1/3 scaled frames were able to be placed parallel to each other and tested on the shake table. The frames were designed as reinforced concrete special moment frames (SMF) for seismic resistance as per seismic detailing provisions of ACI 318-05 [13]. The material strengths assumed for the design were ASTM Grade 60 steel, f_y = 414 MPa (60 ksi), and ordinary type II Portland cement concrete having a 28-day compressive strength of 27.6 MPa (4000 psi).

2.2. Beam Design. The beams were designed as the flexural members of special moment-resisting frames (SMRFs) according to special provisions for seismic design from chapter 21 of the American Concrete Institute code. The maximum design loads for the analysis of the frame were determined from the above load combinations and the storey shear was applied to each storey. The design shear forces are based on the factored dead loads, live loads, plus the shear due to hinging at the ends of the beams for the frames

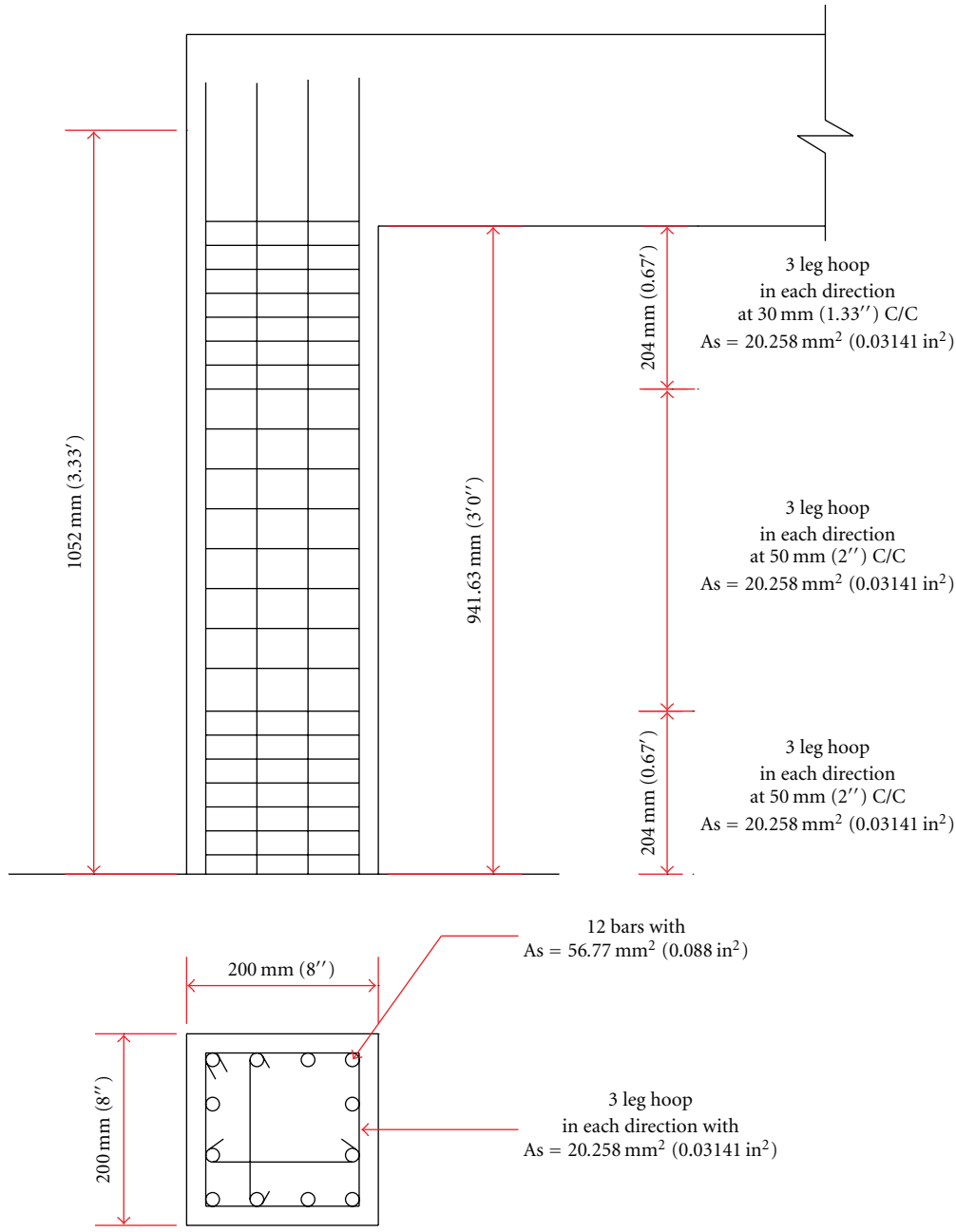

Figure 7: Reinforcement detail of the 1/3rd scaled column.

Table 6: Ground motion details of earthquakes used to excite the structure.

Earthquake event & year	File name	Station	Peak ground acceleration (g)
Northridge (1994)	Nor5	LA—Hollywood Storage	0.778
Landers (1992)	Lan1	Desert Hot Springs	0.875

swaying either to the left or to the right. Beams having cross-section (c/s) 609.6 mm × 609.6 mm (24″ × 24″) were designed according to section 21.3 of the ACI code. The ultimate moment, M_u, reinforcement selected for the beam c/s, nominal moment, φM_n, and the probable moment, M_{pr}, used in the design of the beams B1 and B2 are shown in Tables 1 and 2. The interested reader is referred to ACI 318-05 code for a detailed procedure of beam design for a SMRF. Figure 3 presents the resulting detailing of the reinforcement for the beams.

Figure 8: Formwork before pouring of concrete.

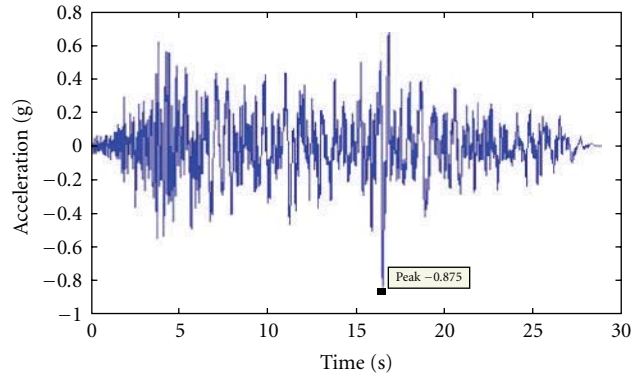

Figure 9: Time-compressed acceleration record for the 1992 Landers earthquake.

Table 7: Test sequence.

Test sequence	Ground motions	Peak ground acceleration (g)
1	Lan1	0.875
2	Nor5	0.778
3	Nor5	0.778
4	Nor5	0.778
5	Nor5	0.973

Figure 10: Shear crack in the column of the SDA concrete frame after test sequence 1.

2.3. Column Design. The Columns were designed as per ACI section 21.4.2 using the strong column weak beam concept. This type of design care is taken to ensure that plastic hinges first form in the beams and not in the columns; hence the risk of lateral instability (leading to collapse) is minimized. The prototype column had a cross-section 608 mm × 608 mm (24″ × 24″) with 12-#8 bars; however, the interaction diagram is not presented here for brevity. From the interaction diagram, $\sum M_{nc}$ was found to be 1,721.89 kN-m (1270 kip-ft) which is greater than 6/5 the value of $\sum M_{nb}$ which was found to be 967.62 kN-m (713.676 kip-ft) when no. 4 bars with 3 leg hoops in each direction are provided as per the requirements of the ACI code to resist shear and for the confinement of longitudinal bars in the column. The beam column joint was designed as per section 21.5 of the ACI code. The detailing of the prototype column is shown in Figure 4.

2.4. Model Scaling Law. The model was scaled by using the Buckingham pi theorem [14]. The Buckingham pi theorem states that any dimensionally homogenous equation involving certain physical quantities can be reduced to an equivalent equation involving a complete set of dimensionless products. Figure 5 shows the plan view for the one-third scale model of the prototype. Design and properties of one third scale model structures have been tested successfully before (see, e.g., [8]). The length factor used for scaling is 3 and Table 3 shows the scale factors for other quantities. The reinforcement bars provided for the prototype beams and columns to resist flexure and shear are no. 8 and no. 4 bars having yield strength of 413.68 MPa (60 ksi). The cross-sectional areas of no. 8 and no. 4 grade 60 bars are 509.68 mm^2 (0.79 in^2) and 129.03 mm^2 (0.2 in^2), respectively. Hence, by referring to Table 3, one can see that a yield force scale factor of 9 is used to find the required area of the reinforcing steel in the model. Thus, bars having areas of 56.8 mm^2 (0.088 in^2) and 14.2 mm^2 (0.022 in^2) must be provided for reinforcement in the model. Threaded steel bar having a diameter of 9.52 mm (3/8″), that is, and cross-sectional area of 71 mm^2 (0.11 in^2) was used, and 5.08 mm (0.2″) diameter galvanized steel wires having cross-area of 20.3 mm^2 (0.0314 in^2) were used as flexural and shear reinforcement in model, respectively. All-thread rods were used instead of no. 3 rebar as the effective area excluding threads is less than that of no. 3 rebar and close to the required area of 56.8 mm^2 (0.088 in^2). Figures 6 and 7 show the reinforcement details of the model.

2.5. Mix Designs. The material properties and compressive strength of the model and the prototype are considered to be the same; hence, the scale factor of one is considered for the mix design since the acceleration and the materials of the model and the prototype are the same, as can be seen in Table 3.

The mix design for the spray dryer ash (SDA) concrete mix was obtained from the study by King [15]. A few modifications were made to the mix design, specifically that SDA was used instead of Class F fly ash as mentioned in the original mix design. Fifty percent of cement and fifty percent of SDA were used for the mix instead of 45% of cement and

Table 8: Damage assessment of Portland cement concrete frame.

Test sequence	Portland cement concrete frame					
	Columns				Beams	
	C1	C2	C3	C4	B1	B1
1	—	—	—	—	—	—
2	—	Shear crack at the outer face of the beam-column joint	Shear crack at both inner and outer faces of the beam-column joints	Shear crack at the inner face of the beam-column joint	—	—
3	Shear crack at the outer face of the beam-column joint	Vertical crack extension towards the end of outer face of the column	Vertical crack extending till the end of the outer face of the column	—	—	Vertical crack at the end of the beam near column C3
4	Vertical crack on the outer face of the column	—	—	Shear crack at the outer face of the beam-column joint	—	—
5	—	—	—	—	—	—

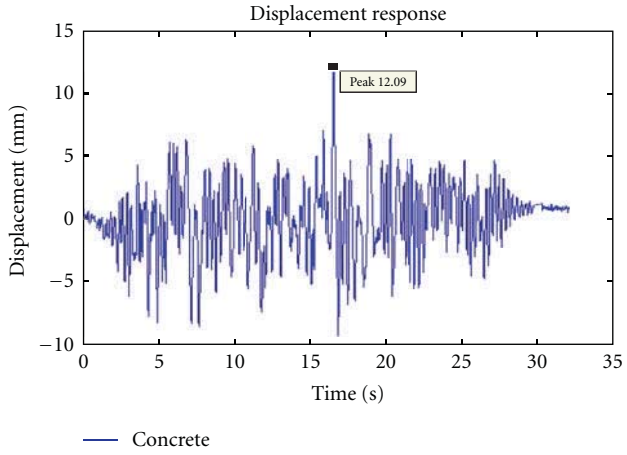

Figure 11: Displacement response of concrete frame, column after test sequence 1.

55% of fly ash as mentioned in their original mix design. Only 19 mm (3/4″) diameter coarse aggregate was used since the model was 1/3 scale, and high-range water reducers were used as mentioned in the mix design. The mix design and the obtained compressive strengths of the SDA concrete are shown in Table 4 and this mix designs for Portland Cement Concrete is shown in Table 5.

Both mix designs targeted a 28-day compressive strength of 31.03 MPa (4500 psi). Both mix designs resulted in compressive strengths exceeding the desired compressive strength but were felt to be reasonable to achieve comparative results and to assess whether a 50% SDA content mix could be used in seismic design. Qualitatively, this difference was accounted for in the performance comparison in the conclusions.

3. Experimental Setup

A 4.57 m (15′) long 1/3 scale portal frame from the center bay of the plan (see Figure 5) was selected for design, construction, and testing. Four portal frames were constructed in total for the experiment. Specifically, two frames were made of ordinary Portland cement concrete having a compressive strength of 56.33 MPa (8170 psi), and two frames were made of concrete in which 50% of the cement was replaced with SDA, having a compressive strength of 46.91 MPa (6803 psi). Figure 8 shows the setup of the formwork just prior to pouring. The column bars were extended about 150 mm (6 inches) out of the formwork so that the two frames could be tied together while testing thus restricting them from out of plane motion. The SDA concrete was poured, and then plain cement concrete was poured into the remaining formwork one day apart. The concrete was allowed to cure for 28 days, and the models were deemed ready for testing. The seismic mass was calculated using a mass similitude factor of 9, by referring to Table 3 and by using the mass similitude procedure outlined in Bracci et al. [8]. The seismic mass to be placed on the model was found to be 8000 kg (17600 lb). Figure 2 shows the setup of models with the seismic mass on the shake table just prior to testing. Three displacement gauges were used to measure the displacement of the frames, one at the neutral axis of each beam and one for shake table displacement.

4. Seismic Test Program

The portal frames were both tested on the uniaxial shake table at Colorado State University using a total of five different earthquakes in succession. The Canoga Park recording of the 1994 Northridge, California earthquake (recorded at a site known as the Hollywood storage facility) and 1992 Landers earthquake were selected as input ground motions. Table 6 provides the peak ground motion details for the scaling of the records used to excite the structure, and Table 7 shows the name, peak ground acceleration, and the test sequence of the earthquakes used in the test of each specimen. Figure 9 shows the time-compressed acceleration response for the 1992 Landers earthquake. The 1994 Northridge earthquake record is not shown here for brevity. Referring to Table 3, one can see that the time

Table 9: Damage assessment of SDA concrete frame.

Test sequence	SDA concrete frame					
	Columns				Beams	
	C1	C2	C3	C4	B1	B2
1	A thick crack at the outer face of the column edge	—	—	Shear crack at the inner face of the beam-column joint	—	—
2	—	—	2 Vertical cracks on the outer face of the column	Vertical crack on the outer face of the column	—	—
3	Diagonal crack at the outer face of the column	—	Vertical crack on the outer face of column	—	—	—
4	—	—	Shear crack at the inner face of the beam-column joint	Shear crack at the inner face of the beam-column joint	—	Vertical crack on the inner face of the beam near column C4
5	—	—	(a) Horizontal crack exactly below the beam-column joint of column C3 and beam B2 (b) Vertical crack at mid height on outer face of the column	(a) Extended vertical crack on the outer face of the column (b) Base of the column damaged (c) Vertical crack at the mid height of the column (d) Horizontal crack exactly below the beam column joint of the column and beam B2	—	—

Table 10: Peak displacement response values of concrete and SDA concrete frames.

Test sequence	Peak displacement response values			
	Concrete frames		SDA concrete frames	
	Column C2, mm	Column C3, mm	Column C2, mm	ColumnC3, mm
1	12.09	11.24	13.85	8.44
2	11.94	10.6	11.46	9.77
3	9.99	10.46	12.89	11.87
4	11.24	10.4	14	9.88
5	13.74	13.46	12.9	11.53

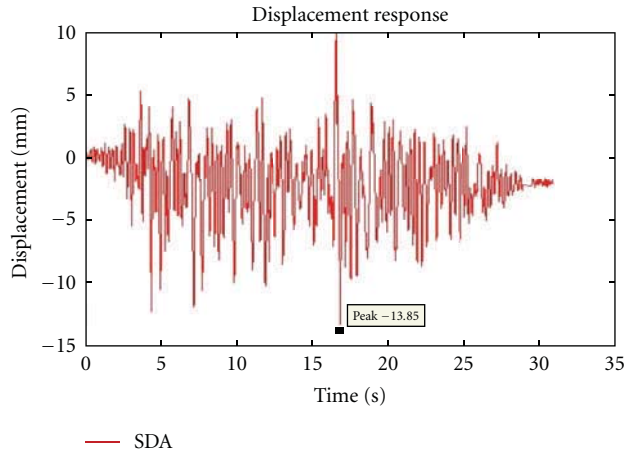

Figure 12: Displacement response of SDA concrete frame, column after test sequence 1.

was scaled by a square root of the length factor. Since the scale factor for acceleration is unity, input acceleration values remain unchanged and time is simply compressed by 1/sqrt(3).

The concrete and SDA frame models were tested on the shake table in the sequence shown in Table 7. Tables 8 and 9 provide a summary of the damage assessment after each test sequence for the Portland cement concrete and SDA concrete frames, respectively.

Referring to the peak responses in Table 10, the peak displacement values of column C3 and Column C2 after test sequence 1 for the Portland cement concrete frame were approximately equal to the peak displacements of Column C3 and Column C2 in the SDA concrete frame. Figure 10 shows a typical shear crack observed in the SDA frame columns after the test sequence. Figures 11 and 12 present the time history of the displacement response for Test 1 at the top of the column for the Portland cement and SDA concrete frames, respectively. Through the inspection of these figures, the one can see that the dynamic behavior is very similar for both the frame types.

By comparing the damage and peak displacement response values in Table 10, it can be seen that until test 2 both the SDA concrete frame and Portland cement concrete frame behaved in a similar manner with respect to their damage levels for the same ground motions, with the exception of the small shear crack. From test 3 to test 4, it can be seen that the Portland cement concrete frame began to perform better than the SDA concrete frame from

a displacement perspective although similar damage was observed in both the frames. After test 5, the SDA frame had suffered slightly more damage overall when compared to that of the concrete frame, but the difference was felt to be negligible considering the number and intensity of the ground motions used as input during the tests. Additionally, the SDA frame, even after being damaged in tests 3 and 4, had a slightly lower peak displacement in test 5.

5. Summary and Conclusions

The objective of this study was to compare the experimental seismic performance of 1/3 scale high SDA content concrete portal frames to conventional Portland cement concrete portal frames when subjected to the same series of earthquake ground motions. By comparing the damage levels and displacement response plots of the SDA frame to that of the Portland cement concrete frame after each earthquake, little difference was found in the response of the frames. It was only after test 3 that the SDA frame did not perform as well when compared to that of the Portland cement concrete frame. However, by the end of test 5 they had performed approximately equally. All three of these shakes were more intense than the current design-basis earthquake for the location these frames were designed. Development of shear cracks at the beam column joints in both Portland cement concrete frames and SDA concrete frames after a test sequence indicated that the frames behaved as per the designed strong column-weak beam concept. Regardless, there was no significant damage or structural failure, such as a collapse, exhibited by either frame. From a strictly structural standpoint, it can be stated that up to fifty percent of cement could be replaced with SDA in a concrete mix in place of ordinary Portland cement concrete for the construction of structural members in high seismic zones. This is underscored by the fact that the SDA mix was slightly weaker in compressive strength and still performed, in general, the same as the Portland cement frame. However, work in the area of durability and corrosion of reinforcement is needed prior to actual implementation of such a high SDA content into structural concrete. Clearly, if this can be studied and shown to be also viable from a ductility standpoint, then contents as high as 50% SDA can be utilized thus reducing the cost of construction. Further, SDA can be recycled and diverted from landfills, thereby moving towards greener construction.

References

[1] Environmental Protection Agency (EPA), April 2010, http://www.epa.gov .

[2] L. V. Heebink, "A review of literature related to the use of spray dryer absorber material. Production, characterization, utilization applications, barriers, and recommendations," Tech. Rep. 1014915, Electric Power Research Institute, 2007.

[3] C. E. Riley, *High-volume use of self-cementing spray dry absorber material for structural applications*, Ph.D. dissertation, Colorado State University, Fort Collins, Colo, USA, 2009.

[4] N. Swamy, A. Sami, R. Ali, and D. D. Theodorakopoulos, "Early strength fly ash concrete for structural applications," *ACI Journal Proceedings*, vol. 80, no. 5, pp. 414–423, 1983.

[5] R. C. Joshi, J. M. Oswell, and G. S. Natt, "Laboratory investigations on concrete and geocrete with high fly ash contents," in *Proceedings of the International Ash Utilization Symposium and Exposition*, vol. 2, 1985.

[6] S. E. Hussain and Rasheeduzzafar, "Corrosion-resistance performance of fly-ash blended cement concrete," *ACI Materials Journal*, vol. 91, no. 3, pp. 264–272, 1994.

[7] M. Pigeon and V. M. Malhotra, "Frost resistance of roller-compacted high-volume fly ash concrete," *Journal of Materials in Civil Engineering*, vol. 7, no. 4, pp. 208–211, 1995.

[8] J. M. Bracci, A. M. Reinhorn, and J. B. Mander, "Seismic resistance of reinforced concrete frame structures designed only for gravity loads—part I: design and properties of one-third scale model structure," Tech. Rep. NCEER -92-0027, 1992.

[9] G. Dinelli, G. Belz, C. E. Majorana, and B. A. Schrefler, "Experimental investigation on the use of fly ash for lightweight precast structural elements," *Materials and Structures/Materiaux et Constructions*, vol. 29, no. 194, pp. 632–638, 1996.

[10] A. Fernandez-Jimenez, I. García-Lodeiro, and A. Palomo, "Durability of alkali-activated fly ash cementitious materials," *Journals of Material Science*, vol. 42, no. 9, pp. 3055–3065, 2007.

[11] J. W. van de Lindt, J. A. H. Carraro, P. R. Heyliger, and C. Choi, "Application and feasibility of coal fly ash and scrap tire fiber as wood wall insulation supplements in residential buildings," *Resources, Conservation and Recycling*, vol. 52, no. 10, pp. 1235–1240, 2008.

[12] ASCE, *Minimum Design Loads for Buildings and other Structures*, American Society of Civil Engineering; Structural Engineering Institute, Reston, Va, USA, 2005.

[13] E. Buckingham, "The principle of similitude," *Nature*, vol. 96, no. 2406, pp. 396–397, 1915.

[14] ACI, *Building Code Requirements for Structural Concrete*, American concrete Institute 318-05, 2005.

[15] B. King, *Making of Better Concrete, Guidelines to Using Fly Ash for High Quality Eco-Friendly Structures*, Green Building Press, 2005.

Hindawi Publishing Corporation
Advances in Civil Engineering
Volume 2011, Article ID 526256, 9 pages
doi:10.1155/2011/526256

Research Article

A Case History Study of the Recycling Efforts from the United States Army Corps of Engineers Hurricane Katrina Debris Removal Mission in Mississippi

Dennis Leroy Brandon, Victor Frank Medina, and Agnes Belinda Morrow

Engineer Research and Development Center, US Army Corps of Engineers, 3909 Halls Ferry Road, Vicksburg, MS 39180, USA

Correspondence should be addressed to Dennis Leroy Brandon, dennis.l.brandon@usace.army.mil

Received 1 March 2011; Revised 9 June 2011; Accepted 15 June 2011

Academic Editor: Monica Prezzi

In support of the Federal Emergency Management Agency (FEMA), the US Army Corps of Engineers (USACE) managed the removal of Hurricane Katrina storm debris in several states. This paper focuses on the debris removal practices in 16 southern Mississippi counties and the recycling efforts. Debris was removed from public and private property. The debris included vegetation, construction material, electronic waste, vehicles, and vessels. The scope of the USACE mission was expanded several times. The scope within the respective counties varied from vegetation only to the removal of every eligible form of debris. The recommendations proposed should enhance recycling efforts during future debris removal missions.

1. Introduction

Hurricane Katrina was the costliest natural disaster in American history, generating more than 90.2 million m^3 of debris across Louisiana, and Mississippi. The Federal Emergency Management Agency (FEMA) assigned the US Army Corps of Engineers (USACE) responsibility for debris removal in localities where local governments were not capable of handling debris removal [1]. The USACE Vicksburg District managed the removal of more than 15.1 million m^3 of debris from 16 southern MS counties (Figure 1): Clarke, Covington, Forrest, George, Greene, Hancock, Harrison, Jackson, Jones, Lamar, Leake, Lincoln, Newton, Perry, Pike, and Walthall [2]. The extent of the USACE mission in each county was determined by the county supervisors or the governing officials in each municipality. Debris removal was conducted between September 2005 and September 2006, and was essentially complete in the northern counties by April 2006. In Hancock, Harrison, and Jackson counties, debris removal continued until September 2006. In these counties, the USACE's expanded mission included debris removal from swimming pools, the removal of concrete foundations, and the removal of vehicles and vessels. This paper reviews the procedures utilized during Hurricane Katrina debris removal and the recycling practices during that mission. In addition, the paper recommends changes from the Katrina experience to enhance recycling.

2. Description of the Corps of Engineers Debris Removal Mission

2.1. Goals of the Federal Debris Removal Mission. The debris removal goal of USACE was to manage all storm debris in a timely, efficient, cost-effective manner that also achieves environmental compliance [3]. To be eligible for removal by the Federal response, the debris removal must be in the "public interest," which was defined as (1) eliminates immediate threats to life, public health and safety, (2) eliminates immediate threats of significant damage to improved property, and (3) ensures economic recovery of the affected community to benefit the community at large [3]. If debris did not meet this criteria, then its removal was the responsibility of the local land owner or the municipality.

2.2. Debris Categories. The debris was categorized as vegetative, household hazardous waste, construction and demolition, white goods, electronic, vehicular, or marine vessel.

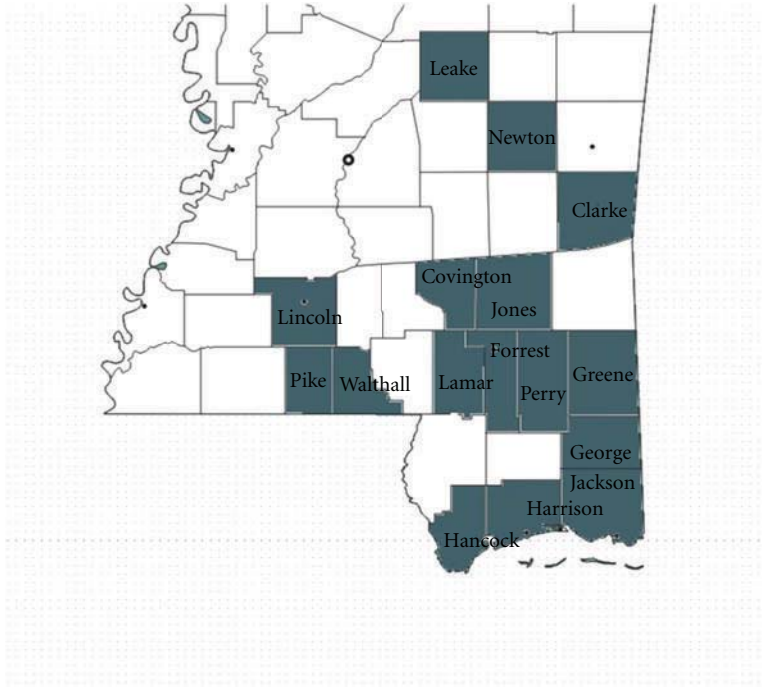

Figure 1: Mississippi County map. Counties that had their debris removal missions managed by the USACE are shaded and have name labels.

Vegetative debris consists of whole trees, tree stumps, tree branches, tree trunks, and other leafy material. A tree is considered hazardous if it is an immediate threat to lives, public health, and safety, or improved property. Leaners are trees leaning at an angle greater than 30 degrees. Hangers are damaged limbs still hanging from tree branches [3]. Leaners and hangers are an immediate threat to life and safety. Leaners and hangers constitute a significant proportion of the vegetative debris removed. Household hazardous waste is used or leftover contents of consumer products that contain chemicals defined in regulatory terms under the Resource Conservation and Recovery Act. These wastes appear on one of the four hazardous waste lists or exhibit one of the following characteristics: ignitability, corrosivity, reactivity, or toxicity. Examples of household hazardous waste include small quantities of normal household cleaning and maintenance products, latex and oil based paint, cleaning solvents, gasoline, oils, swimming pool chemicals, pesticides, and propane gas cylinders. Construction and demolition debris can be defined as damaged components of buildings and structures such as lumber and wood, gypsum wallboard, glass, metal, roofing material, tile, carpeting and floor coverings, window coverings, pipe, concrete, fully cured asphalt, equipment, furnishings, and fixtures. White goods were defined as discarded household appliances such as refrigerators, freezers, air conditions, heat pumps, ovens, ranges, microwave ovens, space heaters, dishwashers, washing machines, clothes dryers and water heaters. Many white goods contain ozone-depleting refrigerants, mercury, or compressor oils that required removal and processing to protect the environment before the white goods could be recycled. Electronic waste (e-waste) refers to electronics that contain hazardous materials, such as cathode ray tubes, computer monitors and televisions. Typically, these products contain minerals and chemicals that require specific disposal methods [3]. Vehicular refer to automobiles, trucks, bases, campers, motorcycles, and golf carts. Marine vessels include boats, trailers, and jet skis.

2.3. Types of Removal. The debris removal efforts were classified as either right of entry (ROE) or right of way (ROW). ROE involves debris removal from private property that was conducted to meet the goals discussed above. Because it involved access to private property, ROE removals required documentation by which a property owner confers to the USACE the right to enter onto private property for debris removal without committing trespass. In instances where the property owner was not available, the USACE obtained documentation from the local government to conduct debris removal. The USACE created an ROE file for each parcel entered. The ROE file documented site hazard assessments, coordination with the owner and subcontractor(s), FEMA approval and any historical preservation society assessment. ROW refers to portions of land over which facilities such as highways, railroads, or power lines are built. These are generally public lands and included land on both sides of the facility up to a private property line [3]. The types of debris placed in the ROW or removed through ROE were determined by local governing officials.

2.4. Debris Management. Figure 2 outlines USACE debris management procedures used during the Hurricane Katrina response. Vegetative debris, construction and demolition

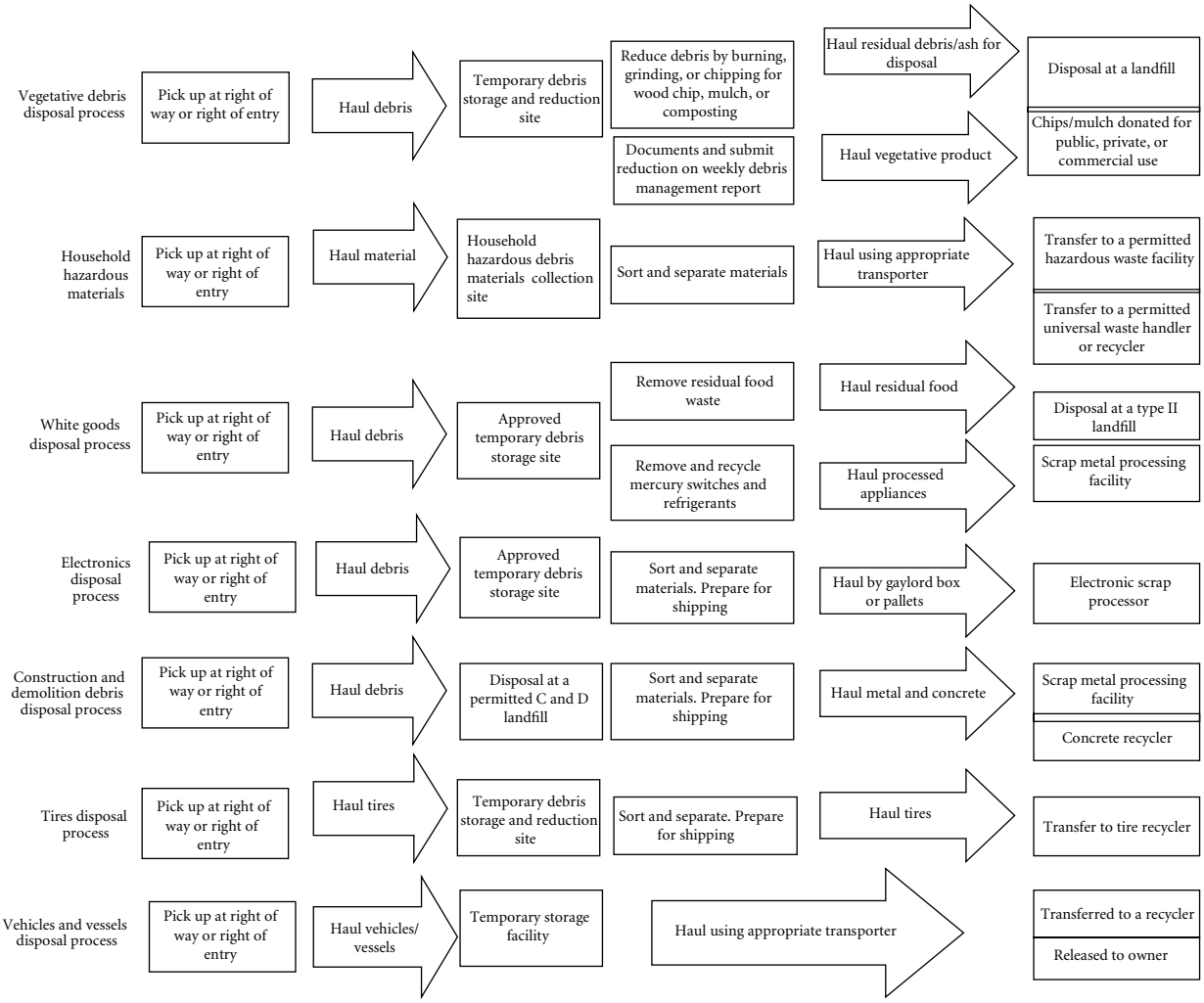

Figure 2

debris, household hazardous waste, white goods, and electronic wastes were segregated and placed in the ROW. Generally, homogenous loads of vegetative debris, white goods, and electronic wastes were transported to temporary debris storage and reduction sites (TDSRS), placed in separate storage locations, further processed, and then reduced or transferred to a recycling facility. Construction and demolition debris was transported to permitted landfills or TDSRS. Household hazardous waste was hauled to collection sites, sorted, and transported to permitted hazardous waste facilities or universal waste handlers. ROE debris removal also involved homogeneous loads of debris removed from private property and debris placed in the ROW. The vegetative debris included downed trees and leaners and hangers removed from ROW or ROE. These were transported to TDSRS sites. The construction and demolition debris was derived from demolition, structural collapse, or offsite sources.

TDSRS were established to facilitate waste reduction and reuse. The USACE established 44 TDSRS in 16 southern Mississippi counties, which were used exclusively for the USACE removal mission (Table 1). TDSRS were established on private property, public property, and permitted landfills [4–6]. Table 2 provides basic debris management costs from the USACE contract with AshBritt Environmental, who served as the primary contractor [2]. Additionally, the USACE performed the removal of storm-damaged vehicles, vessels and removed debris from swimming pools in selected jurisdictions [7]. The USACE base plan was to achieve all debris removal using cost elements of the AshBritt contract. The cost savings discussed in this paper are reductions from the base plan. These costs do not include USACE administrative costs.

2.5. Recycling in the Debris Removal Mission. Recycling disaster-related debris has financial and environmental advantages. These operations can decrease the overall cost of a debris removal operation by reducing the amount of debris that is taken to a landfill. This diminishes the cost of final disposition in the form of tipping fees, which are

Table 1: Debris (m^3) removed from ROE and/or ROW in 16 Mississippi counties.

County	Debris type[@]	Total debris	ROE	ROW	No. TDSRS	Vegetation reduction
Clarke	V; CD	72,509	0	72,509	2	I (2)*
Covington	V; CD; HH; WG; EW	346,223	56,497	289,726	3	I (3)
Forrest	V; CD; HH; WG; EW	1,876,870	255,422	1,621,448	5	I (1); G (5)
George	V; CD; HH; WG; EW	480,970	165,658	315,312	2	G (1)
Greene	V	3,782	0	3,782	1	I (1)
Hancock	V; CD; HH; WG; EW;VV	4,137,377	1,617,215	2,520,162	6	I (1)
Harrison	V; CD; HH; WG; EW;VV	1,046,314	548,391	497,923	1	G (1)
Jackson	V; CD; HH; WG; EW;VV	3,324,483	609,073	2,715,410	6	G (1)
Jones	V; CD; WG	1,474,217	0	1,474,217	4	I (2); G (2)
Lamar	V; CD; HH; WG; EW	1,122,628	212,905	909,723	4	I (1); G (3)
Leake	V; CD	28,602	0	28,602	1	I (1)
Lincoln	V	82,301	0	82,301	2	G (2)
Newton	V; CD	79,820	0	79,820	1	I (1)
Perry	V; CD; HH; WG; EW	417,439	70,006	347,433	2	I (1); G (1)
Pike	V	252,811	0	252,811	2	G (2)
Walthall	V	395,686	0	395,686	2	G (2)
Grand Total		15,142,032	3,535,167	11,606,865	44	I(14); G(20)

[@] V: vegetative; CD: construction and demolition; HH: household hazardous waste; WG: white goods; EW: electronic wastes; VV: vehicles and vessels.
*I (#): incineration reduction method (no. TDSRS where incineration was used).
G (#): grinding reduction method (no. TDSRS where grinding was used).

Table 2: Basic debris management costs from the AshBritt environmental contract [2].

Task	Debris Management Costs
Debris hauling	\$20.93 to \$27.47 per m^3
Tipping fee	\$3.27 to \$4.58 per m^3
Reduction	\$5.89 per m^3
Haul reduced debris	\$6.54 per m^3
ROE debris removal	\$280.00 per crew hour
Extracted stumps	\$250.00 to \$700.00 each
Leaners and hangers	\$50.00 to \$400.00 each
Decommissioning structures	\$2,500.00 each
Demolition	\$45.00 per m^3
Segregation	\$230.00 per crew hour
QA/S&A/site management	\$6.54 per m^3
White goods with putrefied food removal	\$45.00 each

costs charged by landfills to dispose of solid waste in their facilities. In the case of recycling, potential end-use products for specific markets may offset the cost of operations [3].

Conversely, recycling efforts may conflict with the goals of the debris removal. Often, removal had to be done quickly—particularly when rapid removal was needed to create right of ways or to deal with an immediate safety hazard. Debris hauling vehicles usually did not contain separate compartments. Building demolitions many times could not, and even when they could were not, conducted in a step by step manner allowing for separation of recyclable components. However, recycling efforts were implemented in several areas and these are discussed in the next section.

2.6. Implementation of Recycling. The actions of the resident engineer, equipment selected by the subcontractors, and decisions by county and municipal officials were important in recycling performed during the Hurricane Katrina Response. The USACE established one regional office and several local offices that directed removal in one or more counties. Each office was managed by a resident engineer. Some of the recycling efforts discussed in this paper resulted from the personal initiatives of the resident engineer. Interestingly, resident engineers frequently changed positions during the cleanup, which sometimes resulted in changes in recycling efforts. Recycling efforts were also impacted by debris removal and reduction options utilized by contractors. Actual debris removal was conducted by contractors. The AshBritt contract did not specify which debris removal methods and reduction options would be utilized in any locality. In many cases, the contractors made decisions that affected recycling efforts. Finally, county and municipal officials affected recycling. These officials determined the types of debris removed. Because the debris removal requirements and vegetative debris reduction methods varied, county-to-county comparisons are difficult. Further, recycling and reuse efforts varied substantially from location to location and even over time.

3. Description of Recycling Efforts Undertaken as Part of the Corps of Engineers Debris Removal Mission

3.1. Recycling Vegetative Debris. Vegetative debris is generally not hazardous, but can be challenging because it is bulky and consumes a substantial volume of landfill space. During the USACE Katrina response, more than 85% of the vegetative

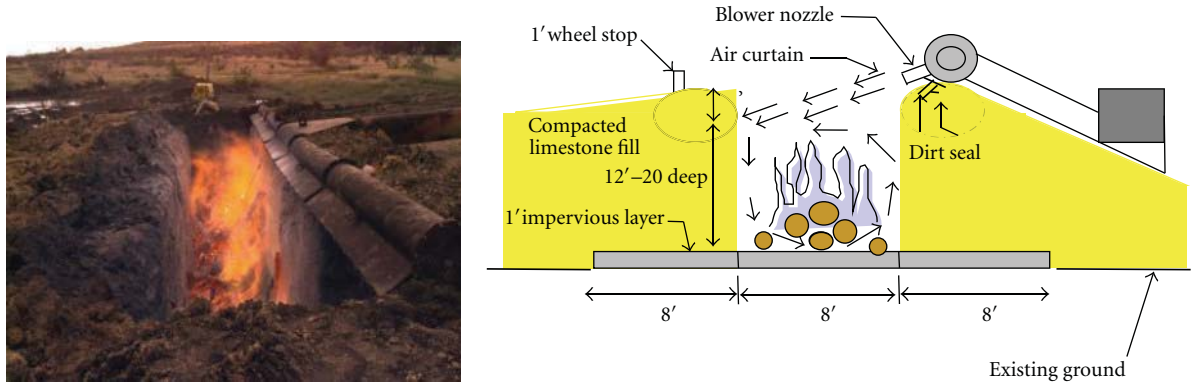

Figure 3: Below-grade air curtain incineration.

debris was hauled to TDSRS. Two methods of vegetative waste reduction were used: incineration and grinding. Air curtain pit (Figure 3) incineration was used at 14 TDSRS (Table 1). Incineration was a very effective means of volume reduction, reportedly achieving 95% volume reduction [3]. Although ash could have some recycling possibilities, such as filler material for bricks or for filler material in road construction, ash was not recycled as part of the USACE Katrina response.

Chipping/grinding operations were used at 20 TDSRS (Table 1), and reportedly achieved a volumetric reduction of up to 75% [3]. Chips ground from vegetative debris were used beneficially as landscaping mulch, and as a boiler fuel source. In several counties, all of the debris hauled to TDSRS was vegetative (Lincoln, Pike, Walthall). For example, in Pike County, 252,811 m^3 (Table 1) of vegetative debris resulted in approximately 63,203 m^3 of mulch. All of the mulch from these three counties was used beneficially. This accomplishment was aided by the local distribution of hand bills, publishing the availability of mulch in local newspapers and an agreement with a chip mill. The Walthall County agreement stated that [8] "... Jones Chip Mill will have the responsibility and obligation of removing and hauling all of the chipped/ground vegetative debris from each of the designated sites above at no cost to the Government ..." This allowed the USACE to save the typical reduced debris hauling and tipping fees (i.e., \$9.81–\$11.12 per m^3; Table 2). Assuming a \$10 hauling and tipping fee, the Pike County costs saved on mulch were over \$600,000. In some cases, large woody debris, such as logs, proved to be valuable resources without any reduction. For example, at one TDSRS in Walthall County, more than 900 logs were separated and donated to the property owner as part of the TDSRS agreement [6]. This resulted in a savings of \$15.70–\$17.01 per m^3 (Table 2). Assuming an average log diameter of 0.38 m and length of 3.05 m and a reduction, hauling, and tipping cost of \$16 per m^3, this resulted in a savings of just over \$5000.

Recycling of the vegetative material had several advantages. Valuable landfill space was conserved for other debris. The chipped vegetative material aided local residents in their recovery efforts and the industrial uses helped local industries, which aided the local economy in its recovery effort. For USACE, the costs savings resulting from landfill disposal costs more than offset any costs of the chipping/grinding operation. Overall, chipping and grinding the vegetative material created the greatest opportunity for recycling. However, this activity did create the potential for an undesirable outcome: fire. Smoldering occurred in several stockpiles of reduced vegetative debris in Lincoln and Pike counties (Figure 4). Mulch piles should be no higher than 4.57 m [3].

Figure 4: Smoldering chips in Lincoln County TDSRS in January 2006.

3.2. Building Materials. Prior to the demolition of any structures, site inspections were performed. These inspections assessed site utilities and identified site hazards (i.e., private wells, septic tanks, field lines, asbestos, flammable products, etc.). The demolition usually involved a trackhoe ripping the structure apart and loading fragments unto trucks. The construction debris was transported to landfills. Asphalt shingles, metal roofing and siding, bricks, CCA treated wood, untreated wood, and flooring materials were not segregated at the ROE (see Section 2.4).

Other household metal components were segregated on TDSRS (Figure 5), baled, and transported to scrap metal processing facilities. Home owners were permitted to move concrete foundations to the ROW for removal. Concrete was hauled to TDSRS (Figure 6) and placed in segregated

Figure 5: Metal segregated at the Firetower TDSRS in Harrison County, MS.

Figure 6: Concrete segregated at the Firetower TDSRS in Harrison County, MS.

Figure 7: White goods placed in ROW to facilitate easy pick up in Pass Christian, MS.

Figure 8: Refrigerant being reclaimed from white goods in Hancock County, MS.

locations. USACE personnel estimated there were 715 m^3 of concrete in Pass Christian, MS, ROW on July 4, 2006 [9]. Concrete from Pass Christian, MS, was used to create aquatic habitat.

3.3. White Goods. Figure 2 summarizes the management of white goods. White goods were placed in the ROW (Figure 7), and subsequently transported to TDSRS (Figure 8) where refrigerants were removed and reclaimed from refrigerators, freezers, and air conditioners by certified technicians [1]. White goods were subsequently compressed, baled, and transported to scrap metal recyclers (Figure 9). This process not only recycled these chemicals, but kept them out of the environment where they can cause environmental damage, particularly ozone depletion [10]. The USACE processed 45,648 white goods in Hancock County and 4,386 white goods in Pass Christian, MS [11].

3.4. Electronic Wastes. Figure 2 summarizes the management of electronic wastes. Electronic wastes were collected from the ROW and transferred to TDSRS. Figure 10 shows a typical collection of electronic components being prepared for transport. E-waste was wrapped on pallets prior to shipping to the recycler (Figure 11).

3.5. Vehicles and Marine Vessels. Vehicles (automobiles, trucks, bases, campers, motorcycles, and golf carts) and marine vessels (boats, trailers, and jet skis) were moved great distances by tidal surge water, flooding, and wind during Hurricane Katrina (Figures 12 and 13). These bulky items frequently blocked roads and access points needed by recovery teams. In addition, they leaked gasoline, diesel fuel, and other hazardous chemicals. Vehicles and vessels were removed from ROW and ROE. For example, in the Pass Christian area, 350 vehicles and 358 marine vessels were removed as part of the debris removal mission [12]. All vehicles and vessels were towed by commercial towing contractors to designated staging locations. Scrap metal from reduced vehicles and vessels was also recycled.

3.6. Tires. As part of the debris management process, tires were segregate at the TDSRS (Figure 14). Tires were subsequently transported to recycling facilities. At least 42.53 metric tons of tires were recycled from Harrison County. Tires from Hancock County were transported to Gulfport Tire Recycling. Documentation shows that 162.61 metric tons of tires were recycled [13].

3.7. Recovery of TDSRS Sites. Following the removal of all storm debris, TDSRS were restored to as near preworking conditions as possible. They were reseeded with either local grasses or tree seedlings as requested by the landowners. The US Fish and Wildlife Service evaluated the design and closure plans for all TDSRS [4, 14, 15].

Figure 9: White goods were compressed, baled, and shipped to recycling facilities. Picture provided courtesy of USACE.

Figure 10: Collection of electronic waste. Picture provided courtesy of USACE.

Figure 11: Electronic waste wrapped for shipping to electronic scrap processors. Picture provided courtesy of USACE.

Figure 12: Vehicles and Vessel removed from Pass Christian, MS.

4. Discussion

4.1. Recycling Vegetative Material Provides the Most Beneficial Effect. In review of the recycling efforts from Katrina, it is clear that recycling of plant material was the greatest success. Grinding and reuse of plant material created a valuable resource that was used in its entirety for those facilities that used this approach. In some cases, plant material was reused as whole logs. Focusing on vegetative material is critical, since this typically makes up a substantial portion of the debris generated during a large storm. All storm-related debris recovery plans should include plans for vegetative recycling.

Another opportunity could involve recycling of ash from burning of plant material. It is not clear if the volume of this material was large enough to justify a recycling effort, but uses for ash exist. Clean ash could be used as a material to make bricks and could also be used as a roadbase material [16].

4.2. Recycling Saves Valuable Landfill Space. The Hurricane Katrina generated more debris than any other natural disaster in US history, over $90 \times 10^6\,m^3$ [15]. For comparison, Hurricane Andrew (1992), for example, generated $33 \times 10^6\,m^3$ of debris in Metro Dade County, FL [17]. Hurricane Inike in Hawaii generated $3.8 \times 10^6\,m^3$, and Hurricane Hugo generated $1.5 \times 10^6\,m^3$ of plant waste. However, in all these cases, the solid waste generated by a disaster can overwhelm existing solid waste disposal systems. Hurricane Hugo's volume of plant debris was on the order of 5- to 15-times the annual solid waste produced in both North and South Carolina [17].

As shown in Table 1, the USACE debris mission in Mississippi totaled over 15 million m^3. If only 10% of this material could be recycled, that would result in a savings of 1.5 million m^3 of landfill space. Jackson is the largest city in the State of Mississippi with a Metro area population of over 500,000. According to a report in 2004, 2.72×10^6 metric tons of solid waste were disposed of in municipal landfills, which corresponds to about $5 \times 10^6\,m^3$ [18]. Therefore, even a 10% recycling rate would result in a substantial reduction in landfill use compared to normal solid waste operations. However, 10% recycling could be a very modest estimate of the potential.

4.3. Recycling Can Be an Effective Means of Dealing with Problematic Materials. Maximizing recovery and recycling could reduce landfilled wastes. Furthermore, recycling could be valuable for keeping problematic materials out of landfills. During Katrina, the recovery of refrigerants reduced the emission of these compounds into the atmosphere, where they could cause destruction of the ozone layer. Gypsum, which is frequently found in sheetrock, is a material that, if landfilled, can cause problem, as it can undergo anaerobic reaction to form foul smelling and potentially toxic hydrogen sulfide gas. However, it is possible to separate and recover

Figure 13: Vessel removed from Pass Christian, MS.

Figure 14: Tires segregated at Firestone TDSRS slated for recycling.

gypsum-containing sheetrock. The recovered gypsum can be utilized for stabilizing soil pH and can be used as a soil fertilizer [19–21].

4.4. Recycling of Debris Can Aid in Recovery. The debris itself, following separation/removal of any hazardous components, can also be a resource for the area to rebuild roads, buildings, and landfills. Inert soils and sediments, ground concrete, and mulched vegetative materials can be used for landfill covers, which are generally needed in large quantities. Concrete, asphalt road base, inert rocks, petroleum-contaminated soils, and ground asphalt shingles can be used by asphalt plants to repair or replace damaged roads [22]. Similarly, ground concrete, rocks, sand, and other materials can be used as aggregate for the new concrete needed for construction. Plant material can be composted and reused as fertilizer to promote new growth at damaged parks. Logs can be used to stabilize slopes and waterways [23]. For example, whole trees or large debris can be placed perpendicular to eroding banks to deflect the current and help to "train" the channel to a desired position. Studies on a Vermont river showed that adequate erosion protection was obtained for 4-5 years by using whole trees that were 0.6 to 0.9 m in diameter [24].

4.5. Building Demolition Is an Area of Potential Improvement. Building demolition can be a challenging issue; complicating building waste issues are home and office furniture, appliances, and computer equipment that is typically mixed with these wastes [25]. Furthermore, hazardous components can also be mixed in with the building material wastes, including asbestos (insulation in older homes, shingles, and flooring), lead (in lead-based paints and old plumbing systems), polychlorinated biphenyls (electrical transformers), chemicals and petroleum products, and mercury from electrical switching equipment [17, 23, 26]. However, the resulting building debris offers a tremendous opportunity for recycling. By assessing a building, before dismantling it, better results can be obtained regarding separation of hazardous and problem wastes and materials can be better recycled [25]. A program to develop guidance to rapidly assess buildings would be useful. Training programs could be developed to quickly train personnel in these techniques [23]. Phased demolition can maximize the recovery or reusable materials.

4.6. Staging Areas Are Critical for Reuse of Debris. Reuse and recycling requires staging areas where materials can be sorted and stockpiled. During Katrina, this was accomplished by establishing TDSRS sites. These areas proved to be very successful. Plans need to incorporate these areas for future disasters. In addition, plans need to include the restoration of these sites by regrading, planting, and so forth.

5. Conclusion and Recommendations

In conclusion, in spite of challenges due to the massive amount of debris generation, the USACE developed an effective approach for recycling debris. Development of TDSRS sites and policies on waste handling contributed to this success. Recycling saved valuable landfill space and provided useful products for recovery. The costs of recycling were partially offset by savings of landfill disposal costs. Strong planning is required for effective recycling to occur.

The USACE should modify the administrative staff to enhance the marketing and beneficial use of storm debris. This includes commercial and private use of reduced vegetative debris (i.e., chips, mulch, fertilizer, ash, etc.) and the use of logs for stream stabilization. This may involve modifying the contract to allow the USACE to determine the vegetative debris reduction method utilized in specific areas. Increased recycling of construction and demolition debris would require an enhanced assessment of structures and a better system of segregating components. The USACE should solicit proposals from recyclers willing to process segregated debris on TDSRS. Implementing these measures would increase USACE TDSRS costs but reduce the total USACE debris management costs (i.e., reduction, hauling, and/or tipping fees).

References

[1] Federal Emergency Management Agency, "Review of FEMA Guidance for Monitoring Debris Removal Operations for Hurricane Katrina," OIG-07-63 August 2007, http://www.dhs.gov/xoig/assets/mgmtrpts/OIG_07-63_Aug07.pdf.

[2] USACE, "Debris Management Overview Briefing," June 2006.

[3] Federal Emergency Management Agency, "Public Assistance Debris Management Guide," FEMA 325, July 2007, http://www.fema.gov/government/grant/pa/demagde.shtm#5.

[4] USACE Emergency Planning Response-Debris Removal Magnolia and MS Field Office, "Field Evaluation Summary for Lincoln, Pike and Walthall Counties, Mississippi for Temporary Debris Reduction Sites (TDRS)," November 2005.

[5] USACE Emergency Field Office—Central, "Hurricane Katrina Debris Reduction Sites (Site Evaluations) Harrison County, Mississippi," November 2005.

[6] USACE Emergency Planning Response—Debris Removal Magnolia and MS Field Office, "Agreement between Mr. Alton Harvey and the USACE," November 2005.

[7] USACE Emergency Field Office—Central, "Hazard mitigation of abandoned swimming pools in pass christian, MS," April 2006.

[8] USACE Emergency Planning Response—Debris Removal Magnolia and MS Field Office, "Agreement between Jones Chip Mill and the USACE," November 2005.

[9] USACE Emergency Field Office—Central, "Concrete and tree assessments in pass christian, MS," July 2006.

[10] Air Conditioning, Heating and Refrigeration Institute. (AHRI), "Refrigerants and our environment," 2009, http://phaseoutfacts.org/Content/RefrigernatsandOurEnvironment_35.aspx.

[11] USACE Vicksburg District, Hurricane Katrina Debris Removal Repository, Emergency Field Office—Central, 1180 General Corps of Engineers Contracts Correspondence Files, Dirty Whites—Pass Christian, 2006.

[12] USACE Vicksburg District, Hurricane Katrina Debris Removal Repository, Emergency Field Office—Central, 1180 General Corps of Engineers Contracts Correspondence Files, Vehicles and Vessels—Pass Christian, 2006.

[13] USACE Vicksburg District, Hurricane Katrina Debris Removal Repository, Emergency Field Office—West, 1180 General Administrative Files, Tire Haul Outs Hancock County, 2006.

[14] USACE Emergency Planning Response—Debris Removal Magnolia and MS Field Office, "Remediation plan harvey temporary reduction site walthall county," April 2006.

[15] M. Jadacki, *Review of FEMA Guidance for Monitoring Debris Removal Operations for Hurricane Katrina*, Department of Homeland Security, Office of Inspector General, Washington, DC, USA, 2007.

[16] C. B. Cheah and M. Ramli, "The implementation of wood waste ash as a partial cement replacement material in the production of structural grade concrete and mortar: an overview," *Resources, Conservation and Recycling*, vol. 55, no. 7, pp. 669–685, 2011.

[17] D. R. Reinhart and P. T. McCreanor, "Disaster debris management—planning tools," Final Report, University of Central Florida and Mercer University, September 1999, Prepared for EPA Region IV, http://www.cece.ucf.edu/people/reinhart/research/DDfinalreport.pdf.

[18] Mississippi Department of Environmental Quality, "Status Report on Solid waste disposal facilities calendar year 2004," Solid Waste Policy, Planning & Grants Branch, Mississippi Department of Environmental Quality, Office of Pollution Control, 2005.

[19] URS Corporation, "Construction waste project," Solid Waste Management Coordinating Board (SWMCB), Twin Cities Metropolitan Area, Memo #1, 2005.

[20] J. P. Zublena, A. R. Rubin, and D. A. Crouse, "Uses of sheetrock (gypsum) as a soil amendment," Soil Science Notes no. 1., Department of Soil Science, North Carolina State University, 1995.

[21] M. McPhee, "C&D recycling in the home court," *BioCycle*, pp. 30–32, November 1997.

[22] R. H. Brickner, "Researching debris generation," *Recycling Today*, pp. 46–52, September 1995.

[23] M. Channell, M. Graves, V. Medina, A. Morrow, D. Brandon, and C. Nestler, *Enhanced Tools and Techniques to Support Debris Management in Disaster Response Missions*, ERDC/EL TR-09-12, USERDC, Vicksburg, Miss, USA, 2009.

[24] F. C. Edminster, W. S. Atkinson, and A. C. McIntyre, *Streambank Erosion Control on the Winooski River, Vermont*, Circular no. 837, United States Department of Agriculture, Washington, DC, USA, 1949.

[25] G. Y. Solis, H. C. Hightower, J. Sussex, and J. Kawaguchi, *Disaster Debris Management*, The Disaster Preparedness Resources Center, University of British Columbia, Center for Emergency Preparedness, Vancouver, Canada, 1995.

[26] J. E. Kurre, "Characterizing construction and demolition debris for lead contamination," *Waste Age*, vol. 28, no. 7, pp. 117–125, 1997.

Hindawi Publishing Corporation
Advances in Civil Engineering
Volume 2011, Article ID 354305, 8 pages
doi:10.1155/2011/354305

Research Article

Cementitious Spray Dryer Ash-Tire Fiber Material for Maximizing Waste Diversion

Charles E. Riley,[1] Rebecca A. Atadero,[2] John W. van de Lindt,[3] and Paul R. Heyliger[2]

[1] *Department of Civil Engineering, Oregon Institute of Technology, 3201 Campus Drive, Klamath Falls, OR 97601, USA*
[2] *Department of Civil and Environmental Engineering, Colorado State University, Campus Delivery 1372, Fort Collins, CO 80523-1372, USA*
[3] *Department of Civil, Construction, and Environmental Engineering, University of Alabama, Tuscaloosa, AL 35487-0205, USA*

Correspondence should be addressed to Rebecca A. Atadero, ratadero@engr.colostate.edu

Received 31 December 2010; Accepted 17 May 2011

Academic Editor: Paola Bandini

Spray dryer absorber (SDA) material, also known as spray dryer ash, is a byproduct of coal combustion and flue gas scrubbing processes that has self-cementing properties similar to those of class C fly ash. SDA material does not usually meet the existing standards for use as a pozzolan in Portland cement concrete due to its characteristically high sulfur content, and thus unlike fly ash, it is rarely put to beneficial use. This paper presents the results of a study with the objective of developing beneficial uses for SDA material in building materials when combined with tire fiber reinforcement originating from a recycling process. Specifically, spray dryer ash was investigated for use as the primary or even the sole binding component in a mortar or concrete. This study differs from previous research in that it focuses on very high contents of spray dryer ash (80 to 100 percent) in a hardened product. The overarching objective is to divert products that are normally sent to landfills and provide benefit to society in beneficial applications.

1. Introduction

Portland cement concretes and mortars are used extensively in construction of buildings, bridges, and other infrastructure ranging from low-strength sidewalks to high-performance airport runways. Despite recent advances in manufacture, Portland cement remains an energy-intensive product that requires mining of raw materials as well as significant energy input and processing. Incorporation of coal fly ash into concrete mixtures is now widely accepted given its capacity to produce an equivalent or even improved hardened concrete product with less Portland cement and, therefore, reduced raw materials extraction and carbon emissions [1]. However, a substantial portion of fly ash produced each year goes unused, and a significant portion of the country's ash material is deemed useless because it is involved in the flue gas desulfurization process within the spray dryer absorbers utilized at many of the United States coal power plants [2]. It is the material from this subset of plants, alternatively called spray dryer absorber material, SDA material, or spray dryer ash, that is the subject of this research.

Spray dryer ash is produced in far smaller quantities than fly ash in the US. The American Coal Ash Association, ACCA, estimates 1.4 million tons for all dry flue gas desulfurization products, of which spray dryer ash makes up a large portion [3]. While nearly 42 percent of all fly ash produced in the United States (approximately 72 million tons annually [3]) is used beneficially, only about 25 percent of dry FGD products was used in 2008 [3]. Furthermore, the Electric Power Research Institute (EPRI) [2] estimates much higher annual production rates for SDA material than does ACAA: between 3.3 and 3.8 million tons, with that number projected to grow to 14 million tons by 2017 as more plants are required to reduce airborne sulfur emissions. Thus, the need for more beneficial applications of this material is critical.

While fly ash use and performance in concrete has been well documented [1], the mechanical properties of hydrated SDA material have not been studied adequately, in part due to concerns that the elevated sulfur levels will lead to sulfate attack in the hardened product [2]. A recent literature review by EPRI [2] surveyed the current uses for SDA and found applications ranging from agriculture to cementitious

Table 1: Bulk chemical composition of rawhide power station SDA.

Compound	Sample 1 Content A (%)	Sample 2 Content B (%)	Sample 3 Content C (%)	ASTM C618 limit for Class C fly ash (2005)	ASTM C 618 limit for class F fly ash (2005)
Silicon dioxide, SiO_2	39.76	29.84		Sum between 50 % and 70 %	Sum greater than 70 %
Aluminum oxide, Al_2O_3	14.31	14.24			
Iron oxide, Fe_2O_3	5.56	5.82			
$SiO_2 + Al_2O_3 + Fe_2O_3$	59.63	49.90	60.63		
Calcium oxide, CaO	23.45	26.48			
Sulfur trioxide, SO_3	6.19	10.01	3.70	5% maximum	5% maximum
Magnesium oxide, MgO	4.06	4.93			
Sodium oxide, Na_2O	1.42	1.66			
Titanium dioxide, TiO_2	1.15	0.98			
Phosphorous pentoxide, P_2O_5	0.98	1.59			
Barium oxide, BaO	0.61	0.68			
Potassium oxide, K_2O	0.53	0.48			
Strontium oxide, SrO	0.33	0.42			
Manganese dioxide, MnO_2	<0.01	0.02			
Moisture	1.86	1.04	1.33	3% maximum	3% maximum
Loss on ignition	1.65	2.85	1.64	6% maximum	6% maximum

A: sampled 4/3/2007 and tested by SGS North America, Inc., Denver, Colo, USA.
B: sampled 7/26/2007 and tested by Wyoming Analytical Laboratories, Inc., Golden, Colo, USA.
C: reported in Little, 2008 [10].

materials to wallboard; however, most of the applications noted in this paper were found in Europe where the composition of SDA is different from that produced at the US electric power plants. In European processes, the fly ash and spray dryer product are collected separately. The fact that US sources combine the fly ash and spray dryer product means not only that the resulting material is more variable, but also that the beneficial properties of the fly ash can be exploited.

The project described here seeks to leverage the self-cementing nature of this material to create a cementitious product with as little Portland cement as possible. Thus, the emphasis of this work is not on achieving the highest possible strength, but in diverting as much waste material as possible into a useful product that maintains adequate properties. In the present study, applications with lower strength requirements (e.g., nonstructural components) are targeted with the cemented SDA combined with fibers collected during the automobile tire recycling process as reinforcement. The results indicate that good compressive and tensile strength is possible. While these results are for a specific SDA material source, they suggest that useful materials may be produced with this presently underutilized industrial byproduct. They also indicate the value of further study of SDA material sources and long-term material performance.

2. Materials and Specimens

Two different types of materials were studied. The first was a material comprised solely of spray dryer ash and water, with some specimens also including recycled polymer fibers from used automobile tires (described in more detail below). Second, mortar specimens manufactured with spray dryer ash, sand conforming to ASTM C33 [4], varied amounts of Portland cement, and recycled polymer fibers were considered.

Table 1 shows details of the chemical composition of three samples of the SDA material produced by the Rawhide power plant in Northern Colorado. The quantities in Table 1 indicate the level of variability present in SDA material from just a single source, thus underscoring a need for site-specific study to ensure the quality control of SDA material as an input. Of particular note is the very high lime content (over

Table 2: Mixture proportions.

Mixture number	Cement type	Cement[a]	SDA[a]	Sand[a]	Water[a]	Fibers[b]
1A	—	0	100	0	40	0
1B	—	0	100	0	35	0
1C	—	0	100	0	30	0
1D	—	0	100	0	25	0
1E	—	0	100	0	25	0.5
1F	—	0	100	0	25	1.0
1G	—	0	100	0	25	2.0
2A	—	0	100	100	40	0
2B	III	5	95	100	40	0
2C	III	10	90	100	40	0
2D	III	15	85	100	40	0
2E	III	20	80	100	40	0
2F	I/II	5	95	100	40	0
2G	I/II	10	90	100	40	0
2H	I/II	15	84	100	40	0
2I	I/II	20	80	100	40	0
2J	I/II	10	90	100	40	1.0
2K	I/II	10	90	100	40	1.5
2L	I/II	10	90	100	40	2.0

[a]These quantities are expressed as a percent by weight relative to the total weight of SDA and cement in the mixture.
[b]Expressed as a percent by weight of the total solids (SDA, cement and sand) in the mixture.

20 percent CaO), which contributes to the self-cementing capacity of the material. The SO_3 content, which is typically slightly in excess of the 5 percent limit for fly ash used in concrete as specified by ASTM C618 [5], is also notable. This excess sulfur has prevented the application of the material in concrete to date, but because the amount of excess is still quite modest, the material merits individual study.

The polymer fibers used in this study were obtained from an automobile tire recycling facility and represented a combination of polymers commonly used as tire reinforcement such as nylon, polyester, and aramid with lengths randomly distributed between approximately 2 mm and 30 mm. The steel wires present in most automotive tires were removed magnetically at early stages of the recycling process. The polymer fibers were interspersed with rubber particles varying from fine dust to larger pieces less than 5 mm in dimension as well as raw chopped fibers that were still twisted together in cords. These recycled fibers were chosen for their compatibility with the theme of waste diversion and sustainable construction, which is a prime motivator for developing a cementitious material with industrial byproducts. Because of variability in fiber size and constitution, all fiber fractions are by weight, as without the density it was not possible to determine a volume fraction. However, given the range of specific gravities of the potential reinforcing fibers, a volume fraction very nearly equal to the weight fraction is reasonable.

The mixture proportions of the specimens are shown in Table 2. Mixtures numbered 1 are spray dryer ash pastes, while those numbered 2 are spray dryer ash-based mortars. Sets 1A through 1D were composed solely of spray dryer ash and water and were intended to study the effect of water-to-ash ratio on the compressive strength of the hardened paste. Sets 1E through 1G included varying percentages of the recycled polymer fibers, in order to investigate their effect on the hydrated ash pastes.

The mortar mixtures had a constant water/cementitious materials ratio of 0.40 but had varying amounts of Portland cement and recycled polymer fibers in an effort to improve on the properties observed in the spray dryer ash pastes. Two types of Portland cement were used. Type I/II was used because it is very commonly available. Type III cement was also used because in the case of fly ash, there is usually a reduced rate of strength gain when mixtures including fly ash are compared to mixtures with just Portland cement, and it was anticipated that the same situation might occur with spray dryer ash. Research by Bilodeau and Malhotra [6] indicated the high early strength properties of Type III cement would bring the strength versus time characteristics of the hydrated ash (Class F fly ash in the case of Bilodeau and Malhotra) closer to those of conventional concrete. This is important for construction scheduling for structural applications and shipping/trucking scheduling for nonstructural construction materials such as siding or roof tiles.

The compressive strengths of the mixtures in Table 2 were investigated using 5.08-cm cubes following the dimensions suggested in ASTM C109 [7]. Mortar testing also included flexural specimens: beams with approximate dimensions 5.08 cm by 5.08 cm by 20.3 cm tested according to ASTM C78 [8] with a 15.2-cm clear span.

For both pastes and mortars, the constituent materials were mixed approximately according to ASTM C 305 [9] to ensure uniformity of the mixtures, which was particularly important for the paste mixtures with a low water/ash ratio.

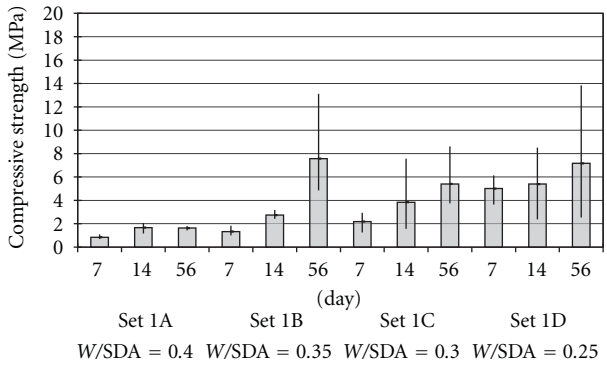

Figure 1: Early compressive strength of hydrated spray dryer ash pastes.

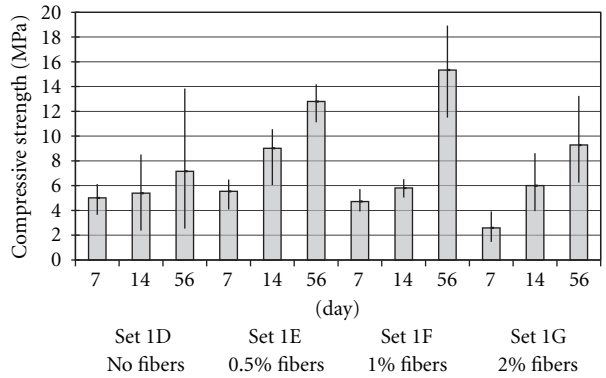

Figure 2: Early compressive strength of hydrated spray dryer ash with fibers.

The sole deviation from ASTM C 305 was the mixing device. A mixing bit and hand drill were used in lieu of a planetary rotary mixer. Paste specimens were cured at approximately 80 percent humidity and between 26 and 32 degrees C (79–90 degrees F). This slightly elevated temperature was meant to accelerate curing, as would be found at a manufacturing plant for a prefabricated building material. The mortar specimens were placed in a more traditional curing room that maintained a relative humidity of approximately 90 percent and a temperature of approximately 22 degrees C (72 degrees F). For both pastes and mortars, the specimens were placed in the curing environment directly after casting and were returned to the curing environment following removal of the molds after approximately one day. Paste tests were conducted at seven-day intervals, with five cubes tested from each mixture. For the mortars, three cubes were tested at seven-day intervals up to 28 days, while three beams were tested at 14 and 28 days for each of the nine mixtures.

3. Discussion

3.1. Hydrated Spray Dryer Ash Pastes. Recall that the objective of this study was to divert as much spray dryer ash as possible from landfilling. Thus, the first experiments evaluated the potential of hydrated spray dryer ash alone in manufactured structural and nonstructural construction products. Early strength gain is an important item of consideration for these materials because manufacturers of commercial products require shipment as quickly as possible, often in as little as seven days. Figure 1 shows the results of 7, 14, and 56 day tests for Sets 1A through 1D. These sets were composed of spray dryer ash pastes with water/ash ratios ranging from 0.40 for Set 1A to 0.25 for Set 1D. Figure 1 shows the average strength as well as the high and low values. Although the compressive strengths showed considerable variability, in general, there is an increase in compressive strength that is inversely linear with water/ash ratio.

Figure 2 shows the results for compressive strength for Sets 1D through 1G with high, low, and average strengths included. These sets all had a fixed water/ash ratio of 0.25 and demonstrate the effect of inclusion of the polymer fibers derived from tire recycling. Set 1D had no fibers, while Sets 1E, 1F, and 1G had increasing fiber fractions as shown in Table 2. Based on the results shown in Figure 2, the fiber reinforcement appears to be beneficial to the compressive strength with an optimum fiber fraction around 1 percent. Set 1E with 0.5 percent fibers (recall, by weight) shows a clear increase in strength over Set 1D with no fibers. It appears that the addition of more fibers (Set 1F with 1 percent and Set 1G with 2 percent) has little impact on the strength, or may even weaken the mixture slightly, perhaps due to greater difficulty in creating a uniform mix. The increase in strength may be attributed to the ability of the fibers to bridge cracks and act as reinforcement in a relatively weak and brittle matrix material. The pictures shown in Figure 3 are examples of the appearance of typical cubes with and without fibers after testing to failure. In general, cubes without fibers fractured into numerous pieces, while cubes with fibers showed cracking and deformation but maintained their general shape even after the initial cracking and the associated significant reduction in capacity. The inclusion of a small amount of fibers leads to a significant (20 to 70 percent) increase in compressive strength, but this increase appears to peak at fairly low fiber weight fractions.

Table 3: Average 56-day compressive strength and modulus of elasticity measured from cube specimens.

Set	Average 56-day compressive strength (MPa)	Average 56-day modulus of elasticity (MPa)
1A	1.63	119.6
1B	7.57	408.4
1C	5.40	382.8
1D	7.16	376.9
1E	12.79	565.9
1F	15.34	557.2
1G	9.28	395.5

The ultimate compressive strength of hydrated spray dryer ash will depend on the specific chemical composition of the ash and the long-term curing conditions. However, it is of interest to know approximate values for the compressive strength for both neat and fiber-reinforced spray dryer ash.

Table 4: Compressive strength for different types of cement, testing ages and percents of cement added (MPa).

		Type I cement (Sets 2F–2I)				Type III cement (Sets 2B–2E)			
Days	0%	5%	10%	15%	20%	5%	10%	15%	20%
7	4.09	17.62	13.03	16.19	15.88	15.18	23.00	19.85	23.04
14	6.91	23.61	17.83	23.92	25.70	20.65	27.09	27.82	24.37
21	8.03	24.43	24.53	32.64	32.84	23.64	29.98	27.06	31.91
28	7.99	27.37	27.15	34.00	37.18	22.87	29.26	29.23	28.79

(a)

(b)

Figure 3: Typical cube appearance after compressive testing without (a) and with (b) polymer fibers.

Table 3 shows the average 56-day compressive strengths and moduli achieved. The modulus of elasticity was calculated from the cube tests using a linear fit to initial portions of the stress-strain curve, and the strain was calculated from the test machine crosshead displacement data collected during the compressive strength tests. For the most part, the trends witnessed in the early strengths are continued at later strengths: decreasing the water/ash ratio results in an increase in strength, and modest use of tire fiber (about 1 percent) yields additional increase that declines with the addition of more fibers.

The highest average strengths observed for the hydrated spray dryer ash with and without fibers were 15.3 MPa and 7.5 MPa, respectively. These strengths were achieved at an age of 56 days and indicate that hydrated spray dryer ash alone is not likely to be suitable for many structural engineering uses. Aesthetically, the finished cubes had limited resistance to scratching or abrasion and for high water ratios especially, seemed to have a chalky finish. The material was also observed to readily absorb water. A cube dipped in water appeared dry in less than one minute because the water had been absorbed into the cube. Based on these results, the mortar mixtures were developed and tested to study potential means of achieving enhanced properties while still utilizing large quantities of spray dryer ash.

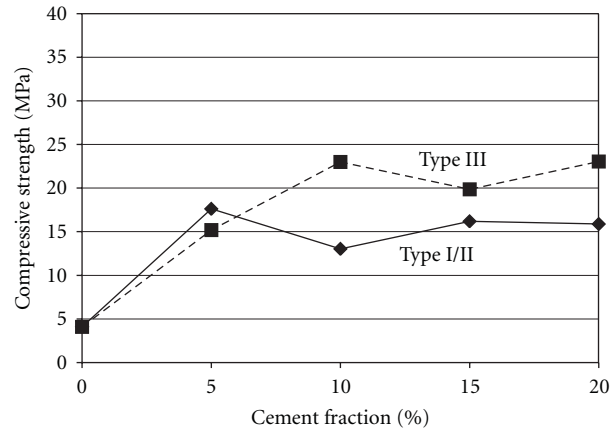

Figure 4: Comparison of compressive strength at 7 days for mixtures with type I/II and type III cement.

3.2. Hydrated Spray Dryer Ash Sanded Mortars. Seeking to improve the properties of the spray dryer ash pastes, the researchers considered the addition of sand and small amounts of Portland cement. To maximize spray dryer ash usage, cement quantities of only five, ten, fifteen, and twenty percent were considered. This can be thought of as the inverse of typical fly ash applications, where smaller amounts of fly ash are used as additives to traditional concrete mixtures. As indicated earlier, both Type I/II and Type III cements were tested.

Table 4 summarizes the results of testing at 7, 14, 21, and 28 days for specimens with varied cement fraction. From this table, it is immediately obvious that the addition of even five percent Portland cement (of either type) has a significant impact on the compressive strength. At 28 days, including five percent of Type I/II cement in the mixture increased the compressive strength over the mixture with just spray dryer ash binder by about 3.4 times, from 8.0 to 27.4 MPa, and the Type III cement increased the compressive strength by nearly 2.7 times, from 8.0 to 22.9 MPa. Figures 4 and 5 compare the effect of the different types of cement at ages of 7 and 28 days, respectively. Figure 4 shows that Type III cement outperformed Type I/II cement at the early age of 7 days, as would be expected from cement

Table 5: Modulus of elasticity for different types of cement, testing ages and percents of cement added (MPa).

	Type I cement (Sets 2F–2I)					Type III cement (Sets 2B–2E)			
Days	0%	5%	10%	15%	20%	5%	10%	15%	20%
7	686	2022	1666	1965	1720	1609	2354	2193	2474
14	1080	2681	2176	2337	2099	1835	2720	3095	2743
21	1051	2773	2612	3208	3122	2513	2612	2643	2938
28	881	2850	3172	3360	2869	2428	2648	2911	2819

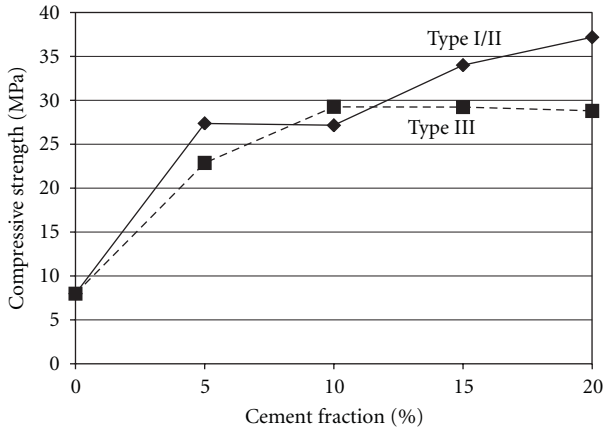

Figure 5: Comparison of compressive strength at 28 days for mixtures with type I/II and type III cement.

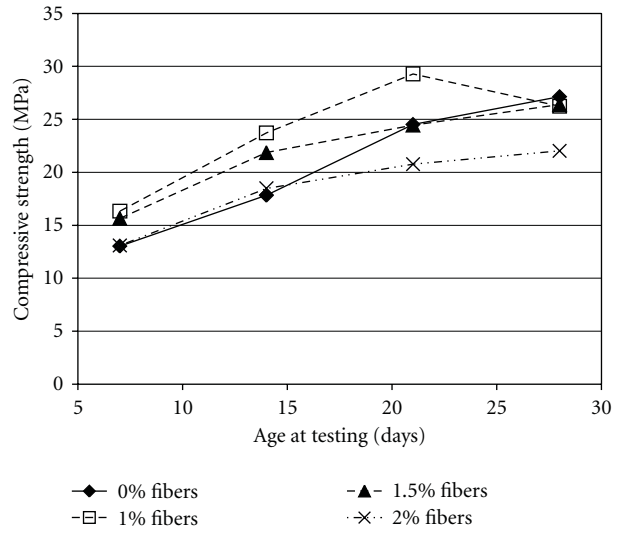

Figure 6: Effect of increasing percentages of recycled polymer fiber on the compressive strength of a mortar with ten percent type I/II cement.

formulated to give high early strengths. However, Figure 5 shows that the long-term strength was generally higher with the addition of Type I/II cement. These figures also show that the increase in strength with the addition of cement is not a linear relationship, as only comparatively modest strength gains occur as the percentage of cement is increased from five to twenty percent. Inherent variability in constituent materials and questionable homogeneity of the mixed materials contribute to some variability in the compressive strength results. However, the coefficients of variation for the three-specimen sets were generally within 10 percent and rarely exceeded 15 percent. In all cases, dramatic compressive strength gains came with very modest (between 5 and 10 percent) additions of cement.

The modulus of elasticity of the test specimens was computed based on results from the compression testing. These results are shown in Table 5. Because cube specimens were used and the strain was calculated from displacement of the loading platen, these stiffness results should be considered estimates. However, they can be used to observe the relative effect resulting from the addition of Portland cement. The addition of cement clearly increases the stiffness, with values of two to three times those for specimens made with SDA material as the only binding agent. However, as with the compressive strength results, there do not appear to be coherent trends in the data relating increased percentages of cement to further increases in stiffness. Essentially, the addition of Portland cement has a significant stiffening effect without respect to the amount of cement.

Table 6: Modulus of elasticity for different percentages of fibers for a mortar made with 10% type I/II cement (MPa).

	% Fibers			
Days	0.0%	1.0%	1.5%	2.0%
7	1666	2034	1724	1839
14	2176	2468	2804	2237
21	2612	2969	2596	2815
28	3172	2697	2739	2861

The effect of polymer fibers on the compressive strength was also considered with the addition of cement. Mortars were prepared with ten percent Type I/II cement and varying fiber contents. Figure 6 shows the results of different fiber contents on the compressive strength over the full testing period. At early ages, it appears that the addition of some fibers is helpful, but over time the strength benefit of the fibers is lost. Furthermore, there appears to be an optimal fiber fraction around 1 percent. The mixtures with 1 percent fibers (by weight) are stronger than the mixtures with 1.5 percent fibers at most ages, and both outperform the mixtures with 2 percent fibers. This result is consistent with the SDA paste results where the addition of 1 percent fibers clearly improved the compressive strength, and 2 percent

Table 7: Modulus of rupture results for different types of cement, testing ages and percents of cement added (MPa).

	Type I cement (Sets 2F–2I)					Type III cement (Sets 2B–2E)			
Days	0%	5%	10%	15%	20%	5%	10%	15%	20%
14	1.19	3.27	2.61	3.74	5.24	2.38	3.14	3.28	3.99
28	1.54	3.05	3.11	4.85	6.44	2.58	3.74	3.34	4.21

fiber addition had a detrimental effect. Results indicating the effect of fiber addition on the modulus of elasticity are shown in Table 6 and show that the addition of fibers to a mixture already containing cement is of little benefit to stiffness. There may be some mild advantage to fiber addition at early ages, but by 28 days the stiffness of specimens with fibers was less than that of the specimens without fibers.

Given the mechanics of failure of a brittle material in compression (shear failure along 45-degree planes and splitting along the axis of loading), the addition of reinforcing fibers to a stiff and brittle matrix may not have a significant impact on compressive strength or stiffness. Thus, the strengthening observed in the SDA paste specimens is likely the result of the weaker and less stiff matrix being reinforced by fibers that are relatively stiffer and thus able to reinforce the matrix prior to cracking. Once the matrix itself is stronger and stiffer, as is the case in the mortars with added cement, fibers can have a detrimental effect (due perhaps to a loss in workability) until cracking has occurred, and the fibers deform sufficiently to carry significant loads. These results are consistent with the highly variable results for fiber-reinforced concrete reported by other authors and summarized by Johnston [11]. Qualitatively, the mortar cubes with fibers behaved similarly to the neat spray dryer ash cubes (shown in Figure 3), remaining intact even after losing their load-carrying capacity.

Flexural testing was conducted at 14 and 28 days for mortar specimens with the addition of both cement and fibers. Table 7 presents the moduli of rupture (MOR) from these tests. The addition of cement appears to increase the flexural strength, although not to the degree witnessed for the compressive strength. The addition of 5 percent Type I/II cement increased the MOR by a factor of 1.98 at 28 days, and the addition of 5 percent Type III cement increased the MOR by a factor of 1.68 at 28 days compared to the cement-free mortar specimens. Figure 7 compares the effect of different percentages of the two different types of cement on the MOR achieved at 28 days. This plot shows that adding increasing percentages of Type I/II cement continues to increase the MOR; however, the continued addition of Type III cement beyond 10 percent appears to offer little benefit.

The addition of fibers to concrete typically provides added capacity to the regions of the test specimen in tension, potentially increasing the overall flexural strength of the specimen. Figure 8 shows the effect of different fiber contents on the flexural strength at both 14 and 28 days. The addition of 1 percent fibers clearly improves the MOR compared to specimens without any fibers at all, with increases of between 10 and 30 percent. However, similar to the results observed in compression, the addition of larger percentages of fibers

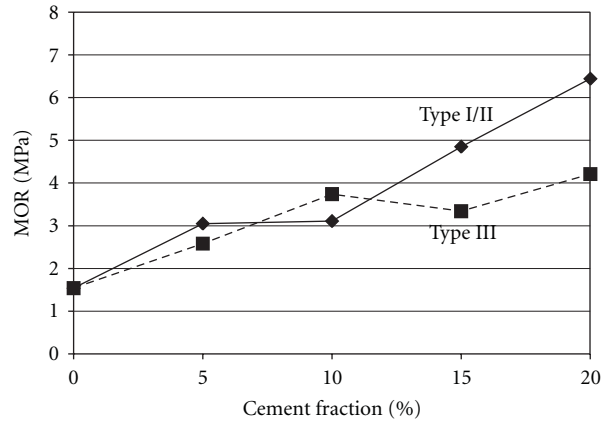

Figure 7: Comparison of MOR at 28 days for mixtures with type I/II and type III cement.

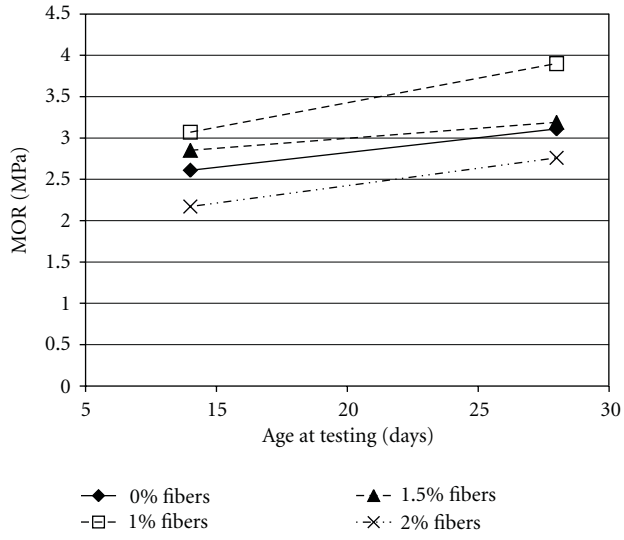

Figure 8: Effect of increasing percentages of recycled polymer fiber on the MOR of a mortar with ten percent type I/II cement.

was not beneficial. The mixture with 1.5 percent fibers had an average MOR approximately equal to the mixture with no fibers, and the mixture with 2 percent fibers actually had a lower MOR than the mixture without fibers. Thus, an optimal fiber content for both flexure and compression exists around 1 percent by weight for these particular materials.

Overall, the mixtures tested with additions of both cement and tire fiber showed significant promise as a potential engineering material. The strengths and stiffnesses showed significant improvement with as little as 5 percent addition

of Portland cement and approximately 1 percent of fibers. Both Type I/II and Type III cements were found to be effective, with Type III cement increasing early strengths, while Type I/II cement produced higher later strengths. In terms of aesthetics and workability, the addition of the cement also eliminated concerns about the chalky finish associated with the SDA-only mixtures. The addition of cement also improved the workability of the pure spray dryer ash mortar, as the spray dryer ash-only mixtures tended to be sticky which made the finishing difficult.

4. Summary and Conclusions

Two phases of testing were used to investigate the use of spray dryer ash as a cementitious material for engineering use. Spray dryer ash alone mixed with water was found to be too weak in compression to offer benefits as a practical engineering material even for moderately structural components such as roof tiles. The addition of recycled polymer fibers increased the strength by a significant amount (10–50 percent), but the resulting strengths were still quite low. Other properties, such as a chalky finish, also indicated that spray dryer ash alone was not suitable as a matrix for most structural engineering applications.

Improvements were found in the properties of sanded mortars through the addition of small amounts of Portland cement to the ash-tire fiber mixture. Compressive strengths at the low end of the range typically considered for conventional concrete (27 MPa) were achieved with only 5% additions of Portland cement. Recycled polymer fibers were shown to benefit the compressive and flexural strengths at additions of around 1 percent by weight, while greater fiber fractions had a limited or detrimental impact on strengths. The fibers were very effective at preventing spalling and loss of material due to fracture and contributed to increased toughness and ductility. This attribute may be desirable for certain applications.

This preliminary testing has been conducted on mortars, and thus, testing of concretes with large aggregate is a necessary next step. If structural applications are to be pursued, these practical applications will also require testing to ensure the durability of the product and its compatibility with reinforcing bar from both a bonding and corrosion perspective. The results of the study presented herein indicate a high potential for useful application of this material and provide justification for further studies focusing on specific applications. Significant waste diversion through beneficial use of spray dryer ash appears to be a viable objective.

Acknowledgements

The authors gratefully acknowledge the Colorado Commission on Higher Education (CCHE) for support of this research through contract no. 07 GAA 00018. The spray dyer ash and recycled tire fibers were provided for this research by the Platte River Power Authority and Jai Tire, respectively. The authors also acknowledge the assistance of the students who worked on this project including Jeff Eulberg, Stephanie Thomas, Balaji Mahalingam, Fredrick Busch, and Karthik Rechan.

References

[1] ACI Committee 232.2, *Use of Fly Ash in Concrete*, American Concrete Institute, Farmington Hills, Mich, USA, 2003.

[2] EPRI, "A review of literature related to the use of spray dryer absorber material-production, characterization, utilization applications, barriers, and recommendations," TR1014915, Electric Power Research Institute, September 2007.

[3] ACAA, "Coal combustion product (CCP) production and use survey," American Coal Ash Association. Aurora, Colo, USA, 2008, http://www.acaa-usa.org/.

[4] ASTM International, *C33 Standard Specification for Concrete Aggregates*, ASTM International, West Conshohocken, Pa, USA, 2008.

[5] ASTM International, *C618 Standard Specification for Coal Fly Ash and Raw or Calcined Natural Pozzolan for Use in Concrete*, ASTM International, West Conshohocken, Pa, USA, 2005.

[6] A. Bilodeau and V. M. Malhotra, "High-volume fly ash system: concrete solution for sustainable development," *ACI Structural Journal*, vol. 97, no. 1, pp. 41–48, 2000.

[7] ASTM International, *C109 Standard Test Method for Compressive Strength of Hydraulic Cement Mortars*, ASTM International, West Conshohocken, Pa, USA, 2008.

[8] ASTM International, *C78 Standard Test Method for Flexural Strength of Concrete*, ASTM International, West Conshohocken, Pa, USA, 2008.

[9] ASTM International, *C305 Standard Practice for Mechanical Mixing of Hydraulic Cement Pastes and Mortars of Plastic Consistency*, ASTM International, West Conshohocken, Pa, USA, 2008.

[10] J. Little, "Spray dryer ash finds a market," *Ash at Work*, no. 1, pp. 10–11, 2008.

[11] C. D. Johnston, *Fiber-Reinforced Cements and Concretes*, Gordon and Breach Science Publishers, Amsterdam, The Netherlands, 2001.

Hindawi Publishing Corporation
Advances in Civil Engineering
Volume 2011, Article ID 808561, 7 pages
doi:10.1155/2011/808561

Research Article

Use of Reclaimed Asphalt Pavement in Conjunction with Ground Improvement: A Case History

Kevin C. Foye

CTI and Associates Inc., 51331 W. Pontiac Trail, Wixom, MI 48393, USA

Correspondence should be addressed to Kevin C. Foye, kfoye@cticompanies.com

Received 2 February 2011; Accepted 17 May 2011

Academic Editor: Paola Bandini

The use of Reclaimed Asphalt Pavement (RAP) in lieu of virgin crushed stone aggregate is becoming a widely accepted practice for a number of construction applications, particularly pavement base courses. A number of laboratory RAP studies have considered the mechanical properties of RAP bases in order to support pavement designs incorporating RAP. These studies have revealed a number of interesting relationships between RAP moisture content, compaction, and stiffness. This paper discusses the experiences of a design-build contractor integrating a geosynthetic ground improvement program with a RAP base during the reconstruction of a 1.95 ha asphalt parking lot. Field observations of base course construction with RAP explore some of the implications of laboratory findings. A number of interesting observations on the technical, construction, and economic issues resulting from the project challenges and the use of RAP are presented.

1. Introduction

The use of Reclaimed Asphalt Pavement (RAP) in lieu of virgin crushed stone aggregate is becoming a widely accepted practice for a number of construction applications, particularly pavement base courses, as evidenced by its inclusion in department of transportation specifications, including Minnesota Department of Transportation (Mn/DOT) [1]. The use of RAP in this application is attractive for a number of reasons: first, it reduces the cost of material production by eliminating quarrying, crushing, and screening operations. Second, for repaving projects, it reduces handling and transportation costs since the RAP is retained onsite for reuse. Third, it reduces the consumption of natural resources and energy, as reflected in the reduced costs in the first two points.

Engineers designing pavements require reliable design guidance to incorporate any material into their design pavement sections. Common flexible pavement design methodologies are largely calibrated to empirical studies while their formulation is informed by commonly measured mechanical properties, especially resilient modulus and various measurements that correlate with resilient modulus (Puppala [2], AASHTO [3]). Hence, studies to support the incorporation of RAP into pavement designs have focused on characterizing its mechanical properties. The mechanical properties of RAP are expected to largely mimic those of crushed stone aggregate due to its similar composition—with the notable exception of residual asphalt binder—and particle-size gradation. Several authors, including Attia and Abdelrahman [4], Mokwa and Peebles [5], and Locander [6] have performed laboratory studies of RAP, focusing on tests of interest to pavement base construction, including Proctor compaction, California Bearing Ratio (CBR), and resilient modulus. The goal of these studies has been to assess the suitability of RAP as a base course material and to offer design guidance to engineers designing pavement sections including RAP.

The contribution of this paper is to share some anecdotal observations regarding the use of RAP to construct the base course of a flexible pavement system. The project presented involved the reclamation and repavement of exist-ing distressed asphalt pavement over a soft subgrade. Field observations regarding the behavior and preparation of RAP not only confirm a number of laboratory observations, but also provide some answers to lingering questions from

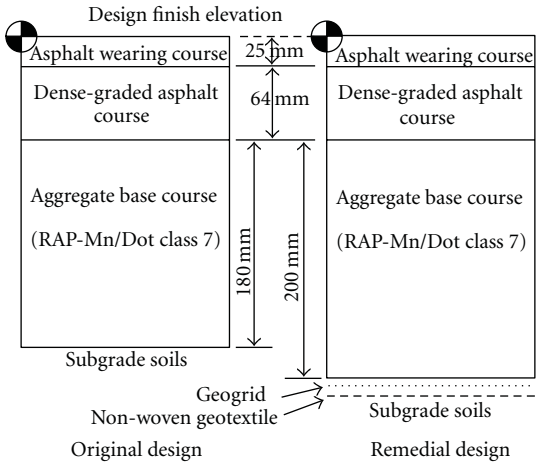

Figure 1: Design pavement cross sections.

Figure 2: Photo showing typical proof rolling test.

the laboratory studies—especially the question of whether or not RAP offers comparable performance to crushed stone aggregate as a base course. Additionally, due to a discovered subgrade problem at the project site, engineers also integrated the planned RAP base into a remedial solution to avoid a costly subgrade replacement. Hence this paper also shares the experiences of the prime contractor integrating a geosynthetic ground improvement program with the RAP recycling. A number of interesting observations on the technical, construction, and economic issues resulting from the project challenges and the use of RAP are presented.

2. Project Background

The project was to rehabilitate a 19,500 m^2 (1.95 ha) asphalt parking lot within the US Army Reserve Facility (owner), Fort Snelling, Minn, USA under the direction of personnel from the US Army Corps of Engineers (USACE), Kansas City, and St. Paul Districts. The parking lot is used to park a number of light- and heavy-duty rubber-tired and tracked vehicles. The existing, 30-year-old parking lot pavement had several low points that did not drain properly, resulting in ponding, moisture damage, and severe alligator cracking to the point of pot holes and loose aggregate. The prime contractor, which includes the author, was responsible for construction of the planned rehabilitation according to design plans and specifications prepared by the USACE's consulting engineer. This responsibility was expanded to include design-build and value engineering services as a result of conditions encountered during the project. Rehabilitation included improving site drainage through regrading, installation of new stormwater collection structures, and construction of new stormwater discharge control features. The existing, distressed asphalt pavement was milled and stockpiled for reuse as RAP in the new pavement base course. The design pavement cross section is shown in Figure 1 as "Original Design." This section was selected by the USACE's consulting engineer because it exactly replaced the existing pavement section: 75–100 mm of asphalt pavement over 175–200 mm of base aggregate. The existing pavement section was determined by soil borings through the parking lot.

Suitability of the subgrade to support the pavement system was assessed by means of a proof rolling test, whereby a loaded rubber-tired water truck is driven over the subgrade and a quality control technician observes the subgrade for signs of deflection, pumping, and/or rutting under the action of the tires (Figure 2). Observed pumping and rutting disqualifies the subgrade. Areas of disqualified subgrade required either compaction or replacement to meet design requirements. In cases where compaction is ineffective in achieving an acceptable subgrade, the contract required the undercutting of the subgrade to a depth of 1 m below top of subgrade elevation and replacement with compacted imported fill.

Following milling of the existing pavement and removal of the existing base material, the paving subcontractor proof rolled the existing subgrade. The quality control technician noted significant deflection, pumping, and rutting of the subgrade during proof rolling, suggesting that the subgrade may be unsuitable to depths greater than 300 to 1000 mm. Consequently, the subgrade was deemed unsuitable for placement of the pavement base. The extent of the permanent rutting, partially shown in Figure 3, indicated that nearly all of the 1.95 ha parking lot subgrade would require improvement.

To further investigate the subsurface profile following the failed proof-roll tests, the prime contractor excavated several test pits into the parking lot subgrade. These test pits revealed the consistent expression of a wet organic silt layer throughout the parking lot footprint. Figure 4 presents a photo of a typical test pit showing the organic silt layer. The organic silt varied in thickness over the site from 300 to 600 mm. A layer of wet, silty sand immediately below the organic silt also appeared to contribute to the poor condition of the subgrade and may also be responsible for the observed pumping during proof-roll testing. The typical depth to the bottom of the wet silt is 1 m below the top of subgrade.

Laboratory testing of the subsurface soils included grain size distribution and Atterberg Limits. Table 1 summarizes the results of the laboratory classification testing. Atterberg

Figure 3: Photo showing typical rutting observed following proof rolling of the existing subgrade.

Figure 4: Example test pit showing, from top to bottom, typical soil profile: residual gray base aggregate, brown silty sand, black organic silt, brown silty sand.

limits were determined for both air-dried and oven-dried samples to assess the potential influence of organic materials. These tests confirmed that the black silt layer classifies as an organic soil. Field testing included the aforementioned proof rolling and Dynamic Cone Penetrometer (DCP) sounding (ASTM D6951 [7]). DCP soundings revealed DCP indices from <15 mm/blow to 90 mm/blow, indicating interpreted CBR values from 1 to >10. Representative values of CBR assessed for the subgrade were between 1 and 3.

Adherence to the project specifications would have required excavation and replacement of the subgrade to a depth of 1 m over the entire 1.95 ha site, resulting in about 19,500 m^3 of additional spoil and imported fill. The prime contractor considered this approach unnecessarily wasteful. Furthermore, the cost to perform this cut and replace improvement was prohibitive to the owner. Therefore, the prime contractor conducted a value engineering assessment of alternative options to address this issue at a significantly lower cost while achieving the performance required for the new pavement.

Table 1: Laboratory subgrade classification test results.

	Atterberg limits			
	Air-dried		Oven-dried	
Soil description	LL	PL	LL	PL
Brown to brownish gray silt	26	21	21	19
Dark brown to black organic silt*	26	16	18	16

*Note: the dark brown to black organic silt was classified as an organic silt since the liquid limit of the oven-dried sample was less than 75% of the liquid limit of the air-dried sample per ASTM D2488.

3. Ground Improvement Approach

Two viable alternative technologies were identified: (1) soil stabilization/modification and (2) geosynthetic reinforcement. For soil stabilization/modification, the prime contractor considered mixing the subgrade with lime, fly ash, or Portland cement. For geosynthetic reinforcement, the prime contractor considered installing a single layer of high-strength geotextile or geogrid reinforcement in combination with a geotextile separator. Because the prime contractor's engineers recognized the relatively high cost of the cut and replace alternative and the need for an effective improvement option, they adopted the "design by cost" methodology described by Koerner [8] in the sense that the selected alternative was designed to appeal to the owner in terms of cost while the technical evaluation satisfied conservative criteria for performance. Accordingly, preliminary estimates suggested that the geogrid/geotextile option would provide the best fit in terms of cost and performance.

Evaluation of the required pavement section using a triaxial geogrid layer as reinforcement was conducted using the methodology of AASHTO [3] in combination with improvement factors recommended by the geogrid manufacturer. Table 2 summarizes the AASHTO [3] layer coefficients assumed in the analysis of the design cross sections. The design 80-kN Equivalent Single-Axle Load (ESAL) traffic was back calculated by taking as input the layer coefficients shown in Table 2, the original design asphalt and base course thicknesses, and a subgrade resilient modulus = 83 MPa. This value of resilient modulus was implied by the subgrade acceptance specifications. The remedial design cross section was selected to deliver equal or greater performance for the same number of ESALs as the original design assuming an actual subgrade resilient modulus = 27 MPa (CBR $\approx$ 3). The resulting design cross section is shown in Figure 1 as "Remedial Design." The geotextile specified for the separator is a 271 g/m^2 needle-punched nonwoven geotextile. The function of the geotextile is to prevent the intrusion of subgrade silt into the overlying base course, ensuring proper interlock of the base aggregate and geogrid. Both the original design and the remedial design analyses considered Mn/DOT class 5 stone aggregate base. The significance of the class 5 aggregate base is discussed in the following sections.

A cost estimate investigation of the stabilization/modification option revealed that a soil improvement cost comparable to the installation of the geotextile and geogrid could only be achieved by reducing the depth of improvement to 380 mm and by changing the soil additive to circulating

Table 2: Summary of AASHTO [3] Design Inputs Used to Analyze Pavement Sections. Original design value for resilient modulus was inferred from project specifications. Design ESALs were back calculated from original design pavement section.

Design Parameter	Original Design Value	Remedial Design Value
Asphalt Wearing Course Layer Coefficient	0.42	0.42
Dense-Graded Asphalt Course Layer Coefficient	0.40	0.40
Aggregate Base Course Layer Coefficient	0.14	0.24
Subgrade Resilient Modulus	83 MPa	27 MPa
Target Design ESALs	176,000	176,000

Figure 5: Photo showing installation of underdrains.

fluidized-bed (CFB) ash at a mixing ratio of 5% by weight. Due to these constraints, the prime contractor decided to abandon the soil stabilization/modification option for the following reasons: (1) limited time was available to conduct the necessary bench-scale testing of the candidate material: (2) if testing determined that a greater mixing ratio or more potent cementing agent were required, the soil stabilization/modification option would be disadvantaged in terms of cost.

4. Implementation of Selected Ground Improvement Method

As part of the original design, the prime contractor installed a number of underdrains extending from the recently installed catch basins. These underdrains consisted of a perforated high-density polyethylene (HDPE) pipe embedded in a stone aggregate-filled trench wrapped in a filter geotextile (Figure 5). The trenches were excavated about 700 mm deep into the subgrade. The effective area drained by these underdrains was limited to less than 10% of the total parking lot. However, their placement at the low points of the regraded parking lot subgrade may facilitate effective drainage of a much larger fraction of the total area. These drains became significant to the improvement of the subgrade due to concerns about the discovery of water trapped within the silty sand above the organic silt layer. The quality control technician noted that visible flow through the installed drains stopped within 4 to 5 hours of installation. Anecdotal accounts of improved subgrade conditions 2 months after the installation of the underdrains suggest that the drains contributed to the subgrade improvement.

After about 2 months of review, and consideration, the owner agreed to the recommended geogrid reinforcement option and construction resumed with the excavation of additional subgrade soil to accommodate the increased pavement section thickness. The geotextile and geogrid were unrolled directly onto the subgrade. Continuity of the geotextile with adjacent rolls was provided by a 900-mm overlap. The geogrid panels were similarly joined by a 900-mm overlap only. Plastic cable ties were used to aid laborers deploying geogrid by temporarily securing panels together. The 900-mm overlap was recommended by the manufacturer for subgrades with CBR values less than 2.

Following placement of the geotextile and geogrid, bulldozers were used to push the RAP base material onto the geogrid, taking care not to track over areas with less than 150 mm of RAP in place or to make sharp turns, which could damage or displace the geogrid. The base course was compacted with vibratory roller compactors. Quality control acceptance of the compacted RAP base course was based on DCP and proof roll testing. According to 2005 Mn/DOT specification (a modified version of the recommendations by Siekmeier et al. [9]), a DCP index of 10 mm/blow or less was required to accept the base course compaction. The paving subcontractor applied additional compactive efforts to failing areas until they passed. Proof rolling was conducted on the base course in response to concerns raised by the asphalt paving subcontractor. Because the subcontractor was not involved in the decision to use geosynthetic reinforcement instead of excavating the subgrade—a considerable change in work—the subcontractor was unconvinced that the geogrid-reinforced RAP could provide a sufficient base atop the soft subgrade. Hence, additional reassurance was provided via proof rolling. Per agreed acceptance criteria, any areas exhibiting rutting during proof rolling were subject to additional compaction. Areas exhibiting no rutting, but visually perceptible deflection, were noted on the site plan for possible warranty relief. The prime contractor agreed to relieve the paving subcontractor of its warranty obligations for these areas if all other measures of workmanship (e.g., asphalt thickness and density) passed design criteria. This arrangement was agreed on because the paving subcontractor was not involved in the ground improvement decision and, therefore, felt it should not be subject to the risk assumed by the pursuit of the less expensive ground improvement alternative.

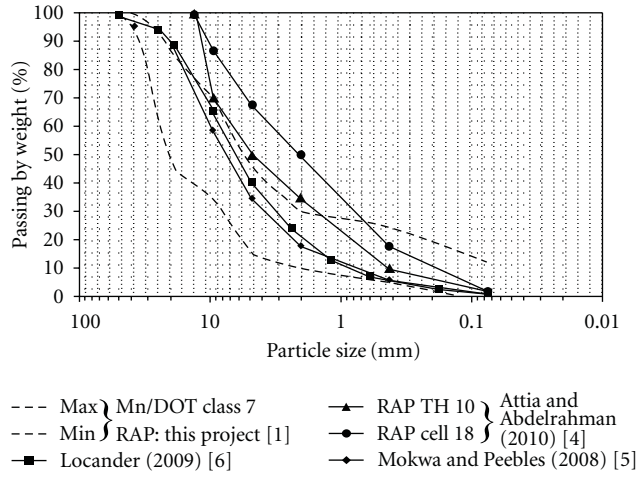

Figure 6: Comparison of Minnesota Department of Transportation (Mn/DOT) class 7 Particle Size Gradation Specification (RAP Used in This project) with Tested RAP Gradations from Selected Studies.

5. RAP Base Suitability: Comparison of Laboratory Studies to Construction Observations

Due to the intense interest in the reuse of RAP, many state and federal research agencies have encouraged the study of the mechanical properties of RAP when used as a base layer material. Accordingly, many authors have published the findings of RAP studies for this application. As with other recycled materials, studies have contemplated the use of RAP both alone and as a component of blended mixtures with stone aggregate manufactured from virgin sources. This paper considers the findings of few authors to compare laboratory observations to field observations of RAP behavior during construction.

Attia and Abdelrahman [4], Mokwa and Peebles [5], and Locander [6] investigated the strength and stiffness properties of RAP and RAP/stone aggregate blends in the laboratory to assess their suitability as pavement base layers. Since gradation is expected to have a significant effect on the behavior of RAP, it is useful to consider if the gradation of the RAP used in this project is comparable to these laboratory studies. The RAP used in this project met the criteria for Mn/DOT class 7 aggregate. Figure 6 plots the particle size gradation bounds for class 7 aggregate together with the gradation curves for the 100% RAP aggregate tested by Attia and Abdelrahman [4], Mokwa and Peebles [5], and Locander [6]. The gradation for RAP investigated by Attia and Abdelrahman [4] is similar to the gradation for Mn/DOT class 5 aggregate—the same specification as the original base design for this project. As seen in Figure 6, the gradations for Mokwa and Peebles [5] and Locander [6] fall within the Mn/DOT class 7 bounds while the RAP studied by Attia and Abdelrahman [4] is finer than Mn/DOT class 7 aggregate. Based on this comparison, the Mn/DOT class 7 RAP used in this project is expected to have properties similar to those tested by the selected studies. Since Mn/DOT class 7 is apparently coarser than RAP studied by Attia and Abdelrahman [4], it is expected to have slightly more favorable properties as a base material, although this relationship is not studied in this paper.

The asphalt binder content of the existing pavement, prior to reclamation, was determined from a single sample analyzed using Mn/DOT Method 1852 [10], a modified version of AASHTO T 164 [11]. This laboratory analysis determined an asphalt content of 4.9% for the existing pavement. This value compares well with RAP studied by Locander [6] (4.65% to 6.2% asphalt content) but is greater than that studied by Attia and Abdelrahman [4] (3.6% to 4% asphalt content).

Several of these authors noted a binding and/or agglomeration effect where residual asphalt binder within RAP causes finer particles to adhere to each other as well as larger particles, reducing the apparent fines fraction of the RAP particle gradation. Accordingly, many of the expected properties (e.g., moisture retention, resistance to flow, and maximum dry density) of materials with a significant fines fraction are likewise reduced.

Laboratory studies of RAP appear to focus on compaction behavior and stiffness, especially resilient modulus, since these are important considerations for design and construction of pavement systems. Mokwa and Peebles [5] conclude that RAP can have lesser or greater stiffness than typical stone aggregate base material depending on the quality of RAP tested. Locander [6] concludes that RAP has stiffness and compaction properties roughly equivalent to stone aggregates routinely used for pavement base layers. Interested in these seemingly conflicting results, Attia and Abdelrahman [4] investigated the relationship between moisture content, density, and stiffness. They conclude, depending on the moisture content and dry density achieved during compaction, that the resilient modulus of 100% RAP and RAP/stone aggregate blends can be less than or greater than comparably prepared Mn/DOT class 5 aggregate base courses. They note that resilient modulus decreases with increasing moisture content during compaction, especially for samples compacted wet of optimum moisture content. Attia and Abdelrahman [4] reason that this decrease is due to a reduction in the dry density achieved during compaction and to the lubricating effect of the additional free water.

Mokwa and Peebles [5] noted that as the RAP fraction of the base layer increases, the moisture content required to achieve optimal compaction decreases. This decrease in moisture content is attributed to the relatively free-draining nature of RAP, since the agglomeration effect mentioned above tends to reduce the amount of fines available to hold water. This result is confirmed by Attia and Abdelrahman [4]. Accordingly, RAP has a relatively narrow range of comparably low-moisture contents to facilitate optimum compaction when compared to virgin stone aggregate, such as Mn/DOT class 5. Thus, the concern for construction articulated by the results of Attia and Abdelrahman [4] is that too much water will be added to RAP in the field, preventing compaction from achieving comparable properties and resulting pavement base performance as other aggregates.

In the case of the project described in this paper, the field experience shows clearly that the RAP base required the continual addition of water to facilitate compaction. The quality control technician noted that the RAP drained rapidly and the surface also dried, hampering compaction efforts. With the frequent addition of water via water truck, compaction was much more effective, achieving a firm base in fewer compactor passes, passing DCP testing and exhibiting no rutting or deflection under proof rolling. After acclimating to the pace of water addition required, the paving subcontractor was able to compact the entire parking lot base course in a week with a single compactor. Compaction succeeded in producing a base condition where proof rolling exhibited only barely perceptible deflection in limited locations. As a result, all parties were pleased with the quality of the base prior to asphalt pavement placement. Furthermore, both asphalt layers were placed and compacted without incident over the entire parking lot area.

Attia and Abdelrahman [4] noted that because RAP drains freely, it is not susceptible to freeze-thaw damage (i.e., reduction in resilient modulus following a freeze-thaw cycle). They obtained this conclusion since the water inside their RAP samples was allowed to drain during the test. This observation contrasts with compaction testing, since the closed-bottom compaction molds used for compaction and resilient modulus testing would not permit the draining of water and corresponding reduction in moisture content during compaction. It appears that the observations of the parking lot construction are consistent with both the freeze-thaw finding and the compaction results since, in the field, water was able to drain from the RAP base material. Accordingly, it is very difficult under field conditions, with a properly graded subgrade, to excessively water RAP bases to the point where compaction and performance goals are not being met. Therefore, the findings of Attia and Abdelrahman [4], Mokwa and Peebles [5], and Locander [6], considered together with the field observations on this project, suggest that RAP base courses can be readily constructed with properties comparable to similarly prepared virgin stone aggregate base courses.

6. Conclusion

The project described in this report was successfully concluded at a cost (about $200,000) that is significantly less than that espoused by the original cut and replace specification (about $890,000) for unacceptable subgrades. The successful application of geogrid reinforcement in conjunction with the RAP base aggregate allowed the completion of the project in a timely manner with high-quality results. This design change not only continued the planned recycling of the asphalt pavement, but effectively resulted in the recycling of the entire subgrade, reducing the time, energy, and money consumed to replace it. The scrutiny of the base construction motivated by the paving subcontractor concerns about the geosynthetics allowed a number of useful, detailed observations. Specifically, observations related to the drainage and compaction behavior appear to be timely and can help to focus future laboratory studies of RAP. The original project specification substituting Mn/DOT class 7 RAP for class 5 stone aggregate appears to have been supported by the project outcomes as well as the findings of Attia and Abdelrahman [4], Mokwa and Peebles [5], and Locander [6].

The project also highlights a number of contractual issues worth considering on any project incorporating relatively new technologies, whether the technology in question is recycled materials or geosynthetics. First, risk is implied in any technical decision to reduce construction cost through the use of less conventional technology. Notions of conventional technology can be both geographically and institutionally specific. Thus, a technology does not need to be new in absolute terms to receive resistance from project participants. The apportionment of the risk and corresponding reward needs to be considered by all project stakeholders when dealing with problems such as the soft subgrade described in this paper. Second, the experience of this project suggests that the design-build framework has some efficiencies when addressing these concerns since it is possible for the prime contractor to negotiate both the design and workmanship obligations of the overall project team amongst its participants. It is also noteworthy that CFB ash could have been implemented given sufficient laboratory study. However, given the prime contractor's relative familiarity with geosynthetics and the original project schedule, geogrid reinforcement was the most competitive ground improvement option.

In conclusion, this project illustrates the successful implementation of RAP in what is rapidly becoming a commonplace application. The use of a RAP base in conjunction with geogrid reinforcement is more novel and also appears to be a complete success. Together, these technologies allowed the successful completion of the project, avoiding a significant waste of money, time, resources, and energy.

Acknowledgments

This project was funded by the 88th Regional Support Command (RSC). The author is grateful for the contributions of Josephine Newton-Lund, US Army Corps of Engineers, Kansas City District and Howard Dahlby of J. M. Waller Associates, Inc.

References

[1] *Standard Specifications for Construction*, Minnesota Department of Transportation, 2005.

[2] A. J. Puppala, *Estimating Stiffness of Subgrade and Unbound Materials for Pavement Design*, NCHRP Synthesis 382, Washington, DC, USA, 2008.

[3] AASHTO, *Guide for Design of Pavement Structures*, AASHTO, Washington, DC, USA, 1993.

[4] M. Attia and M. Abdelrahman, "Sensitivity of untreated reclaimed asphalt pavement to moisture, density, and freeze thaw," *Journal of Materials in Civil Engineering*, vol. 22, no. 12, pp. 1260–1269, 2010.

[5] R. L. Mokwa and C. S. Peebles, "Strength, stiffness, and compressibility of RAP/aggregate blends," *Pavement Mechanics and Performance*, no. 154, pp. 247–255, 2008.
[6] R. Locander, "Analysis of Using Reclaimed Asphalt Pavement (RAP) as a Base Course Material," Colorado Department of Transportation—Research Report CDOT-2009-5, p. 66, 2009.
[7] ASTM, *Standard Test Method for Use of the Dynamic Cone Penetrometer in Shallow Pavement Applications*, ASTM, West Conshohocken, Pa, USA, 2003, D6951-03.
[8] R. M. Koerner, *Designing with Geosynthetics*, Prentice Hall, Upper Saddle River, NJ, USA, 5th edition, 2005.
[9] J. A. Siekmeier, D. Young, and D. Beberg, "Comparison of the Dynamic Cone Penetrometer with Other Tests During Subgrade and Granular Base Characterization in Minnesota," in *Nondestructive Testing of Pavements and Backcalculation of Moduli: Third Volume*, S. D. Tayabji and E. O. Likanen, Eds., American Society for Testing and Materials, West Conshohocken, Pa, USA, 1999, ASTM STP 1375.
[10] "1852: Quantitative Extraction of Bituminous Mixtures (Centrifuge)," Lab Manual, p. 7, Minnesota Department of Transportation, 2010.
[11] AASHTO, *Standard Method of Test for Quantitative Extraction of Asphalt Binder from Hot Mix Asphalt (HMA)*, Washington, DC, USA, 2010, T 164.